

1 **Ice, Cloud, and Land Elevation Satellite 2 (ICESat-2)**

2  
3 **Algorithm Theoretical Basis Document (ATBD)**

4  
5 **for**

6  
7 **Land - Vegetation Along-Track Products (ATL08)**

8  
9  
10  
11 **Contributions by Land/Vegetation SDT Team Members**  
12 **and ICESat-2 Project Science Office**

13 **(Amy Neuenschwander, Katherine Pitts, Benjamin Jelley, John Robbins,**  
14 **Brad Klotz, Sorin Popescu, Ross Nelson, David Harding, Dylan Pederson,**  
15 **and Ryan Sheridan)**

16  
17  
18 **ATBD prepared by**

19 **Amy Neuenschwander and**

20 **Katherine Pitts**

21  
22  
23 **15 January 2020**

24 **(Corresponds to release 003 of the ICESat-2 ATL08 data)**

25  
26  
27 **Content reviewed: technical approach, assumptions, scientific soundness,**  
28 **maturity, scientific utility of the data product**



33  
34

### ATL08 algorithm and product change history

ATBD Version	Change
2016 Nov	Product segment size changed from 250 signal photons to 100 m using five 20m segments from ATL03 (Sec 2)
2016 Nov	Filtered signal classification flag removed from classed_pc_flag (Sec 2.3.2)
2016 Nov	DRAGANN signal flag added (Sec 2.3.4)
2016 Nov	Do not report segment statistics if too few ground photons within segment (Sec 4.15 (3))
2016 Nov	Product parameters added: h_canopy_uncertainty, landsat_flag, d_flag, delta_time_beg, delta_time_end, night_flag, msw_flag (Sec 2)
2017 May	Revised region boundaries to be separated by continent (Sec 2)
2017 May	Alternative DRAGANN parameter calculation added (Sec 4.3.1)
2017 May	Set canopy flag = 0 when <i>L-km</i> segment is over Antarctica or Greenland regions (Sec 4.4 (1))
2017 May	Change initial canopy filter search radius from 3 m to 15 m (Sec 4.9 (6))
2017 May	Product parameters removed: h_rel_ph, terrain_thresh
2017 May	Product parameters added: segment_id, segment_id_beg, segment_id_end, dem_flag, surf_type (Sec 2)
2017 July	Urban flag added (Sec 2.4.17)
2017 July	Dynamic point spread function added (Sec 4.11 (6))
2017 July	Methodology for processing <i>L-km</i> segments with buffer added (Sec 4.1 (2), Sec 4.17)
2017 July	Revised alternative DRAGANN methodology ( <del>see bolded text in</del> Sec 4.3.1)
2017 July	Added post-DRAGANN filtering methodology (Sec 4.7)
2017 July	Updated SNR to be estimated from superset of ATL03 and DRAGANN found signal used for processing ATL08 (Sec <a href="#">2.5.18</a> )
2017 September	More details added to DRAGANN description (Sec 4.3), and corrections to DRAGANN implementation (Sec 3.1.1, Sec 4.3 (9))
2017 September	Added Appendix A – very detailed DRAGANN description
2017 September	Revised alternative DRAGANN methodology (see bolded text in Sec 4.3.1)
2017 September	Clarified SNR calculation (Sec <a href="#">2.5.18</a> , Sec 4.3 (18))
2017 September	Added cloud flag filtering option (Sec <a href="#">Error! Reference source not found.</a> )
2017 September	Added top of canopy median surface filter (Sec 3.5 (a), Sec 4.10 (3), Sec 4.12 (1-3))

Deleted: 2.5.1

Deleted: 2.5.1

Deleted: 1

2017 September	Modified 500 canopy photon segment filter (Sec 3.5 (c), Sec 4.12 (6))
2017 November	Added solar_azimuth, solar_elevation, and n_seg_ph to Reference Data group; parameters were already in product (Sec 2.4)
2017 November	Specified number of ground photons threshold for relative canopy product calculations (Sec 4.16 (2)); no number of ground photons threshold for absolute canopy heights (Sec 4.16.1 (1))
2017 November	Changed the ATL03 signal used in superset from all ATL03 signal (signal_conf_ph flags 1-4) to the medium-high confidence flags (signal_conf_ph flags 3-4) (Sec 3.1, Sec 4.3 (17))
2017 November	Removed Date parameter from Table 2.4 since UTC date is in file metadata
2018 March	Clarified that cloud flag filtering option should be turned off by default (Sec <a href="#">Error! Reference source not found.</a> )
2018 March	Changed h_diff_ref QA threshold from 10 m to 25 m (Table 5.2)
2018 March	Added absolute canopy height quartiles, canopy_h_quartile_abs ( <i>Later removed</i> )
2018 March	Removed psf_flag from main product; psf_flag will only be a QAQC alert (Sec 5.2)
2018 March	Added an Asmooth filter based on the reference DEM value (Sec 4.6 (4-5))
2018 March	Changed relief calculation to 95 <sup>th</sup> – 5 <sup>th</sup> signal photon heights. (Sec 4.6 (6))
2018 March	Adjusted the Asmooth smoothing methodology (Sec 4.6 (8))
2018 March	Recalculate the Asmooth surface after filtering outlying noise from signal, then detrend signal height data (Sec 4.7 (3-4))
2018 March	Added option to run alternative DRAGANN process again in high noise cases (Sec <a href="#">4.3.3</a> )
2018 March	Changed global land cover reference to MODIS Global Mosaics product (Sec 2.4.14)
2018 March	Adjusted the top of canopy median filter thresholds based on SNR (Sec 4.12 (1-2))
2018 March	Added a final photon classification QA check (Sec 4.14, Table 5.2)
2018 March	Added slope adjusted terrain parameters ( <i>Later removed</i> )
2018 June	Replaced slope adjusted terrain parameters with terrain best fit parameter (Sec 2.1.14, 4.15 (2.e))
2018 June	Clarified source for water mask (Sec 2.4.15)
2018 June	Clarified source for urban mask (Sec 2.4.17)
2018 June	Added expansion to the terrain_slope calculation (Sec 4.15)
2018 June	Removed canopy_d_quartile

Deleted: 1

Deleted: 4.3.2

2018 June	Removed canopy_quartile_heights and canopy_quartile_heights_abs, replaced with canopy_h_metrics (Secs 2.2.3, 4.16 (6), 4.16.1 (5))
2018 *** draft 1	Delta_time specified as mid-segment time, rather than mean segment time (Sec 2.4.5)
2018 *** draft 1	QA/QC products to be reported on a per orbit basis, rather than per region (Sec 5.2)
2018 *** draft 1	Added more detail to landsat_flag description (Sec 2.2.23)
2018 *** draft 1	Added psf_flag back into ATL08 product, as it is also needed for the QA product (Sec 2.5.12)
2018 *** draft 1	Specified that the sigma_h value reported here is the mean of the ATL03 reported sigma_h values (Sec 2.5.7)
2018 *** draft 1	Removed n_photons from all subgroups
2018 *** draft 1	<p>Better defined the interpolation and smoothing methods used throughout:</p> <ul style="list-style-type: none"> <li>• <a href="#">Error! Reference source not found.</a> (3): <ul style="list-style-type: none"> <li>• Interpolation – nearest</li> <li>• 4.6 (5): Interpolation – PCHIP</li> <li>• 4.6 (8): Smoothing – moving average</li> <li>• 4.7 (3): Interpolation – PCHIP</li> <li>• 4.7 (3): Smoothing – moving average</li> <li>• 4.8 (10): Smoothing – moving average</li> <li>• 4.8 (11): Interpolation – linear</li> <li>• 4.8 (12): Smoothing – moving average</li> <li>• 4.8 (13): Interpolation – linear</li> <li>• 4.8 (14): Smoothing – moving average</li> <li>• 4.8 (15): Smoothing – Savitzky-Golay</li> <li>• 4.8 (16): Interpolation – linear</li> <li>• 4.8 (21): Interpolation – PCHIP</li> </ul> </li> <li>• 4.10 (10): Interpolation – linear</li> <li>• 4.11 (all): Smoothing – moving average</li> <li>• 4.10 (6.b): Interpolation – linear</li> <li>• 4.12 (1.a): Interpolation – linear</li> <li>• 4.12 (1.c): Smoothing – lowess</li> <li>• 4.12 (4): Interpolation – PCHIP</li> <li>• 4.12 (7): Interpolation – PCHIP</li> <li>• 4.12 (9): Smoothing – moving average</li> <li>• 4.15 (2.e.i.1): Interpolation – linear</li> </ul>
2018 *** draft 1	Added ref_elev and ref_azimuth back in (it was mistakenly removed in a previous version; Secs 2.5.3, 2.5.4)
2018 *** draft 1	Clarified wording of h_canopy_quad definition (Sec 2.2.17)
2018 *** draft 1	Updated segment_snowcover description to match the ATL09 snow_ice parameter it references (Sec 2.4.16) and added product reference to <a href="#">Table 4.2</a>

Deleted: 1

Deleted: 3

Deleted: 4

Deleted: 5

Deleted: 6

Deleted: 7

Deleted: 8

Deleted: 9

Deleted: 14

Deleted: Table

2018 *** draft 1	Added ph_ndx_beg (Sec <a href="#">2.5.22</a> ); parameter was already on product
2018 *** draft 1	Added dem_removal_flag for QA purposes (Sec 2.4.11; Table 5.2)
2018 *** draft 2	Reformatted QA/QC trending and trigger alert list into a table for better clarification ( <a href="#">Table 5.3</a> )
2018 *** draft 2	Replaced n_photons in Table 5.2 with n_te_photons, n_ca_photons, and n_toc_photons
2018 *** draft 2	Removed beam_number from Table 2.5. Beam number and weak/strong designation within gtx group attributes.
2018 *** draft 2	Clarified calculation of h_te_best_fit (Sec 4.15 (2.e))
2018 *** draft 2	Changed h_canopy and h_canopy_abs to be 98 <sup>th</sup> percentile height (Table 2.2, Sec 2.2.5, Sec 2.2.6, Sec 4.16 (4), Sec 4.16.1 (3))
2018 *** draft 2	Separated h_canopy_metrics_abs from h_canopy_metrics (Table 2.2, Sec 2.2.3, Sec 4.16.1 (5))
2018 October	Removed 99 <sup>th</sup> percentile from h_canopy_metrics and h_canopy_metrics_abs (Table 2.2, Sec 2.2.3, Sec 2.2.4, Sec 4.16 (4), Sec 4.16.1 (5))
2018 December	Renamed and reworded Section 4.3.1 to better indicate that the DRAGANN preprocessing step is not optional
2018 December	Specified that DRAGANN should use along-track time, and added time rescaling step (Sec 4.3 (1 - 4))
2018 December	Added DRAGANN changes made to better capture sparse canopy in cases of low noise rates (Sec 4.3, Appendix A)
2018 December	Made corrections to DRAGANN description regarding the determination of the noise Gaussian (Sec 3.1.1, Sec 4.3)
2018 December	Removed h_median_canopy and h_median_canopy_abs, as they are equivalent to canopy_h_metrics(50) and canopy_h_metrics_abs(50) (Table 2.2, Sec 4.16 (5), Sec 4.16.1 (4))
2018 December	Removed the requirement that > 5% ground photons required to calculate relative canopy height parameters (Table 2.2, Sec 4.16 (2))
2018 December	Added canopy relative height confidence flag (canopy_rh_conf) based on the percentage of ground and canopy photons in a segment (Table 2.2, Sec 4.16 (2))
2018 December	Added ATL09 layer_flag to ATL08 output (Table 2.5, <a href="#">Table 4.2</a> )
2019 February	Adjusted cloud filtering to be based on ATL09 backscatter analysis rather than cloud flags (Sec 4.1)
2019 March 5	Updated ATL09-based product descriptions reported on ATL08 product (Secs 2.5.13, 2.5.14, 2.5.15, 2.5.16)
2019 March 5	Updated cloud-based low signal filter methodology, and moved to first step of ATL08 processing (Sec 4.1)

Deleted: 2.5.2

Deleted: Table

Deleted: Table

2019 March 13	Replace canopy_closure with new landsat_perc parameter (Table 2.2, Sec 2.2.24)
2019 March 13	Change ATL08 product output regions to match ATL03 regions (Sec 2), but keep ATL08 regions internally and report in new parameter atl08_regions (Table 2.4, Sec 2.4.19)
2019 March 13	Add methodology for handling short ATL08 processing segments at the end of an ATL03 granule (Sec 4.2), and output distance the processing segment length is extended into new parameter last_seg_extend (Table 2.4, Sec 2.4.20)
2019 March 13	Add preprocessing step for removing atmospheric and ocean tide corrections from ATL03 heights ( <i>Later removed</i> )
2019 March 27	Remove preprocessing step for removing atmospheric and ocean tide corrections from ATL03 heights, since those values are now removed from the ATL03 photon heights.
2019 March 27	Replaced ATL03 region figure with corrected version (Figure 2.2)
2019 March 27	Specified that at least 50 classed photons are required to create the 100 m land and canopy products (Secs 2, 4.15(1), 4.16(1))
2019 March 27	Clarified that any non-extended segments would report a land_seg_extend value of 0 (Sec 4.2, Sec 2.4.20)
2019 April 30	Fixed the error in Eqn 1.4 for the sigma topo value
<b>2019 May 13</b>	Specified for cloud flag carry-over from ATL09 that ATL08 will report the highest cloud flag if an 08 segment straddles two 09 segments. (Section 2.5)
<b>2019 May 13</b>	Changed parameter cloud_flag_asr to cloud_flag_atm since the cloud_flag_asr is likely not to work over land due to varying surface reflectance (Sec, 2.5)
<b>2019 May 13</b>	Add ATL09 parameter cloud_fold_flag to the ATL08 data product for future qa/qc checks for low clouds. (Secs, 2.5)
<b>2019 May 13</b>	Clarification on the calculation of gradient for slope that feeds into the calculation of the point spread function (Sec 4.11)
<b>2019 July 8</b>	Changed Landsat canopy cover percentage to 3 % (from original value of 5%) (Section 4.4)
<b>2019 July 8</b>	Added a QA method for DRAGANN flags to help remove false positives (now Section 4.3.1)
<b>2019 July 8</b>	Set the window size to 9 rather than SmoothSize for the final ground finding step. (Section 4.11 and 4.12)
<b>2019 July 8</b>	Added a brightness flag to land segments. (Section 2.4.21)
<b>2019 November 12</b>	Added subset_te_flag to (Section 2.1) which indicate 100 m segments that are populated by less than 100 m worth of data

<b>2019 November 12</b>	Added subset_can_flag (section 2.2) which indicate 100 m segments that are populated by less than 100 m worth of data
<b>2020 January 5</b>	Clarified the interpolation of values (latitude, longitude, delta time) when the 100 m segments are populated by less than 100 m worth of data. (Section 2.4.3 and 2.4.4)
<b>2020 January 13</b>	Fine-tuned the methodology to improve ground finding by first histogramming the photons to improve detecting the ground in cases of dense canopy. (Section 4.8)
<b>2020 January 13</b>	Updated ATL08 HDF5 file organization figure in Section 2.1

53  
54



## 82 Contents

83	List of Tables .....	<a href="#">15</a>	Deleted: 13
84	List of Figures .....	<a href="#">16</a>	Deleted: 14
85	1 INTRODUCTION .....	<a href="#">18</a>	Deleted: 16
86	1.1. Background.....	<a href="#">19</a>	Deleted: 17
87	1.2 Photon Counting Lidar.....	<a href="#">21</a>	Deleted: 19
88	1.3 The ICESat-2 concept.....	<a href="#">22</a>	Deleted: 20
89	1.4 Height Retrieval from ATLAS.....	<a href="#">25</a>	Deleted: 23
90	1.5 Accuracy Expected from ATLAS .....	<a href="#">27</a>	Deleted: 25
91	1.6 Additional Potential Height Errors from ATLAS .....	<a href="#">29</a>	Deleted: 27
92	1.7 Dense Canopy Cases.....	<a href="#">29</a>	Deleted: 27
93	1.8 Sparse Canopy Cases .....	<a href="#">30</a>	Deleted: 28
94	2. ATL08: DATA PRODUCT .....	<a href="#">31</a>	Deleted: 29
95	2.1 Subgroup: Land Parameters.....	<a href="#">34</a>	Deleted: 32
96	2.1.1 Georeferenced_segment_number_beg .....	<a href="#">35</a>	Deleted: 33
97	2.1.2 Georeferenced_segment_number_end.....	<a href="#">35</a>	Deleted: 33
98	2.1.3 Segment_terrain_height_mean .....	<a href="#">36</a>	Deleted: 34
99	2.1.4 Segment_terrain_height_med.....	<a href="#">36</a>	Deleted: 34
100	2.1.5 Segment_terrain_height_min.....	<a href="#">36</a>	Deleted: 34
101	2.1.6 Segment_terrain_height_max.....	<a href="#">37</a>	Deleted: 34
102	2.1.7 Segment_terrain_height_mode .....	<a href="#">37</a>	Deleted: 35
103	2.1.8 Segment_terrain_height_skew .....	<a href="#">37</a>	Deleted: 35
104	2.1.9 Segment_number_terrain_photons .....	<a href="#">37</a>	Deleted: 35
105	2.1.10 Segment height_interp .....	<a href="#">37</a>	Deleted: 35
106	2.1.11 Segment h_te_std .....	<a href="#">38</a>	Deleted: 36
107	2.1.12 Segment_terrain_height_uncertainty.....	<a href="#">38</a>	Deleted: 36
108	2.1.13 Segment_terrain_slope.....	<a href="#">38</a>	Deleted: 36

162	2.1.14	Segment_terrain_height_best_fit.....	38	Deleted: 36
163	2.2	Subgroup: Vegetation Parameters.....	39	Deleted: 37
164	2.2.1	Georeferenced_segment_number_beg .....	42	Deleted: 39
165	2.2.2	Georeferenced_segment_number_end.....	42	Deleted: 39
166	2.2.3	Canopy_height_metrics_abs.....	42	Deleted: 40
167	2.2.4	Canopy_height_metrics.....	43	Deleted: 40
168	2.2.5	Absolute_segment_canopy_height .....	43	Deleted: 40
169	2.2.6	Segment_canopy_height.....	43	Deleted: 40
170	2.2.7	Absolute_segment_mean_canopy.....	44	Deleted: 41
171	2.2.8	Segment_mean_canopy.....	44	Deleted: 41
172	2.2.9	Segment_dif_canopy.....	44	Deleted: 41
173	2.2.10	Absolute_segment_min_canopy .....	44	Deleted: 41
174	2.2.11	Segment_min_canopy .....	44	Deleted: 41
175	2.2.12	Absolute_segment_max_canopy.....	44	Deleted: 42
176	2.2.13	Segment_max_canopy.....	45	Deleted: 42
177	2.2.14	Segment_canopy_height_uncertainty .....	45	Deleted: 42
178	2.2.15	Segment_canopy_openness.....	46	Deleted: 43
179	2.2.16	Segment_top_of_canopy_roughness.....	46	Deleted: 43
180	2.2.17	Segment_canopy_quadratic_height .....	46	Deleted: 43
181	2.2.18	Segment_number_canopy_photons.....	46	Deleted: 43
182	2.2.19	Segment_number_top_canopy_photons .....	46	Deleted: 44
183	2.2.20	Centroid_height.....	47	Deleted: 44
184	2.2.21	Segment_rel_canopy_conf.....	47	Deleted: 44
185	2.2.22	Canopy_flag.....	47	Deleted: 44
186	2.2.23	Landsat_flag.....	47	Deleted: 44
187	2.2.24	Landsat_perc .....	47	Deleted: 45
188	2.3	Subgroup: Photons .....	48	Deleted: 45

243	2.3.1	Indices_of_classed_photons .....	<a href="#">49</a>	Deleted: 46
244	2.3.2	Photon_class .....	<a href="#">49</a>	Deleted: 46
245	2.3.3	Georeferenced_segment_number.....	<a href="#">49</a>	Deleted: 46
246	2.3.4	DRAGANN_flag.....	<a href="#">50</a>	Deleted: 46
247	2.4	Subgroup: Reference data .....	<a href="#">50</a>	Deleted: 46
248	2.4.1	Georeferenced_segment_number_beg .....	<a href="#">51</a>	Deleted: 48
249	2.4.2	Georeferenced_segment_number_end.....	<a href="#">52</a>	Deleted: 48
250	2.4.3	Segment_latitude .....	<a href="#">52</a>	Deleted: 49
251	2.4.4	Segment_longitude .....	<a href="#">53</a>	Deleted: 49
252	2.4.5	Delta_time.....	<a href="#">53</a>	Deleted: 49
253	2.4.6	Delta_time_beg.....	<a href="#">53</a>	Deleted: 49
254	2.4.7	Delta_time_end .....	<a href="#">54</a>	Deleted: 49
255	2.4.8	Night_Flag.....	<a href="#">54</a>	Deleted: 49
256	2.4.9	Segment_reference_DTM .....	<a href="#">54</a>	Deleted: 49
257	2.4.10	Segment_reference_DEM_source.....	<a href="#">54</a>	Deleted: 50
258	2.4.11	Segment_reference_DEM_removal_flag.....	<a href="#">54</a>	Deleted: 50
259	2.4.12	Segment_terrain_difference.....	<a href="#">54</a>	Deleted: 50
260	2.4.13	Segment_terrain flag.....	<a href="#">55</a>	Deleted: 50
261	2.4.14	Segment_landcover .....	<a href="#">55</a>	Deleted: 50
262	2.4.15	Segment_watermask.....	<a href="#">55</a>	Deleted: 51
263	2.4.16	Segment_snowcover .....	<a href="#">55</a>	Deleted: 51
264	2.4.17	Urban_flag.....	<a href="#">55</a>	Deleted: 51
265	2.4.18	Surface_type .....	<a href="#">56</a>	Deleted: 51
266	2.4.19	ATL08_region.....	<a href="#">56</a>	Deleted: 52
267	2.4.20	Last_segment_extend.....	<a href="#">56</a>	Deleted: 52
268	2.5	Subgroup: Beam data .....	<a href="#">57</a>	Deleted: 52
269	2.5.1	Georeferenced_segment_number_beg .....	<a href="#">59</a>	Deleted: 55

324	2.5.2	Georeferenced_segment_number_end.....	<a href="#">60</a>	<b>Deleted:</b> 55
325	2.5.3	Beam_coelevation .....	<a href="#">60</a>	<b>Deleted:</b> 55
326	2.5.4	Beam_azimuth .....	<a href="#">60</a>	<b>Deleted:</b> 56
327	2.5.5	ATLAS_Pointing_Angle.....	<a href="#">60</a>	<b>Deleted:</b> 56
328	2.5.6	Reference_ground_track.....	<a href="#">60</a>	<b>Deleted:</b> 56
329	2.5.7	Sigma_h.....	<a href="#">61</a>	<b>Deleted:</b> 56
330	2.5.8	Sigma_along .....	<a href="#">61</a>	<b>Deleted:</b> 56
331	2.5.9	Sigma_across .....	<a href="#">61</a>	<b>Deleted:</b> 57
332	2.5.10	Sigma_topo .....	<a href="#">61</a>	<b>Deleted:</b> 57
333	2.5.11	Sigma_ATLAS_LAND.....	<a href="#">62</a>	<b>Deleted:</b> 57
334	2.5.12	PSF_flag.....	<a href="#">62</a>	<b>Deleted:</b> 57
335	2.5.13	Layer_flag.....	<a href="#">62</a>	<b>Deleted:</b> 57
336	2.5.14	Cloud_flag_atm.....	<a href="#">62</a>	<b>Deleted:</b> 58
337	2.5.15	MSW .....	<a href="#">62</a>	<b>Deleted:</b> 58
338	2.5.16	Cloud Fold Flag.....	<a href="#">63</a>	<b>Deleted:</b> 58
339	2.5.17	Computed_Apparent_Surface_Reflectance.....	<a href="#">63</a>	<b>Deleted:</b> 58
340	2.5.18	Signal_to_Noise_Ratio .....	<a href="#">63</a>	<b>Deleted:</b> 59
341	2.5.19	Solar_Azimuth.....	<a href="#">63</a>	<b>Deleted:</b> 59
342	2.5.20	Solar_Elevation.....	<a href="#">64</a>	<b>Deleted:</b> 59
343	2.5.21	Number_of_segment_photons.....	<a href="#">64</a>	<b>Deleted:</b> 59
344	2.5.22	Photon_Index_Begin.....	<a href="#">64</a>	<b>Deleted:</b> 59
345	3	ALGORITHM METHODOLOGY .....	<a href="#">65</a>	<b>Deleted:</b> 60
346	3.1	Noise Filtering .....	<a href="#">65</a>	<b>Deleted:</b> 60
347	3.1.1	DRAGANN .....	<a href="#">66</a>	<b>Deleted:</b> 61
348	3.2	Surface Finding .....	<a href="#">70</a>	<b>Deleted:</b> 65
349	3.2.1	De-trending the Signal Photons .....	<a href="#">72</a>	<b>Deleted:</b> 67
350	3.2.2	Canopy Determination.....	<a href="#">72</a>	<b>Deleted:</b> 67

405	3.2.3	Variable Window Determination .....	<a href="#">74</a>	<b>Deleted: 69</b>
406	3.2.4	Compute descriptive statistics .....	<a href="#">75</a>	<b>Deleted: 70</b>
407	3.2.5	Ground Finding Filter (Iterative median filtering).....	<a href="#">77</a>	<b>Deleted: 72</b>
408	3.3	Top of Canopy Finding Filter.....	<a href="#">78</a>	<b>Deleted: 73</b>
409	3.4	Classifying the Photons.....	<a href="#">79</a>	<b>Deleted: 74</b>
410	3.5	Refining the Photon Labels .....	<a href="#">79</a>	<b>Deleted: 74</b>
411	3.6	Canopy Height Determination.....	<a href="#">84</a>	<b>Deleted: 79</b>
412	3.7	Link Scale for Data products .....	<a href="#">84</a>	<b>Deleted: 79</b>
413	4.	ALGORITHM IMPLEMENTATION.....	<a href="#">85</a>	<b>Deleted: 80</b>
414	4.1	Cloud based filtering.....	<a href="#">88</a>	<b>Deleted: 83</b>
415	4.2	Preparing ATL03 data for input to ATL08 algorithm.....	<a href="#">90</a>	<b>Deleted: 85</b>
416	4.3	Noise filtering via DRAGANN .....	<a href="#">91</a>	<b>Deleted: 86</b>
417	4.3.1	DRAGANN Quality Assurance .....	<a href="#">94</a>	<b>Deleted: 89</b>
418	4.3.2	Preprocessing to dynamically determine a DRAGANN parameter .....	<a href="#">95</a>	<b>Deleted: 90</b>
419	4.3.3	Iterative DRAGANN processing.....	<a href="#">98</a>	<b>Deleted: 93</b>
420	4.4	Is Canopy Present .....	<a href="#">99</a>	<b>Deleted: 94</b>
421	4.5	Compute Filtering Window .....	<a href="#">99</a>	<b>Deleted: 94</b>
422	4.6	De-trend Data.....	<a href="#">99</a>	<b>Deleted: 94</b>
423	4.7	Filter outlier noise from signal.....	<a href="#">100</a>	<b>Deleted: 95</b>
424	4.8	Finding the initial ground estimate.....	<a href="#">101</a>	<b>Deleted: 96</b>
425	4.9	Find the top of the canopy (if canopy_flag = 1) .....	<a href="#">104</a>	<b>Deleted: 98</b>
426	4.10	Compute statistics on de-trended data.....	<a href="#">105</a>	<b>Deleted: 99</b>
427	4.11	Refine Ground Estimates .....	<a href="#">106</a>	<b>Deleted: 100</b>
428	4.12	Canopy Photon Filtering .....	<a href="#">107</a>	<b>Deleted: 102</b>
429	4.13	Compute individual Canopy Heights .....	<a href="#">110</a>	<b>Deleted: 104</b>
430	4.14	Final photon classification QA check.....	<a href="#">110</a>	<b>Deleted: 104</b>
431	4.15	Compute segment parameters for the Land Products .....	<a href="#">111</a>	<b>Deleted: 105</b>

467  
468  
469  
470  
471  
472  
473  
474

4.16 Compute segment parameters for the Canopy Products..... [113](#)

    4.16.1 Canopy Products calculated with absolute heights..... [115](#)

4.17 Record final product without buffer ..... [115](#)

5 DATA PRODUCT VALIDATION STRATEGY ..... [117](#)

    5.1 Validation Data..... [117](#)

    5.2 Internal QC Monitoring..... [120](#)

6 REFERENCES..... [126](#)

**Deleted:** 108

**Deleted:** 109

**Deleted:** 110

**Deleted:** 111

**Deleted:** 114

**Deleted:** 120

497 **List of Tables**

498	Table 2.1. Summary table of land parameters on ATL08.....	<a href="#">34</a>	<b>Deleted:</b> 32
499	Table 2.2. Summary table of canopy parameters on ATL08.....	<a href="#">40</a>	<b>Deleted:</b> 37
500	Table 2.3. Summary table for photon parameters for the ATL08 product.....	<a href="#">48</a>	<b>Deleted:</b> 45
501	Table 2.4. Summary table for reference parameters for the ATL08 product.....	<a href="#">50</a>	<b>Deleted:</b> 47
502	Table 2.5. Summary table for beam parameters for the ATL08 product.....	<a href="#">57</a>	<b>Deleted:</b> 52
503	Table 3.1. Standard deviation ranges utilized to qualify the spread of photons within		
504	moving window.....	<a href="#">76</a>	<b>Deleted:</b> 71
505	Table 4.1. Input parameters to ATL08 classification algorithm.....	<a href="#">85</a>	<b>Deleted:</b> 80
506	Table 4.2. Additional external parameters referenced in ATL08 product.....	<a href="#">86</a>	<b>Deleted:</b> 81
507	Table 5.1. Airborne lidar data vertical height (Z accuracy) requirements for		
508	validation data.....	<a href="#">117</a>	<b>Deleted:</b> 109
509	Table 5.2. ATL08 parameter monitoring.....	<a href="#">120</a>	<b>Deleted:</b> 112
510	Table 5.3. QA/QC trending and triggers.....	<a href="#">124</a>	<b>Deleted:</b> 116
511			

553 **List of Figures**

554	Figure 1.1. Various modalities of lidar detection. Adapted from Harding, 2009. ....	22	Deleted: 20
555	Figure 1.2. Schematic of 6-beam configuration for ICESat-2 mission. The laser		
556	energy will be split into 3 laser beam pairs – each pair having a weak spot (1X) and a		
557	strong spot (4X).....	24	Deleted: 22
558	Figure 1.3. Illustration of off-nadir pointing scenarios. Over land (green regions) in		
559	the mid-latitudes, ICESat-2 will be pointed away from the repeat ground tracks to		
560	increase the density of measurements over terrestrial surfaces.....	25	Deleted: 23
561	Figure 1.4. Illustration of the point spread function, also referred to as Znoise, for a		
562	series of photons about a surface. ....	27	Deleted: 25
563	Figure 2.1. HDF5 data structure for ATL08 products .....	32	Deleted: 30
564	Figure 2.2. ATL03 granule regions; graphic from ATL03 ATBD (Neumann et al.).....	33	Deleted: 31
565	Figure 2.3. ATL08 product regions.....	34	Deleted: 32
566	Figure 2.4. Illustration of canopy photons (red dots) interaction in a vegetated area.		
567	Relative canopy heights, $H_i$ , are computed by differencing the canopy photon height		
568	from an interpolated terrain surface.....	40	Deleted: 37
569	Figure 3.1. Combination of noise filtering algorithms to create a superset of input		
570	data for surface finding algorithms.....	66	Deleted: 61
571	Figure 3.2. Histogram of the number of photons within a search radius. This		
572	histogram is used to determine the threshold for the DRAGANN approach. ....	68	Deleted: 63
573	Figure 3.3. Output from DRAGANN filtering. Signal photons are shown as blue.....	70	Deleted: 65
574	Figure 3.4. Flowchart of overall surface finding method.....	71	Deleted: 66
575	Figure 3.5. Plot of Signal Photons (black) from 2014 MABEL flight over Alaska and		
576	de-trended photons (red).....	72	Deleted: 67
577	Figure 3.6. Shape Parameter for variable window size.....	75	Deleted: 70
578	Figure 3.7. Illustration of the standard deviations calculated for each moving		
579	window to identify the amount of spread of signal photons within a given window.		
580	.....	77	Deleted: 72
581	Figure 3.8. Three iterations of the ground finding concept for $L$ -km segments with		
582	canopy.....	78	Deleted: 73



616 617	Figure 3.9. Example of the intermediate ground and top of canopy surfaces calculated from MABEL flight data over Alaska during July 2014.....	81	<b>Deleted:</b> 76
618 619 620 621	Figure 3.10. Example of classified photons from MABEL data collected in Alaska 2014. Red photons are photons classified as terrain. Green photons are classified as top of canopy. Canopy photons (shown as blue) are considered as photons lying between the terrain surface and top of canopy.....	82	<b>Deleted:</b> 77
622 623 624 625	Figure 3.11. Example of classified photons from MABEL data collected in Alaska 2014. Red photons are photons classified as terrain. Green photons are classified as top of canopy. Canopy photons (shown as blue) are considered as photons lying between the terrain surface and top of canopy.....	83	<b>Deleted:</b> 78
626 627 628 629	Figure 3.12. Example of classified photons from MABEL data collected in Alaska 2014. Red photons are photons classified as terrain. Green photons are classified as top of canopy. Canopy photons (shown as blue) are considered as photons lying between the terrain surface and top of canopy.....	83	<b>Deleted:</b> 78
630 631 632	Figure 5.1. Example of <i>L-km</i> segment classifications and interpolated ground surface.....	123	<b>Deleted:</b> 115

638 **1 INTRODUCTION**

639 This document describes the theoretical basis and implementation of the  
640 processing algorithms and data parameters for Level 3 land and vegetation heights  
641 for the non-polar regions of the Earth. The ATL08 product contains heights for both  
642 terrain and canopy in the along-track direction as well as other descriptive  
643 parameters derived from the measurements. At the most basic level, a derived surface  
644 height from the ATLAS instrument at a given time is provided relative to the WGS-84  
645 ellipsoid. Height estimates from ATL08 can be compared with other geodetic data and  
646 used as input to higher-level ICESat-2 products, namely ATL13 and ATL18. ATL13  
647 will provide estimates of inland water-related heights and associated descriptive  
648 parameters. ATL18 will consist of gridded maps for terrain and canopy features.

649 The ATL08 product will provide estimates of terrain heights, canopy heights,  
650 and canopy cover at fine spatial scales in the along-track direction. Along-track is  
651 defined as the direction of travel of the ICESat-2 satellite in the velocity vector.  
652 Parameters for the terrain and canopy will be provided at a fixed step-size of 100 m  
653 along the ground track referred to as a segment. A fixed segment size of 100 m was  
654 chosen to provide continuity of data parameters on the ATL08 data product. From an  
655 analysis perspective, it is difficult and cumbersome to attempt to relate canopy cover  
656 over variable lengths. Furthermore, a segment size of 100 m will facilitate a simpler  
657 combination of along-track data to create the gridded products.

658 We anticipate that the signal returned from the weak beam will be sufficiently  
659 weak and may prohibit the determination of both a terrain and canopy segment  
660 height, particularly over areas of dense vegetation. However, in more arid regions we  
661 anticipate producing a terrain height for both the weak and strong beams.

662 In this document, section 1 provides a background of lidar in the ecosystem  
663 community as well as describing photon counting systems and how they differ from  
664 discrete return lidar systems. Section 2 provides an overview of the Land and  
665 Vegetation parameters and how they are defined on the data product. Section 3  
666 describes the basic methodology that will be used to derive the parameters for ATL08.

667 Section 4 describes the processing steps, input data, and procedure to derive the data  
668 parameters. Section 5 will describe the test data and specific tests that NASA's  
669 implementation of the algorithm should pass in order to determine a successful  
670 implementation of the algorithm.

671

### 672 **1.1. Background**

673 The Earth's land surface is a complex mosaic of geomorphic units and land  
674 cover types resulting in large variations in terrain height, slope, roughness, vegetation  
675 height and reflectance, often with the variations occurring over very small spatial  
676 scales. Documentation of these landscape properties is a first step in understanding  
677 the interplay between the formative processes and response to changing conditions.  
678 Characterization of the landscape is also necessary to establish boundary conditions  
679 for models which are sensitive to these properties, such as predictive models of  
680 atmospheric change that depend on land-atmosphere interactions. Topography, or  
681 land surface height, is an important component for many height applications, both to  
682 the scientific and commercial sectors. The most accurate global terrain product was  
683 produced by the Shuttle Radar Topography Mission (SRTM) launched in 2000;  
684 however, elevation data are limited to non-polar regions. The accuracy of SRTM  
685 derived elevations range from 5 – 10 m, depending upon the amount of topography  
686 and vegetation cover over a particular area. ICESat-2 will provide a global distribution  
687 of geodetic measurements (of both the terrain surface and relative canopy heights)  
688 which will provide a significant benefit to society through a variety of applications  
689 including sea level change monitoring, forest structural mapping and biomass  
690 estimation, and improved global digital terrain models.

691 In addition to producing a global terrain product, monitoring the amount and  
692 distribution of above ground vegetation and carbon pools enables improved  
693 characterization of the global carbon budget. Forests play a significant role in the  
694 terrestrial carbon cycle as carbon pools. Events, such as management activities  
695 (Krankina et al. 2012) and disturbances can release carbon stored in forest above

696 ground biomass (AGB) into the atmosphere as carbon dioxide, a greenhouse gas that  
697 contributes to climate change (Ahmed et al. 2013). While carbon stocks in nations  
698 with continuous national forest inventories (NFIs) are known, complications with NFI  
699 carbon stock estimates exist, including: (1) ground-based inventory measurements  
700 are time consuming, expensive, and difficult to collect at large-scales (Houghton  
701 2005; Ahmed et al. 2013); (2) asynchronously collected data; (3) extended time  
702 between repeat measurements (Houghton 2005); and (4) the lack of information on  
703 the spatial distribution of forest AGB, required for monitoring sources and sinks of  
704 carbon (Houghton 2005). Airborne lidar has been used for small studies to capture  
705 canopy height and in those studies canopy height variation for multiple forest types  
706 is measured to approximately 7 m standard deviation (Hall et al., 2011).

707         Although the spatial extent and changes to forests can be mapped with existing  
708 satellite remote sensing data, the lack of information on forest vertical structure and  
709 biomass limits the knowledge of biomass/biomass change within the global carbon  
710 budget. Based on the global carbon budget for 2015 (Quere et al., 2015), the largest  
711 remaining uncertainties about the Earth's carbon budget are in its terrestrial  
712 components, the global residual terrestrial carbon sink, estimated at  $3.0 \pm 0.8$   
713 GtC/year for the last decade (2005-2014). Similarly, carbon emissions from land-use  
714 changes, including deforestation, afforestation, logging, forest degradation and  
715 shifting cultivation are estimated at  $0.9 \pm 0.5$  GtC /year. By providing information on  
716 vegetation canopy height globally with a higher spatial resolution than previously  
717 afforded by other spaceborne sensors, the ICESat-2 mission can contribute  
718 significantly to reducing uncertainties associated with forest vegetation carbon.

719         Although ICESat-2 is not positioned to provide global biomass estimates due  
720 to its profiling configuration and somewhat limited detection capabilities, it is  
721 anticipated that the data products for vegetation will be complementary to ongoing  
722 biomass and vegetation mapping efforts. Synergistic use of ICESat-2 data with other  
723 space-based mapping systems is one solution for extended use of ICESat-2 data.  
724 Possibilities include NASA's Global Ecosystems Dynamics Investigation (GEDI) lidar

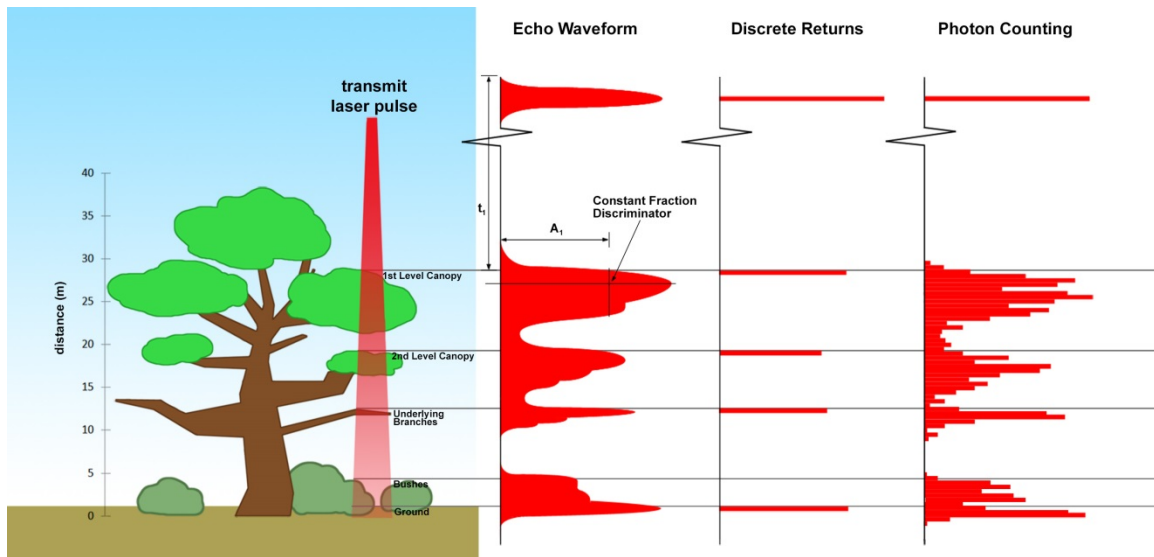
725 planned to fly onboard the International Space Station (ISS) or imaging sensors, such  
726 as Landsat 8, or NASA/ISRO –NISAR radar mission.

727

## 728 **1.2 Photon Counting Lidar**

729 Rather than using an analog, full waveform system similar to what was utilized  
730 on the ICESat/GLAS mission, ICESat-2 will employ a photon counting lidar. Photon  
731 counting lidar has been used successfully for ranging for several decades in both the  
732 science and defense communities. Photon counting lidar systems operate on the  
733 concept that a low power laser pulse is transmitted and the detectors used are  
734 sensitive at the single photon level. Due to this type of detector, any returned photon  
735 whether from the reflected signal or solar background can trigger an event within the  
736 detector. A discussion regarding discriminating between signal and background noise  
737 photons is discussed later in this document. A question of interest to the ecosystem  
738 community is to understand where within the canopy is the photon likely to be  
739 reflected. Figure 1.1 is an example of three different laser detector modalities: full  
740 waveform, discrete return, and photon counting. Full waveform sensors record the  
741 entire temporal profile of the reflected laser energy through the canopy. In contrast,  
742 discrete return systems have timing hardware that record the time when the  
743 amplitude of the reflected signal energy exceeds a certain threshold amount. A photon  
744 counting system, however, will record the arrival time associated with a single  
745 photon detection that can occur anywhere within the vertical distribution of the  
746 reflected signal. If a photon counting lidar system were to dwell over a surface for a  
747 significant number of shots (i.e. hundreds or more), the vertical distribution of the  
748 reflected photons will resemble a full waveform. Thus, while an individual photon  
749 could be reflected from anywhere within the vertical canopy, the probability  
750 distribution function (PDF) of that reflected photon would be the full waveform.  
751 Furthermore, the probability of detecting the top of the tree is not as great as  
752 detecting reflective surfaces positioned deeper into the canopy where the bulk of  
753 leaves and branches are located. As one might imagine, the PDF will differ according

754 to canopy structure and vegetation physiology. For example, the PDF of a conifer tree  
755 will look different than broadleaf trees.



756

757 Figure 1.1. Various modalities of lidar detection. Adapted from Harding, 2009.

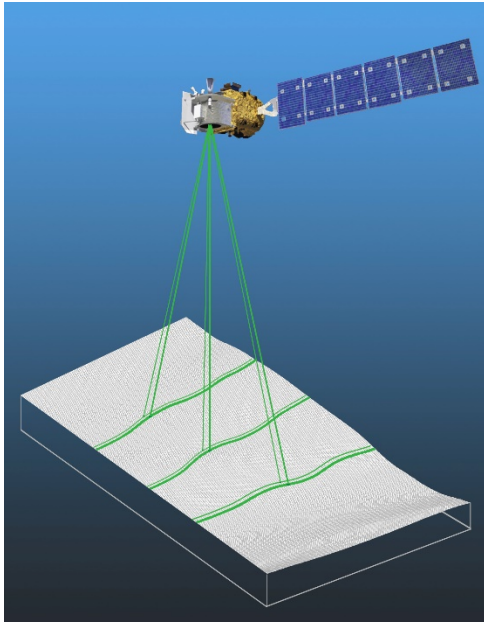
758 A cautionary note, the photon counting PDF that is illustrated in Figure 1.1 is  
759 merely an illustration if enough photons (i.e. hundreds of photons or more) were to  
760 be reflected from a target. In reality, due to the spacecraft speed, ATLAS will record 0  
761 – 4 photons per transmit laser pulse over vegetation.

762

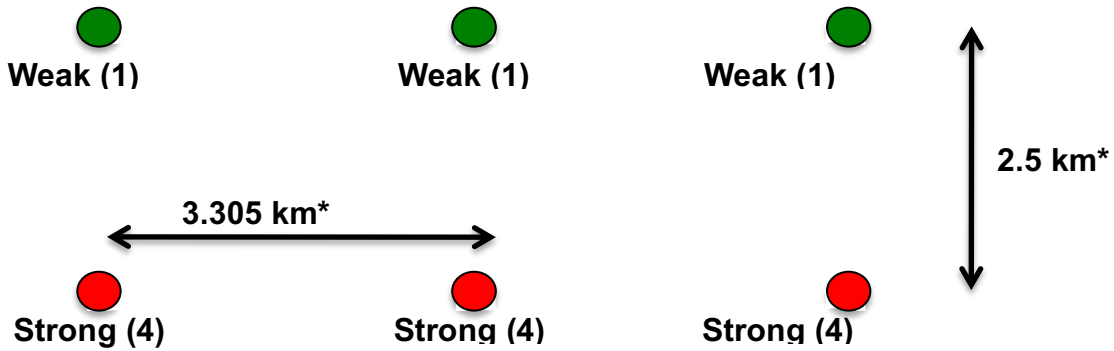
### 763 1.3 The ICESat-2 concept

764 The Advanced Topographic Laser Altimeter System (ATLAS) instrument  
765 designed for ICESat-2 will utilize a different technology than the GLAS instrument  
766 used for ICESat. Instead of using a high-energy, single-beam laser and digitizing the  
767 entire temporal profile of returned laser energy, ATLAS will use a multi-beam,  
768 micropulse laser (sometimes referred to as photon-counting). The travel time of each  
769 detected photon is used to determine a range to the surface which, when combined  
770 with satellite attitude and pointing information, can be geolocated into a unique XYZ  
771 location on or near the Earth's surface. For more information on how the photons  
772 from ICESat-2 are geolocated, refer to ATL03 ATBD. The XYZ positions from ATLAS

773 are subsequently used to derive surface and vegetation properties. The ATLAS  
774 instrument will operate at 532 nm in the green range of the electromagnetic (EM)  
775 spectrum and will have a laser repetition rate of 10 kHz. The combination of the laser  
776 repetition rate and satellite velocity will result in one outgoing laser pulse  
777 approximately every 70 cm on the Earth's surface and each spot on the surface is ~13  
778 m in diameter. Each transmitted laser pulse is split by a diffractive optical element in  
779 ATLAS to generate six individual beams, arranged in three pairs (Figure 1.2). The  
780 beams within each pair have different transmit energies ('weak' and 'strong', with an  
781 energy ratio of approximately 1:4) to compensate for varying surface reflectance. The  
782 beam pairs are separated by ~3.3 km in the across-track direction and the strong and  
783 weak beams are separated by ~2.5 km in the along-track direction. As ICESat-2 moves  
784 along its orbit, the ATLAS beams describe six tracks on the Earth's surface; the array  
785 is rotated slightly with respect to the satellite's flight direction so that tracks for the  
786 fore and aft beams in each column produce pairs of tracks - each separated by  
787 approximately 90 m.



788

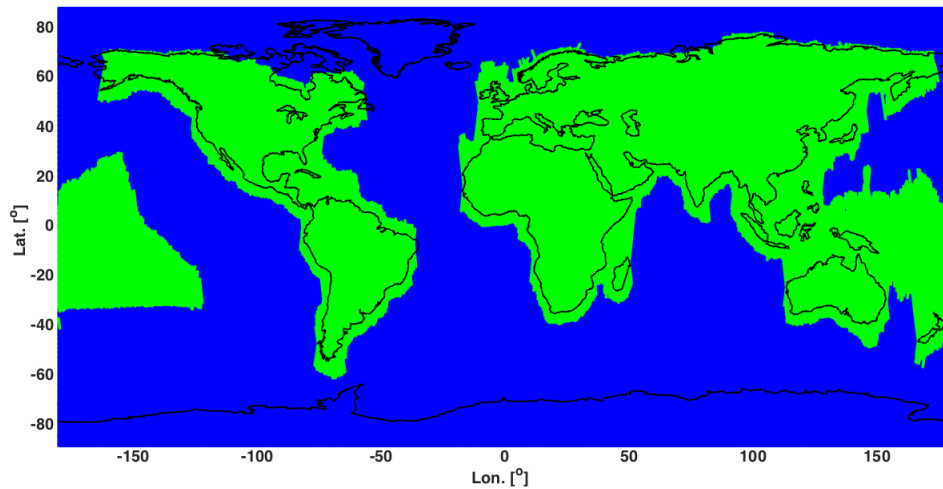


789

790 Figure 1.2. Schematic of 6-beam configuration for ICESat-2 mission. The laser energy will  
 791 be split into 3 laser beam pairs – each pair having a weak spot (1X) and a strong spot (4X).

792 The motivation behind this multi-beam design is its capability to compute  
 793 cross-track slopes on a per-orbit basis, which contributes to an improved  
 794 understanding of ice dynamics. Previously, slope measurements of the terrain were  
 795 determined via repeat-track and crossover analysis. The laser beam configuration as  
 796 proposed for ICESat-2 is also beneficial for terrestrial ecosystems compared to GLAS  
 797 as it enables a denser spatial sampling in the non-polar regions. To achieve a spatial  
 798 sampling goal of no more than 2 km between equatorial ground tracks, ICESat-2 will  
 799 be off-nadir pointed a maximum of 1.8 degrees from the reference ground track  
 800 during the entire mission.





801

802 Figure 1.3. Illustration of off-nadir pointing scenarios. Over land (green regions) in the  
 803 mid-latitudes, ICESat-2 will be pointed away from the repeat ground tracks to increase the  
 804 density of measurements over terrestrial surfaces.

805 ICESat-2 is designed to densely sample the Earth's surface, permitting  
 806 scientists to measure and quantitatively characterize vegetation across vast  
 807 expanses, e.g., nations, continents, globally. ICESat-2 will acquire synoptic  
 808 measurements of vegetation canopy height, density, the vertical distribution of  
 809 photosynthetically active material, leading to improved estimates of forest biomass,  
 810 carbon, and volume. In addition, the orbital density, i.e., the number of orbits per unit  
 811 area, at the end of the three year mission will facilitate the production of gridded  
 812 global products. ICESat-2 will provide the means by which an accurate "snapshot" of  
 813 global biomass and carbon may be constructed for the mission period.

814

#### 815 **1.4 Height Retrieval from ATLAS**

816 Light from the ATLAS lasers reaches the earth's surface as flat disks of down-  
 817 traveling photons approximately 50 cm in vertical extent and spread over  
 818 approximately 14 m horizontally. Upon hitting the earth's surface, the photons are  
 819 reflected and scattered in every direction and a handful of photons return to the

820 ATLAS telescope's focal plane. The number of photon events per laser pulse is a  
821 function of outgoing laser energy, surface reflectance, solar conditions, and scattering  
822 and attenuation in the atmosphere. For highly reflective surfaces (such as land ice)  
823 and clear skies, approximately 10 signal photons from a single strong beam are  
824 expected to be recorded by the ATLAS instrument for a given transmit laser pulse.  
825 Over vegetated land where the surface reflectance is considerably less than snow or  
826 ice surfaces, we expect to see fewer returned photons from the surface. Whereas  
827 snow and ice surfaces have high reflectance at 532 nm (typical Lambertian  
828 reflectance between 0.8 and 0.98 (Martino, GSFC internal report, 2010)), canopy and  
829 terrain surfaces have much lower reflectance (typically around 0.3 for soil and 0.1 for  
830 vegetation) at 532 nm. As a consequence we expect to see 1/3 to 1/9 as many photons  
831 returned from terrestrial surfaces as from ice and snow surfaces. For vegetated  
832 surfaces, the number of reflected signal photon events per transmitted laser pulse is  
833 estimated to range between 0 to 4 photons.

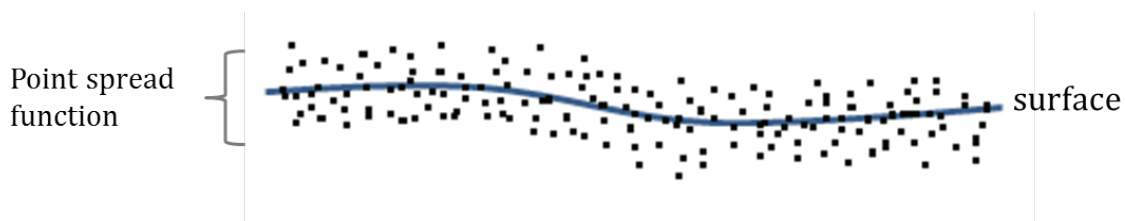
834 The time measured from the detected photon events are used to compute a  
835 range, or distance, from the satellite. Combined with the precise pointing and attitude  
836 information about the satellite, the range can be geolocated into a XYZ point (known  
837 as a geolocated photon) above the WGS-84 reference ellipsoid. In addition to  
838 recording photons from the reflected signal, the ATLAS instrument will detect  
839 background photons from sunlight which are continually entering the telescope. A  
840 primary objective of the ICESat-2 data processing software is to correctly  
841 discriminate between signal photons and background photons. Some of this  
842 processing occurs at the ATL03 level and some of it also occurs within the software  
843 for ATL08. At ATL03, this discrimination is done through a series of three steps of  
844 progressively finer resolution with some processing occurring onboard the satellite  
845 prior to downlink of the raw data. The ATL03 data product produces a classification  
846 between signal and background (i.e. noise) photons, and further discussion on that  
847 classification process can be read in the ATL03 ATBD. In addition, all geophysical  
848 corrections (e.g. ocean tide, solid earth tide models, etc.) are not applied to the  
849 position of the individual geolocated photons at the ATL03 level, but they are

850 provided on the data product if there exists a need to apply them. Thus, all of the  
851 heights processed in the ATL08 algorithm consists of the ATL03 heights with respect  
852 to the WGS-84 ellipsoid.

853

### 854 **1.5 Accuracy Expected from ATLAS**

855 There are a variety of elements that contribute to the elevation accuracy that  
856 are expected from ATLAS and the derived data products. Elevation accuracy is a  
857 composite of ranging precision of the instrument, radial orbital uncertainty,  
858 geolocation knowledge, forward scattering in the atmosphere, and tropospheric path  
859 delay uncertainty. The ranging precision seen by ATLAS will be a function of the laser  
860 pulse width, the surface area potentially illuminated by the laser, and uncertainty in  
861 the timing electronics. The requirement on radial orbital uncertainty is specified to  
862 be less than 4 cm and tropospheric path delay uncertainty is estimated to be 3 cm. In  
863 the case of ATLAS, the ranging precision for flat surfaces, is expected to have a  
864 standard deviation of approximately 25 cm. The composite of each of the errors can  
865 also be thought of as the spread of photons about a surface (see Figure 1.4) and is  
866 referred to as the point spread function or Znoise.



867

868 Figure 1.4. Illustration of the point spread function, also referred to as Znoise, for a series  
869 of photons about a surface.

870 The estimates of  $\sigma_{Orbit}$ ,  $\sigma_{troposphere}$ ,  $\sigma_{forwardscattering}$ ,  $\sigma_{pointing}$ , and  $\sigma_{timing}$   
871 for a photon will be represented on the ATL03 data product as the final geolocated  
872 accuracy in the X, Y, and Z (or height) direction. In reality, these parameters have  
873 different temporal and spatial scales, however until ICESat-2 is on orbit, it is uncertain  
874 how these parameters will vary over time. As such, Equation 1.1 may change once the

875 temporal aspects of these parameters are better understood. For a preliminary  
 876 quantification of the uncertainties, Equation 1.1 is valid to incorporate the instrument  
 877 related factors.

$$878 \quad \sigma_Z = \sqrt{\sigma_{Orbit}^2 + \sigma_{trop}^2 + \sigma_{forwardscattering}^2 + \sigma_{pointing}^2 + \sigma_{timing}^2} \quad \text{Eqn. 1.1}$$

879

880 Although  $\sigma_Z$  on the ATL03 product represents the best understanding of the  
 881 uncertainty for each geolocated photon, it does not incorporate the uncertainty  
 882 associated with local slope of the topography. The slope component to the geolocation  
 883 uncertainty is a function of both the geolocation knowledge of the pointing (which is  
 884 required to be less than 6.5 m) multiplied by the tangent of the surface slope. In a case  
 885 of flat topography ( $\leq 1$  degree slope),  $\sigma_Z \leq 25$  cm, whereas in the case of a 10 degree  
 886 surface slope,  $\sigma_Z = 119$  cm. The uncertainty associated with the local slope will be  
 887 combined with  $\sigma_Z$  to produce the term  $\sigma_{AtlasLand}$ .

$$888 \quad \sigma_{AtlasLand} = \sqrt{\sigma_Z^2 + \sigma_{topo}^2} \quad \text{Eqn. 1.2}$$

$$889 \quad \sigma_{topo} = \quad \text{Eqn. 1.3}$$

890 Ultimately, the uncertainty that will be reported on the data product ATL08  
 891 will include the  $\sigma_{AtlasLand}$  term and the local rms values of heights computed within  
 892 each data parameter segment. For example, calculations of terrain height will be  
 893 made on photons classified as terrain photons (this process is described in the  
 894 following sections). The uncertainty of the terrain height for a segment is described  
 895 in Equation 1.4, where the root mean square term of  $\sigma_{AtlasLand}$  and rms of terrain  
 896 heights are normalized by the number of terrain photons for that given segment.

$$897 \quad \sigma_{ATL08_{segment}} = \sqrt{\sigma_{AtlasLand}^2 + \sigma_{Zrms_{segment\_class}}^2} \quad \text{Eqn. 1.4}$$

898

899 **1.6 Additional Potential Height Errors from ATLAS**

900 Some additional potential height errors in the ATL08 terrain and vegetation  
901 product can come from a variety of sources including:

902 a. Vertical sampling error. ATLAS height estimates are based on a  
903 random sampling of the surface height distribution. Photons may  
904 be reflected from anywhere within the PDF of the reflecting surface;  
905 more specifically, anywhere from within the canopy. A detailed  
906 look at the potential effect of vertical sampling error is provided in  
907 Neuenschwander and Magruder (2016).

908 b. Background noise. Random noise photons are mixed with the  
909 signal photons so classified photons will include random outliers.

910 c. Complex topography. The along-track product may not always  
911 represent complex surfaces, particularly if the density of ground  
912 photons does not support an accurate representation.

913 d. Vegetation. Dense vegetation may preclude reflected photon  
914 events from reaching the underlying ground surface. An incorrect  
915 estimation of the underlying ground surface will subsequently lead  
916 to an incorrect canopy height determination.

917 e. Misidentified photons. The product from ATL03 combined with  
918 additional noise filtering may not identify the correct photons as  
919 signal photons.

920

921 **1.7 Dense Canopy Cases**

922 Although the height accuracy produced from ICESat-2 is anticipated to be  
923 superior to other global height products (e.g. SRTM), for certain biomes photon  
924 counting lidar data as it will be collected by the ATLAS instrument present a challenge  
925 for extracting both the terrain and canopy heights, particularly for areas of dense

926 vegetation. Due to the relatively low laser power, we anticipate that the along-track  
927 signal from ATLAS may lose ground signal under dense forest (e.g. >96% canopy  
928 closure) and in situations where cloud cover obscures the terrestrial signal. In areas  
929 having dense vegetation, it is likely that only a handful of photons will be returned  
930 from the ground surface with the majority of reflections occurring from the canopy.  
931 A possible source of error can occur with both the canopy height estimates and the  
932 terrain heights if the vegetation is particularly dense and the ground photons were  
933 not correctly identified.

934

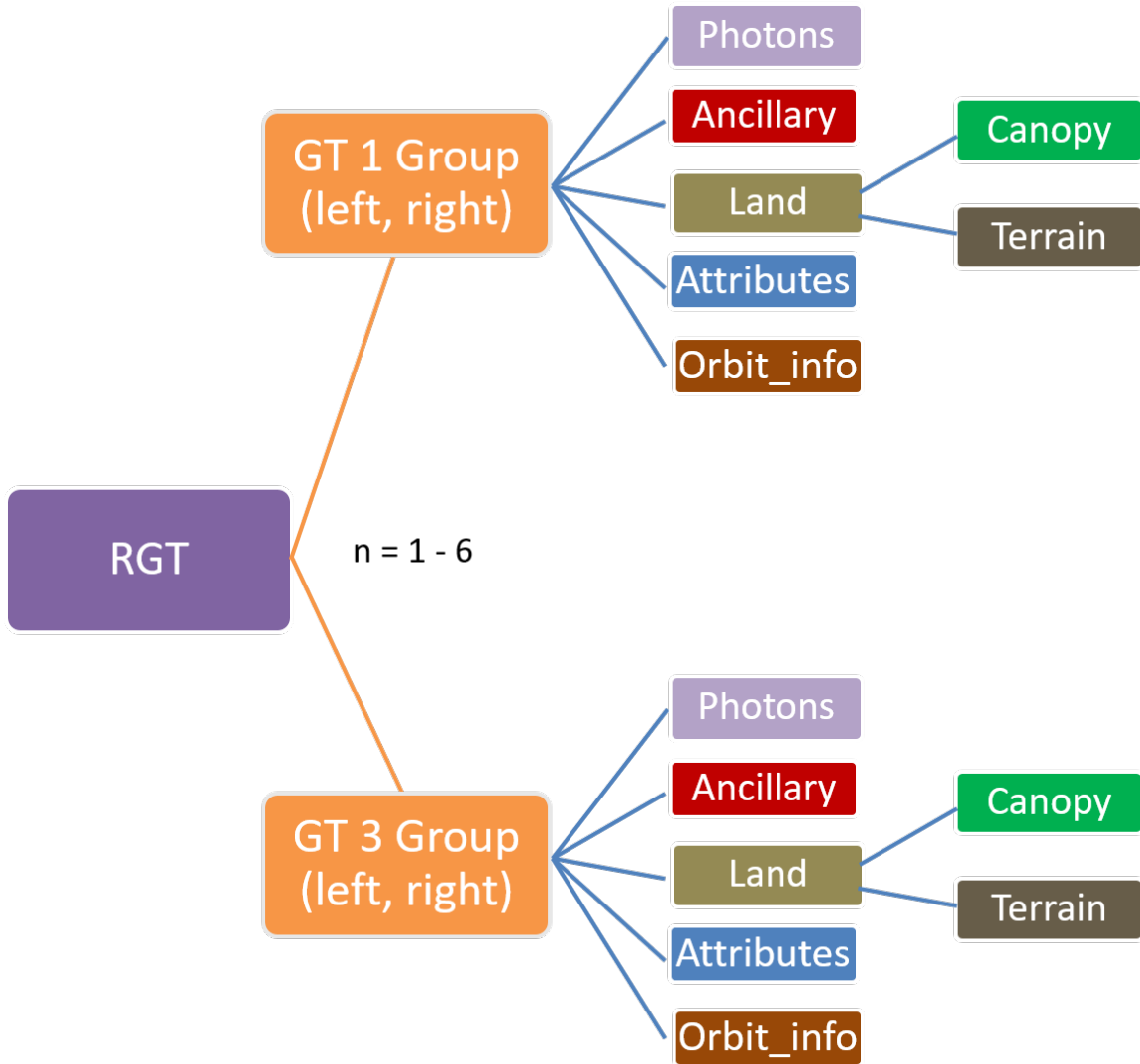
### 935 **1.8 Sparse Canopy Cases**

936 Conversely, sparse canopy cases also pose a challenge to vegetation height  
937 retrievals. In these cases, expected reflected photon events from sparse trees or  
938 shrubs may be difficult to discriminate between solar background noise photons. The  
939 algorithms being developed for ATL08 operate under the assumption that signal  
940 photons are close together and noise photons will be more isolated in nature. Thus,  
941 signal (in this case canopy) photons may be incorrectly identified as solar background  
942 noise on the data product. Due to the nature of the photon counting processing,  
943 canopy photons identified in areas that have extremely low canopy cover <15% will  
944 be filtered out and reassigned as noise photons.

945

## 946 **2. ATL08: DATA PRODUCT**

947           The ATL08 product will provide estimates of terrain height, canopy height,  
948 and canopy cover at fine spatial scales in the along-track direction. In accordance with  
949 the HDF-driven structure of the ICESat-2 products, the ATL08 product will  
950 characterize each of the six Ground Tracks (GT) associated with each Reference  
951 Ground Track (RGT) for each cycle and orbit number. Each ground track group has a  
952 distinct beam number, distance from the reference track, and transmit energy  
953 strength, and all beams will be processed independently using the same sequence of  
954 steps described within ATL08. Each ground track group (GT) on the ATL08 product  
955 contains subgroups for land and canopy heights segments as well as beam and  
956 reference parameters useful in the ATL08 processing. In addition, the labeled photons  
957 that are used to determine the data parameters will be indexed back to the ATL03  
958 products such that they are available for further, independent analysis. A layout of  
959 the ATL08 HDF product is shown in Figure 2.1. The six GTs are numbered from left to  
960 right, regardless of satellite orientation.



961

962 Figure 2.1. HDF5 data structure for ATL08 products

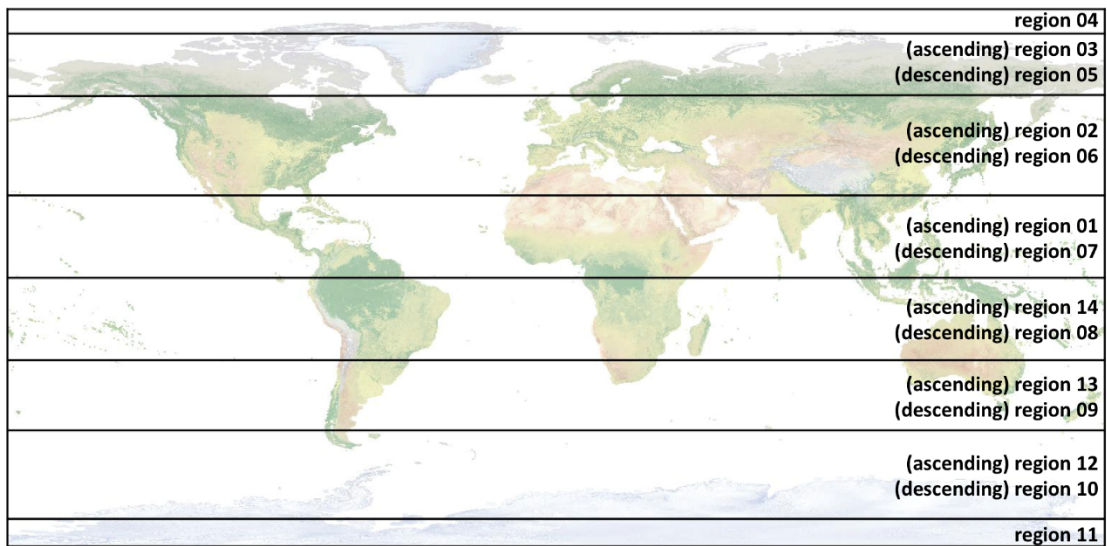
963

964 For each data parameter, terrain surface elevation and canopy heights will be  
 965 provided at a fixed segment size of 100 meters along the ground track. Based on the  
 966 satellite velocity and the expected number of reflected photons for land surfaces, each  
 967 segment should have more than 100 signal photons, but in some instances there may  
 968 be less than 100 signal photons per segment. If a segment has less than 50 classed  
 969 (i.e., labeled by ATL08 as ground, canopy, or top of canopy) photons we feel this  
 970 would not accurately represent the surface. Thus, an invalid value will be reported in



971 all height fields. In the event that there are more than 50 classed photons, but a terrain  
 972 height cannot be determined due to an insufficient number of ground photons, (e.g.  
 973 lack of photons penetrating through dense canopy), the only reported terrain height  
 974 will be the interpolated surface height.

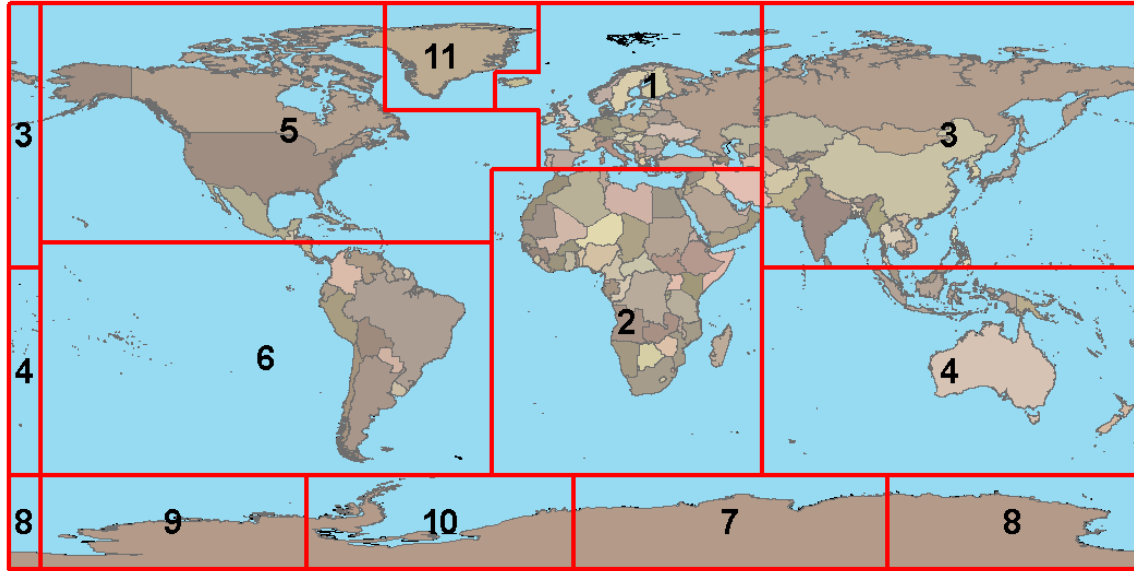
975 The ATL08 product will be produced per granule based on the ATL03 defined  
 976 regions (see Figure 2.2). Thus, the ATL08 file/name convention scheme will match  
 977 the file/naming convention for ATL03 –in attempt for reducing complexity to allow  
 978 users to examine both data products.



979

980 Figure 2.2. ATL03 granule regions; graphic from ATL03 ATBD (Neumann et al.).

981 The ATL08 product additionally has its own internal regions, which are  
 982 roughly assigned by continent, as shown by Figure 2.3. For the regions covering  
 983 Antarctica (regions 7, 8, 9, 10) and Greenland (region 11), the ATL08 algorithm will  
 984 assume that no canopy is present. These internal ATL08 regions will be noted in the  
 985 ATL08 product (see parameter atl08\_region in Section 2.4.19). Note that the regions  
 986 for each ICESat-2 product are not the same.



987

988 Figure 2.3. ATL08 product regions.

989

990 **2.1 Subgroup: Land Parameters**

991 ATL08 terrain height parameters are defined in terms of the absolute height  
 992 above the reference ellipsoid.

993 Table 2.1. Summary table of land parameters on ATL08.

Group	Data type	Description	Source
<b>segment_id_beg</b>	Integer	First along-track segment_id number in 100-m segment	ATL03
<b>segment_id_end</b>	Integer	Last along-track segment_id number in 100-m segment	ATL03
<b>h_te_mean</b>	Float	Mean terrain height for segment	computed
<b>h_te_median</b>	Float	Median terrain height for segment	computed
<b>h_te_min</b>	Float	Minimum terrain height for segment	computed
<b>h_te_max</b>	Float	Maximum terrain height for segment	computed
<b>h_te_mode</b>	Float	Mode of terrain height for segment	computed
<b>h_te_skew</b>	Float	Skew of terrain height for segment	computed

<b>n_te_photons</b>	Integer	Number of ground photons in segment	computed
<b>h_te_interp</b>	Float	Interpolated terrain surface height at mid-point of segment	computed
<b>h_te_std</b>	Float	Standard deviation of ground heights about the interpolated ground surface	computed
<b>h_te_uncertainty</b>	Float	Uncertainty of ground height estimates. Includes all known uncertainties such as geolocation, pointing angle, timing, radial orbit errors, etc.	computed from Equation 1.4
<b>terrain_slope</b>	Float	Slope of terrain within segment	computed
<b>h_te_best_fit</b>	Float	Best fit terrain elevation at the 100 m segment mid-point location	computed
<b>subset_te_flag</b>	Integer	Quality flag indicating the terrain photons populating the 100 m segment statistics are derived from less than 100 m worth of photons	computed

994

995 **2.1.1 Georeferenced\_segment\_number\_beg**

996 (parameter = segment\_id\_beg). The first along-track segment\_id in each 100-m  
997 segment. Each 100-m segment consists of five sequential 20-m segments provided  
998 from the ATL03 product, which are labeled as segment\_id. The segment\_id is a seven  
999 digit number that uniquely identifies each along track segment, and is written at the  
1000 along-track geolocation segment rate (i.e. ~20m along track). The four digit RGT  
1001 number can be combined with the seven digit segment\_id number to uniquely define  
1002 any along-track segment number. Values are sequential, with 0000001 referring to  
1003 the first segment after the equatorial crossing of the ascending node.

1004 **2.1.2 Georeferenced\_segment\_number\_end**

1005 (parameter = segment\_id\_end). The last along-track segment\_id in each 100-m  
1006 segment. Each 100-m segment consists of five sequential 20-m segments provided  
1007 from the ATL03 product, which are labeled as segment\_id. The segment\_id is a seven  
1008 digit number that uniquely identifies each along track segment, and is written at the

1009 along-track geolocation segment rate (i.e. ~20m along track). The four digit RGT  
1010 number can be combined with the seven digit segment\_id number to uniquely define  
1011 any along-track segment number. Values are sequential, with 0000001 referring to  
1012 the first segment after the equatorial crossing of the ascending node.

### 1013 **2.1.3 Segment\_terrain\_height\_mean**

1014 (parameter = h\_te\_mean). Estimated mean of the terrain height above the  
1015 reference ellipsoid derived from classified ground photons within the 100 m segment.  
1016 If a terrain height cannot be directly determined within the segment (i.e. there are not  
1017 a sufficient number of ground photons), only the interpolated terrain height will be  
1018 reported. Required input data is classified point cloud (i.e. photons labeled as either  
1019 canopy or ground in the ATL08 processing). This parameter will be derived from only  
1020 classified ground photons.

### 1021 **2.1.4 Segment\_terrain\_height\_med**

1022 (parameter = h\_te\_median). Median terrain height above the reference  
1023 ellipsoid derived from the classified ground photons within the 100 m segment. If  
1024 there are not a sufficient number of ground photons, an invalid value will be reported  
1025 –no interpolation will be done. Required input data is classified point cloud (i.e.  
1026 photons labeled as either canopy or ground in the ATL08 processing). This parameter  
1027 will be derived from only classified ground photons.

### 1028 **2.1.5 Segment\_terrain\_height\_min**

1029 (parameter = h\_te\_min). Minimum terrain height above the reference ellipsoid  
1030 derived from the classified ground photons within the 100 m segment. If there are  
1031 not a sufficient number of ground photons, an invalid value will be reported –no  
1032 interpolation will be done. Required input data is classified point cloud (i.e. photons  
1033 labeled as either canopy or ground in the ATL08 processing). This parameter will be  
1034 derived from only classified ground photons.

1035 **2.1.6** Segment\_terrain\_height\_max

1036 (parameter = h\_te\_max). Maximum terrain height above the reference  
1037 ellipsoid derived from the classified ground photons within the 100 m segment. If  
1038 there are not a sufficient number of ground photons, an invalid value will be reported  
1039 –no interpolation will be done. Required input data is classified point cloud (i.e.  
1040 photons labeled as either canopy or ground in the ATL08 processing). This parameter  
1041 will be derived from only classified ground photons.

1042 **2.1.7** Segment\_terrain\_height\_mode

1043 (parameter = h\_te\_mode). Mode of the classified ground photon heights above  
1044 the reference ellipsoid within the 100 m segment. If there are not a sufficient number  
1045 of ground photons, an invalid value will be reported –no interpolation will be done.  
1046 Required input data is classified point cloud (i.e. photons labeled as either canopy or  
1047 ground in the ATL08 processing). This parameter will be derived from only classified  
1048 ground photons.

1049 **2.1.8** Segment\_terrain\_height\_skew

1050 (parameter = h\_te\_skew). The skew of the classified ground photons within the  
1051 100 m segment. If there are not a sufficient number of ground photons, an invalid  
1052 value will be reported –no interpolation will be done. Required input data is classified  
1053 point cloud (i.e. photons labeled as either canopy or ground in the ATL08 processing).  
1054 This parameter will be derived from only classified ground photons.

1055 **2.1.9** Segment\_number\_terrain\_photons

1056 (parameter = n\_te\_photons). Number of terrain photons identified in segment.

1057 **2.1.10** Segment\_height\_interp

1058 (parameter = h\_te\_interp). Interpolated terrain surface height above the  
1059 reference ellipsoid from ATL08 processing at the mid-point of each segment. This  
1060 interpolated surface is the FINALGROUND estimate (described in section 4.9).

1061 **2.1.11 Segment h\_te\_std**

1062 (parameter = h\_te\_std). Standard deviations of terrain points about the  
1063 interpolated ground surface within the segment. Provides an indication of surface  
1064 roughness.

1065 **2.1.12 Segment\_terrain\_height\_uncertainty**

1066 (parameter = h\_te\_uncertainty). Uncertainty of the mean terrain height for the  
1067 segment. This uncertainty incorporates all systematic uncertainties (e.g. timing,  
1068 orbits, geolocation, etc.) as well as uncertainty from errors of identified photons. This  
1069 parameter is described in Section 1, Equation 1.4. If there are not a sufficient number  
1070 of ground photons, an invalid value will be reported –no interpolation will be done.  
1071 Required input data is classified point cloud (i.e. photons labeled as either canopy or  
1072 ground in the ATL08 processing). This parameter will be derived from only classified  
1073 ground photons. The  $\sigma_{segmentclass}$  term in Equation 1.4 represents the standard  
1074 deviation of the terrain height residuals about the FINALGROUND estimate.

1075 **2.1.13 Segment\_terrain\_slope**

1076 (parameter = terrain\_slope). Slope of terrain within each segment. Slope is  
1077 computed from a linear fit of the terrain photons. It estimates the rise [m] in relief  
1078 over each segment [100 m]; e.g., if the slope value is 0.04, there is a 4 m rise over the  
1079 100 m segment. Required input data are the classified terrain photons.

1080 **2.1.14 Segment\_terrain\_height\_best\_fit**

1081 (parameter = h\_te\_best\_fit). The best fit terrain elevation at the mid-point  
1082 location of each 100 m segment. The mid-segment terrain elevation is determined by  
1083 selecting the best of three fits – linear, 3<sup>rd</sup> order and 4<sup>th</sup> order polynomials – to the  
1084 terrain photons and interpolating the elevation at the mid-point location of the 100  
1085 m segment. For the linear fit, a slope correction and weighting is applied to each  
1086 ground photon based on the distance to the slope height at the center of the segment.

1087 **2.1.15 Subset\_te\_flag {1:5}**

1088 (parameter = subset\_te\_flag). This flag indicates the quality distribution of  
1089 identified terrain photons within each 100 m on a gesegment basis. The purpose of  
1090 this flag is to provide the user with an indication whether the photons contributing to  
1091 the terrain estimate are evenly distributed or only partially distributed (i.e. due to  
1092 cloud cover or signal attenuation). A 100 m ATL08 segment is comprised of 5 geo-  
1093 segments and we are populating a flag for each geosegment. subset\_te\_flags:

1094 -1: no data within geosegment available for analysis

1095 0: indicates no ground photons within geosegment

1096 1: indicates ground photons within geosegment

1097 For example, an 100 m ATL08 segment might have the following  
1098 subset\_te\_flags: {-1 -1 0 1 1} which would translate that no signal photons (canopy or  
1099 ground) were available for processing in the first two geosegments. Geosegment 3  
1100 was found to have photons, but none were labeled as ground photons. Geosegment 4  
1101 and 5 had valid labeled ground photons. Again, the motivation behind this flag is to  
1102 inform the user that, in this example, the 100 m estimate are being derived from only  
1103 40 m worth of data.

1104

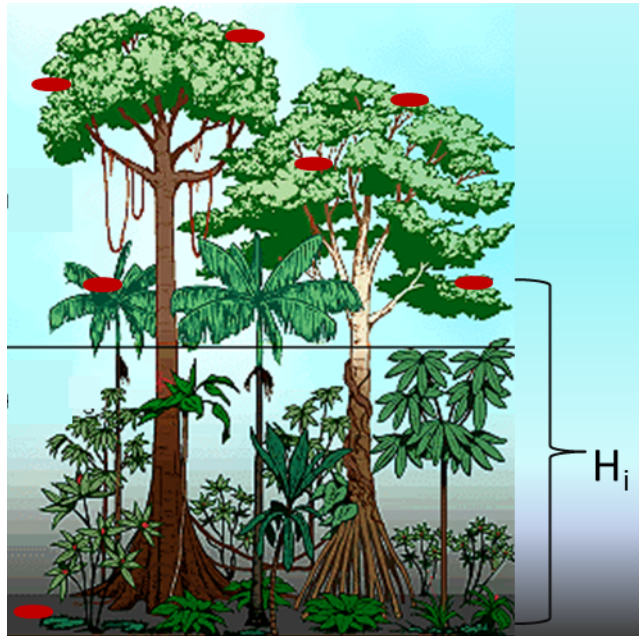
## 1105 **2.2 Subgroup: Vegetation Parameters**

1106 Canopy parameters will be reported on the ATL08 data product in terms of both  
1107 the absolute height above the reference ellipsoid as well as the relative height above  
1108 an estimated ground. The relative canopy height,  $H_i$ , is computed as the height from  
1109 an identified canopy photon minus the interpolated ground surface for the same  
1110 horizontal geolocation (see Figure 2.3). Thus, each identified signal photon above an  
1111 interpolated surface (including a buffer distance based on the instrument point  
1112 spread function) is by default considered a canopy photon. Canopy parameters will



1113 only be computed for segments where more than 5% of the classed photons are  
 1114 classified as canopy photons.

1115



1116

1117 Figure 2.4. Illustration of canopy photons (red dots) interaction in a vegetated area.  
 1118 Relative canopy heights,  $H_i$ , are computed by differencing the canopy photon height from  
 1119 an interpolated terrain surface.

1120 Table 2.2. Summary table of canopy parameters on ATL08.

Group	Data type	Description	Source
<b>segment_id_beg</b>	Integer	First along-track segment_id number in 100-m segment	ATL03
<b>segment_id_end</b>	Integer	Last along-track segment_id number in 100-m segment	ATL03
<b>canopy_h_metrics_abs</b>	Float	Absolute (H##) canopy height metrics calculated at the following percentiles: 25, 50, 60, 70, 75, 80, 85, 90, 95.	computed
<b>canopy_h_metrics</b>	Float	Relative (RH##) canopy height metrics calculated at the following percentiles: 25, 50, 60, 70, 75, 80, 85, 90, 95.	computed
<b>h_canopy_abs</b>	Float	98% height of all the individual absolute canopy heights for segment.	computed



<b>h_canopy</b>	Float	98% height of all the individual relative canopy heights for segment.	computed
<b>h_mean_canopy_abs</b>	Float	Mean of individual absolute canopy heights within segment	computed
<b>h_mean_canopy</b>	Float	Mean of individual relative canopy heights within segment	computed
<b>h_dif_canopy</b>	Float	Difference between h_canopy and canopy_h_metrics(50)	computed
<b>h_min_canopy_abs</b>	Float	Minimum of individual absolute canopy heights within segment	computed
<b>h_min_canopy</b>	Float	Minimum of individual relative canopy heights within segment	computed
<b>h_max_canopy_abs</b>	Float	Maximum of individual absolute canopy heights within segment. Should be equivalent to H100	computed
<b>h_max_canopy</b>	Float	Maximum of individual relative canopy heights within segment. Should be equivalent to RH100	computed
<b>h_canopy_uncertainty</b>	Float	Uncertainty of the relative canopy height (h_canopy)	computed
<b>canopy_openness</b>	Float	STD of relative heights for all photons classified as canopy photons within the segment to provide inference of canopy openness	computed
<b>toc_roughness</b>	Float	STD of relative heights of all photons classified as top of canopy within the segment	computed
<b>h_canopy_quad</b>	Float	Quadratic mean canopy height	computed
<b>n_ca_photons</b>	Integer4	Number of canopy photons within 100 m segment	computed
<b>n_toc_photons</b>	Integer4	Number of top of canopy photons within 100 m segment	computed
<b>centroid_height</b>	Float	Absolute height above reference ellipsoid associated with the centroid of all signal photons	computed
<b>canopy_rh_conf</b>	Integer	Canopy relative height confidence flag based on percentage of ground and canopy photons within a segment: 0 (<5% canopy), 1 (>5% canopy, <5% ground), 2 (>5% canopy, >5% ground)	computed
<b>canopy_flag</b>	Integer	Flag indicating that canopy was detected using the Landsat Tree Cover Continuous Fields data product	computed
<b>landsat_flag</b>	Integer	Flag indicating that Landsat Tree Cover Continuous Fields data product had more than 50% values >100 for L-km segment	computed

<b>landsat_perc</b>	Float	Average percentage value of the valid (value <= 100) Landsat Tree Cover Continuous Fields product for each 100 m segment	
<b>subset_can_flag</b>	Integer	Quality flag indicating the canopy photons populating the 100 m segment statistics are derived from less than 100 m worth of photons	computed

1121

1122 **2.2.1 Georeferenced\_segment\_number\_beg**

1123 (parameter = segment\_id\_beg). The first along-track segment\_id in each 100-m  
 1124 segment. Each 100-m segment consists of five sequential 20-m segments provided  
 1125 from the ATL03 product, which are labeled as segment\_id. The segment\_id is a seven  
 1126 digit number that uniquely identifies each along track segment, and is written at the  
 1127 along-track geolocation segment rate (i.e. ~20m along track). The four digit RGT  
 1128 number can be combined with the seven digit segment\_id number to uniquely define  
 1129 any along-track segment number. Values are sequential, with 0000001 referring to  
 1130 the first segment after the equatorial crossing of the ascending node.

1131 **2.2.2 Georeferenced\_segment\_number\_end**

1132 (parameter = segment\_id\_end). The last along-track segment\_id in each 100-m  
 1133 segment. Each 100-m segment consists of five sequential 20-m segments provided  
 1134 from the ATL03 product, which are labeled as segment\_id. The segment\_id is a seven  
 1135 digit number that uniquely identifies each along track segment, and is written at the  
 1136 along-track geolocation segment rate (i.e. ~20m along track). The four digit RGT  
 1137 number can be combined with the seven digit segment\_id number to uniquely define  
 1138 any along-track segment number. Values are sequential, with 0000001 referring to  
 1139 the first segment after the equatorial crossing of the ascending node.

1140 **2.2.3 Canopy\_height\_metrics\_abs**

1141 (parameter = canopy\_h\_metrics\_abs). The absolute height metrics (H##) of  
 1142 classified canopy photons above the ellipsoid. The height metrics are sorted based on  
 1143 a cumulative distribution and calculated at the following percentiles: 25, 50, 60, 70,

1144 75, 80, 85, 90, 95. These height metrics are often used in the literature to characterize  
1145 vertical structure of vegetation. One important distinction of these canopy height  
1146 metrics compared to those derived from other lidar systems (e.g., LVIS or GEDI) is  
1147 that the ICESat-2 canopy height metrics are heights above the ground surface. These  
1148 metrics do not include the ground photons. Required input data are the absolute  
1149 canopy heights of all canopy photons.

#### 1150 **2.2.4** Canopy\_height\_metrics

1151 (parameter = canopy\_h\_metrics). Relative height metrics above the estimated  
1152 terrain surface (RH##) of classified canopy photons. The height metrics are sorted  
1153 based on a cumulative distribution and calculated at the following percentiles: 25,  
1154 50, 60, 70, 75, 80, 85, 90, 95. These height metrics are often used in the literature to  
1155 characterize vertical structure of vegetation. One important distinction of these  
1156 canopy height metrics compared to those derived from other lidar systems (e.g., LVIS  
1157 or GEDI) is that the ICESat-2 canopy height metrics are heights above the ground  
1158 surface. These metrics do not include the ground photons. Required input data are  
1159 relative canopy heights above the estimated terrain surface for all canopy photons.

#### 1160 **2.2.5** Absolute\_segment\_canopy\_height

1161 (parameter = h\_canopy\_abs). The absolute 98% height of classified canopy  
1162 photon heights above the ellipsoid. The absolute height from classified canopy  
1163 photons are sorted into a cumulative distribution, and the height associated with the  
1164 98% height is reported.

#### 1165 **2.2.6** Segment\_canopy\_height

1166 (parameter = h\_canopy). The relative 98% height of classified canopy photon  
1167 heights above the estimated terrain surface. Relative canopy heights have been  
1168 computed by differencing the canopy photon height from the estimated terrain  
1169 surface in the ATL08 processing. The relative canopy heights are sorted into a  
1170 cumulative distribution, and the height associated with the 98% height is reported.

1171 **2.2.7** Absolute\_segment\_mean\_canopy

1172 (parameter = h\_mean\_canopy\_abs). The absolute mean canopy height for the  
1173 segment. Absolute canopy heights are the photons heights above the reference  
1174 ellipsoid. These heights are averaged.

1175 **2.2.8** Segment\_mean\_canopy

1176 (parameter = h\_mean\_canopy). The mean canopy height for the segment.  
1177 Relative canopy heights have been computed by differencing the canopy photon  
1178 height from the estimated terrain surface in the ATL08 processing. These heights are  
1179 averaged.

1180 **2.2.9** Segment\_dif\_canopy

1181 (parameter = h\_dif\_canopy). Difference between h\_canopy and  
1182 canopy\_h\_metrics(50). This parameter is one metric used to describe the vertical  
1183 distribution of the canopy within the segment.

1184 **2.2.10** Absolute\_segment\_min\_canopy

1185 (parameter = h\_min\_canopy\_abs). The minimum absolute canopy height for  
1186 the segment. Required input data is classified point cloud (i.e. photons labeled as  
1187 either canopy or ground in the ATL08 processing).

1188 **2.2.11** Segment\_min\_canopy

1189 (parameter = h\_min\_canopy). The minimum relative canopy height for the  
1190 segment. Required input data is classified point cloud (i.e. photons labeled as either  
1191 canopy or ground in the ATL08 processing).

1192 **2.2.12** Absolute\_segment\_max\_canopy

1193 (parameter = h\_max\_canopy\_abs). The maximum absolute canopy height for  
1194 the segment. This product is equivalent to H100 metric reported in the literature. This  
1195 parameter, however, has the potential for error as random solar background noise  
1196 may not have been fully rejected. It is recommended that h\_canopy or h\_canopy\_abs

1197 (i.e., the 98% canopy height) be considered as the top of canopy measurement.  
1198 Required input data is classified point cloud (i.e. photons labeled as either canopy or  
1199 ground in the ATL08 processing).

#### 1200 **2.2.13** Segment\_max\_canopy

1201 (parameter = h\_max\_canopy). The maximum relative canopy height for the  
1202 segment. This product is equivalent to RH100 metric reported in the literature. This  
1203 parameter, however, has the potential for error as random solar background noise  
1204 may not have been fully rejected. It is recommended that h\_canopy or h\_canopy\_abs  
1205 (i.e., the 98% canopy height) be considered as the top of canopy measurement.  
1206 Required input data is classified point cloud (i.e. photons labeled as either canopy or  
1207 ground in the ATL08 processing).

#### 1208 **2.2.14** Segment\_canopy\_height\_uncertainty

1209 (parameter = h\_canopy\_uncertainty). Uncertainty of the relative canopy  
1210 height for the segment. This uncertainty incorporates all systematic uncertainties  
1211 (e.g. timing, orbits, geolocation, etc.) as well as uncertainty from errors of identified  
1212 photons. This parameter is described in Section 1, Equation 1.4. If there are not a  
1213 sufficient number of ground photons, an invalid value will be reported -no  
1214 interpolation will be done. In the case for canopy height uncertainty, the parameter  
1215  $\sigma_{segmentclass}$  is comprised of both the terrain uncertainty within the segment but also  
1216 the top of canopy residuals. Required input data is classified point cloud (i.e. photons  
1217 labeled as either top of canopy or ground in the ATL08 processing). This parameter  
1218 will be derived from only classified top of canopy photons. The canopy height  
1219 uncertainty is derived from Equation 1.4, shown below as Equation 1.5, represents  
1220 the standard deviation of the terrain points and the standard deviation of the top of  
1221 canopy height photons.

$$1222 \sigma_{ATL08segment\_ch} = \text{Eqn 1.5}$$

1223

1224 **2.2.15** Segment\_canopy\_openness

1225 (parameter = canopy\_openness). Standard deviation of relative canopy  
1226 heights within each segment. This parameter will potentially provide an indicator of  
1227 canopy openness as a greater standard deviation of heights indicates greater  
1228 penetration of the laser energy into the canopy. Required input data is classified point  
1229 cloud (i.e. photons labeled as either canopy or ground in the ATL08 processing).

1230 **2.2.16** Segment\_top\_of\_canopy\_roughness

1231 (parameter = toc\_roughness). Standard deviation of relative top of canopy  
1232 heights within each segment. This parameter will potentially provide an indicator of  
1233 canopy variability. Required input data is classified point cloud (i.e. photons labeled  
1234 as the top of the canopy in the ATL08 processing).

1235 **2.2.17** Segment\_canopy\_quadratic\_height

1236 (parameter = h\_canopy\_quad). The quadratic mean relative height of classified  
1237 canopy photons. The quadratic mean height is computed as:

1238 
$$qmh = \sqrt{\sum_{i=1}^{n\_ca\_photons} \frac{h_i^2}{n\_ca\_photons}}$$

1239 **2.2.18** Segment\_number\_canopy\_photons

1240 (parameter = n\_ca\_photons). Number of canopy photons within each segment.  
1241 Required input data is classified point cloud (i.e. photons labeled as either canopy or  
1242 ground in the ATL08 processing).

1243 **2.2.19** Segment\_number\_top\_canopy\_photons

1244 (parameter = n\_toc\_photons). Number of top of canopy photons within each  
1245 segment. Required input data is classified point cloud (i.e. photons labeled as top of  
1246 canopy in the ATL08 processing).

1247 **2.2.20** Centroid\_height

1248 (parameter = centroid\_height). Optical centroid of all photons classified as  
1249 either canopy or ground points within a segment. The heights used in this calculation  
1250 are absolute heights above the reference ellipsoid. This parameter is equivalent to the  
1251 centroid height produced on ICESat GLA14.

1252 **2.2.21** Segment\_rel\_canopy\_conf

1253 (parameter = canopy\_rh\_conf). Canopy relative height confidence flag based  
1254 on percentage of ground photons and percentage of canopy photons, relative to the  
1255 total classified (ground and canopy) photons within a segment: 0 (<5% canopy), 1  
1256 (>5% canopy and <5% ground), 2 (>5% canopy and >5% ground). This is a measure  
1257 based on the quantity, not the quality, of the classified photons in each segment.

1258 **2.2.22** Canopy\_flag

1259 (parameter = canopy\_flag). Flag indicating that canopy was detected using the  
1260 Landsat Continuous Cover product for the *L-km* segment. Currently, if more than 3%  
1261 of the Landsat CC pixels along the profile have canopy in them, we make the  
1262 assumption canopy is present along the entire *L-km* segment.

1263 **2.2.23** Landsat\_flag

1264 (parameter = landsat\_flag). Flag indicating that more than 50% of the Landsat  
1265 Tree Cover Continuous Fields product have values >100 (indicating water, cloud,  
1266 shadow, or filled values) for the *L-km* segment. Canopy is assumed present along the  
1267 *L-km* segment if landsat\_flag is 1.

1268 **2.2.24** Landsat\_perc

1269 (parameter = landsat\_perc). Average percentage value of the valid (value <=  
1270 100) Landsat Tree Cover Continuous Fields product pixels that overlap within each  
1271 100 m segment.

1272 **2.2.25 Subset\_can\_flag {1:5}**  
 1273 (parameter = subset\_can\_flag). This flag indicates the distribution of identified  
 1274 canopy photons within each 100 m. The purpose of this flag is to provide the user  
 1275 with an indication whether the photons contributing to the canopy height estimates  
 1276 are evenly distributed or only partially distributed (i.e. due to cloud cover or signal  
 1277 attenuation). A 100 m ATL08 segment is comprised of 5 geo-segments.  
 1278 subset\_can\_flags:

1279 -1: no data within geosegment available for analysis

1280 0: indicates no canopy photons within geosegment

1281 1: indicates canopy photons within geosegment

1282 For example, a 100 m ATL08 segment might have the following  
 1283 subset\_can\_flags: {-1 -1 -1 1 1} which would translate that no photons (canopy or  
 1284 ground) were available for processing in the first three geosegments. Geosegment 4  
 1285 and 5 had valid labeled canopy photons. Again, the motivation behind this flag is to  
 1286 inform the user that, in this example, the 100 m estimate are being derived from only  
 1287 40 m worth of data.

1288

1289

1290 **2.3 Subgroup: Photons**

1291 The subgroup for photons contains the classified photons that were used to  
 1292 generate the parameters within the land or canopy subgroups. Each photon that is  
 1293 identified as being likely signal will be classified as: 0 = noise, 1 = ground, 2 = canopy,  
 1294 or 3 = top of canopy. The index values for each classified photon will be provided such  
 1295 that they can be extracted from the ATL03 data product for independent evaluation.

1296 Table 2.3. Summary table for photon parameters for the ATL08 product.

Group	Data Type	Description	Source
-------	-----------	-------------	--------



<b>classed_PC_indx</b>	Float	Indices of photons tracking back to ATL03 that surface finding software identified and used within the creation of the data products.	ATL03
<b>classed_PC_flag</b>	Integer	Classification flag for each photon as either noise, ground, canopy, or top of canopy.	computed
<b>ph_segment_id</b>	Integer	Georeferenced bin number (20-m) associated with each photon	ATL03
<b>d_flag</b>	Integer	Flag indicating whether DRAGANN labeled the photon as noise or signal	computed

1297

1298 **2.3.1** Indices\_of\_classed\_photons

1299 (parameter = classed\_PC\_indx). Indices of photons tracking back to ATL03 that  
 1300 surface finding software identified and used within the creation of the data products  
 1301 for a given segment.

1302 **2.3.2** Photon\_class

1303 (parameter = classed\_PC\_flag). Classification flags for a given segment. 0 =  
 1304 noise, 1 = ground, 2 = canopy, 3 = top of canopy. The final ground and canopy  
 1305 classification are flags 1-3. The full canopy is the combination of flags 2 and 3.

1306 **2.3.3** Georeferenced\_segment\_number

1307 (parameter = ph\_segment\_id). The segment\_id associated with every photon in  
 1308 each 100-m segment. Each 100-m segment consists of five sequential 20-m segments  
 1309 provided from the ATL03 product, which are labeled as segment\_id. The segment\_id  
 1310 is a seven digit number that uniquely identifies each along track segment, and is  
 1311 written at the along-track geolocation segment rate (i.e. ~20m along track). The four  
 1312 digit RGT number can be combined with the seven digit segment\_id number to  
 1313 uniquely define any along-track segment number. Values are sequential, with

1314 0000001 referring to the first segment after the equatorial crossing of the ascending  
 1315 node.

1316 **2.3.4 DRAGANN\_flag**

1317 (parameter = d\_flag). Flag indicating the labeling of DRAGANN noise filtering for  
 1318 a given photon. 0 = noise, 1=signal.

1319

1320 **2.4 Subgroup: Reference data**

1321 The reference data subgroup contains parameters and information that are  
 1322 useful for determining the terrain and canopy heights that are reported on the  
 1323 product. In addition to position and timing information, these parameters include the  
 1324 reference DEM height, reference landcover type, and flags indicating water or snow.

1325 Table 2.4. Summary table for reference parameters for the ATL08 product.

Group	Data Type	Description	Source
<b>segment_id_beg</b>	Integer	First along-track segment_id number in 100-m segment	ATL03
<b>segment_id_end</b>	Integer	Last along-track segment_id number in 100-m segment	ATL03
<b>latitude</b>	Float	Center latitude of signal photons within each segment	ATL03
<b>longitude</b>	Float	Center longitude of signal photons within each segment	ATL03
<b>delta_time</b>	Float	Mid-segment GPS time in seconds past an epoch. The epoch is provided in the metadata at the file level	ATL03
<b>delta_time_beg</b>	Float	Delta time of the first photon in the segment	ATL03
<b>delta_time_end</b>	Float	Delta time of the last photon in the segment	ATL03
<b>night_flag</b>	Integer	Flag indicating whether the measurements were acquired during night time conditions	computed
<b>dem_h</b>	Float4	Reference DEM elevation	external
<b>dem_flag</b>		Source of reference DEM	external

<b>dem_removal_flag</b>	Integer	Quality check flag to indicate > 20% photons removed due to large distance from dem_h	computed
<b>h_dif_ref</b>	Float4	Difference between h_te_median and dem_h	computed
<b>terrain_flg</b>	Integer	Terrain flag quality check to indicate a deviation from the reference DTM	computed
<b>segment_landcover</b>	Integer4	Reference landcover for segment derived from best global landcover product available	external
<b>segment_watermask</b>	Integer4	Water mask indicating inland water produced from best sources available	external
<b>segment_snowcover</b>	Integer4	Daily snow cover mask derived from best sources	external
<b>urban_flag</b>	Integer	Flag indicating segment is located in an urban area	external
<b>surf_type</b>	Integer1	Flags describing surface types: 0=not type, 1=is type. Order of array is land, ocean, sea ice, land ice, inland water.	ATL03
<b>atl08_region</b>	Integer	ATL08 region(s) encompassed by ATL03 granule being processed	computed
<b>last_seg_extend</b>	Float	The distance (km) that the last ATL08 processing segment in a file is either extended or overlapped with the previous ATL08 processing segment	computed
<b>brightness_flag</b>	Integer	Flag indicating that the ground surface is bright (e.g. snow-covered or other bright surfaces)	computed

1326

#### 1327 **2.4.1** Georeferenced\_segment\_number\_beg

1328 (parameter = segment\_id\_beg). The first along-track segment\_id in each 100-m  
 1329 segment. Each 100-m segment consists of five sequential 20-m segments provided  
 1330 from the ATL03 product, which are labeled as segment\_id. The segment\_id is a seven  
 1331 digit number that uniquely identifies each along track segment, and is written at the

1332 along-track geolocation segment rate (i.e. ~20m along track). The four digit RGT  
1333 number can be combined with the seven digit segment\_id number to uniquely define  
1334 any along-track segment number. Values are sequential, with 0000001 referring to  
1335 the first segment after the equatorial crossing of the ascending node.

#### 1336 **2.4.2** Georeferenced\_segment\_number\_end

1337 (parameter = segment\_id\_end). The last along-track segment\_id in each 100-m  
1338 segment. Each 100-m segment consists of five sequential 20-m segments provided  
1339 from the ATL03 product, which are labeled as segment\_id. The segment\_id is a seven  
1340 digit number that uniquely identifies each along track segment, and is written at the  
1341 along-track geolocation segment rate (i.e. ~20m along track). The four digit RGT  
1342 number can be combined with the seven digit segment\_id number to uniquely define  
1343 any along-track segment number. Values are sequential, with 0000001 referring to  
1344 the first segment after the equatorial crossing of the ascending node.

#### 1345 **2.4.3** Segment\_latitude

1346 (parameter = latitude). Center latitude of signal photons within each segment.  
1347 Each 100 m segment consists of 5 20m ATL03 geosegments. In most cases, there will  
1348 be signal photons in each of the 5 geosegments necessary for calculating a latitude  
1349 value. For instances where the 100 m ATL08 is not fully populated with photons (e.g.  
1350 photons drop out due to clouds or signal attenuation), the latitude will be interpolated  
1351 to the mid-point of the 100 m segment. To implement this interpolation, we confirm  
1352 that each 100 m segment is comprised of at least 3 unique ATL03 geosegments IDs,  
1353 indicating that data is available near the mid-point of the land segment. If less than 3  
1354 ATL03 segments are available, the coordinate is interpolated based on the ratio of  
1355 delta time at the centermost ATL03 segment and that of the centermost photon, thus  
1356 applying the centermost photon's coordinates to represent the land segment with a  
1357 slight adjustment. In some instances, the latitude and longitude will require  
1358 extrapolation to estimate a mid-100 m segment location. It is possible that in these  
1359 extremely rare cases, the latitude and longitude could not represent the true center  
1360 of the 100 m segment. We encourage the user to investigate the parameters

1361 segment\_te\_flag and segment\_can\_flag which provide information as to the number  
1362 and distribution of signal photons within each 100 m segment.

#### 1363 **2.4.4** Segment\_longitude

1364 (parameter = longitude). Center longitude of signal photons within each  
1365 segment. Each 100 m segment consists of 5 20m geosegments. In most cases, there  
1366 will be signal photons in each of the 5 geosegments necessary for calculating a  
1367 longitude value. For instances where the 100 m ATL08 is not fully populated with  
1368 photons (e.g. photons drop out due to clouds or signal attenuation), the latitude will  
1369 be interpolated to the mid-point of the 100 m segment. To implement this  
1370 interpolation, we confirm that each 100 m segment is comprised of at least 3 unique  
1371 ATL03 geosegments IDs, indicating that data is available near the mid-point of the  
1372 land segment. If less than 3 ATL03 segments are available, the coordinate is  
1373 interpolated based on the ratio of delta time at the centermost ATL03 segment and  
1374 that of the centermost photon, thus applying the centermost photon's coordinates to  
1375 represent the land segment with a slight adjustment. In some instances, the latitude  
1376 and longitude will require extrapolation to estimate a mid-100 m segment location. It  
1377 is possible that in these extremely rare cases, the latitude and longitude could not  
1378 represent the true center of the 100 m segment. We encourage the user to investigate  
1379 the parameters segment\_te\_flag and segment\_can\_flag which provide information as to  
1380 the number and distribution of signal photons within each 100 m segment.

#### 1381 **2.4.5** Delta\_time

1382 (parameter = delta\_time). Mid-segment GPS time for the segment in seconds  
1383 past an epoch. The epoch is listed in the metadata at the file level.

#### 1384 **2.4.6** Delta\_time\_beg

1385 (parameter = delta\_time\_beg). Delta time for the first photon in the segment  
1386 in seconds past an epoch. The epoch is listed in the metadata at the file level.

1387 **2.4.7** Delta\_time\_end

1388 (parameter = delta\_time\_end). Delta time for the last photon in the segment  
1389 in seconds past an epoch. The epoch is listed in the metadata at the file level.

1390 **2.4.8** Night\_Flag

1391 (parameter = night\_flag). Flag indicating the data were acquired in night  
1392 conditions: 0 = day, 1 = night. Night flag is set when solar elevation is below 0.0  
1393 degrees.

1394 **2.4.9** Segment\_reference\_DTM

1395 (parameter = dem\_h). Reference terrain height value for segment determined  
1396 by the “best” DEM available based on data location. All heights in ICESat-2 are  
1397 referenced to the WGS 84 ellipsoid unless clearly noted otherwise. DEM is taken from  
1398 a variety of ancillary data sources: GIMP, GMTED, MSS. The DEM source flag indicates  
1399 which source was used.

1400 **2.4.10** Segment\_reference\_DEM\_source

1401 (parameter = dem\_flag). Indicates source of the reference DEM height. Values:  
1402 0=None, 1=GIMP, 2=GMTED, 3=MSS.

1403 **2.4.11** Segment\_reference\_DEM\_removal\_flag

1404 (parameter = dem\_removal\_flag). Quality check flag to indicate > 20%  
1405 classified photons removed from land segment due to large distance from dem\_h.

1406 **2.4.12** Segment\_terrain\_difference

1407 (parameter = h\_dif\_ref). Difference between h\_te\_median and dem\_h. Since the  
1408 mean terrain height is more sensitive to outliers, the median terrain height will be  
1409 evaluated against the reference DEM. This parameter will be used as an internal data  
1410 quality check with the notion being that if the difference exceeds a threshold (TBD) a  
1411 terrain quality flag (terrain\_flg) will be triggered.

1412 **2.4.13 Segment\_terrain flag**

1413 (parameter = terrain\_flg). Terrain flag to indicate confidence in the derived  
1414 terrain height estimate. If h\_dif\_ref exceeds a threshold (TBD) the terrain\_flg  
1415 parameter will be set to 1. Otherwise, it is 0.

1416 **2.4.14 Segment\_landcover**

1417 (parameter = segment\_landcover). Segment landcover will be based on best  
1418 available global landcover product used for reference. One potential source is the 0.5  
1419 km global mosaics of the standard MODIS land cover product (Channan et al, 2015;  
1420 Friedl et al, 2010; available online at <http://glcf.umd.edu/data/lc/index.shtml>). Here,  
1421 17 classes are defined ranging from evergreen (needle and broadleaf forest),  
1422 deciduous (needle and broadleaf forest), shrublands, woodlands, savanna and  
1423 grasslands, agriculture, to urban. The most current year processed for this product is  
1424 based on MODIS measurements from 2012.

1425 **2.4.15 Segment\_watermask**

1426 (parameter = segment\_watermask). Water mask (i.e., flag) indicating inland  
1427 water as referenced from the Global Raster Water Mask at 250 m spatial resolution  
1428 (Carroll et al, 2009; available online at <http://glcf.umd.edu/data/watermask/>). 0 =  
1429 no water; 1 = water.

1430 **2.4.16 Segment\_snowcover**

1431 (parameter = segment\_snowcover). Daily snowcover mask (i.e., flag)  
1432 indicating a likely presence of snow or ice within each segment produced from best  
1433 available source used for reference. The snow mask will be the same snow mask as  
1434 used for ATL09 Atmospheric Products: NOAA snow-ice flag. 0=ice free water;  
1435 1=snow free land; 2=snow; 3=ice.

1436 **2.4.17 Urban\_flag**

1437 (parameter = urban\_flag). The urban flag indicates that a segment is likely  
1438 located over an urban area. In these areas, buildings may be misclassified as canopy,

1439 and thus the canopy products may be incorrect. The urban flag is sourced from the  
1440 “urban and built up” classification on the MODIS land cover product (Channan et al,  
1441 2015; Friedl et al, 2010; available online at  
1442 <http://glcf.umd.edu/data/lc/index.shtml>). 0 = not urban; 1 = urban.

#### 1443 **2.4.18** Surface\_type

1444 (parameter = surf\_type). The surface type for a given segment is determined at  
1445 the major frame rate (every 200 shots, or ~140 meters along-track) and is a two-  
1446 dimensional array surf\_type(n, nsurf), where n is the major frame number, and nsurf  
1447 is the number of possible surface types such that surf\_type(n, isurf) is set to 0 or 1  
1448 indicating if surface type isurf is present (1) or not (0), where isurf = 1 to 5 (land,  
1449 ocean, sea ice, land ice, and inland water) respectively.

#### 1450 **2.4.19** ATL08\_region

1451 (parameter = atl08\_region). The ATL08 regions that encompass the ATL03  
1452 granule being processed through the ATL08 algorithm. The ATL08 regions are shown  
1453 by Figure 2.3. In ATL08 regions 11 (Greenland) and 7 - 10 (Antarctica), the  
1454 canopy\_flag is automatically set to false for ATL08 processing.

#### 1455 **2.4.20** Last\_segment\_extend

1456 (parameter = last\_seg\_extend). The distance (km) that the last ATL08 10 km  
1457 processing segment is either extended beyond 10 km or uses data from the previous  
1458 10 km processing segment to allow for enough data for processing the ATL03 photons  
1459 through the ATL08 algorithm. If the last portion of an ATL03 granule being processed  
1460 would result in a segment with less than 3.4 km (170 geosegments) worth of data,  
1461 that last portion is added to the previous 10 km processing window to be processed  
1462 together as one extended ATL08 processing segment. The resulting last\_seg\_extend  
1463 value would be a positive value of distance beyond 10 km that the ATL08 processing  
1464 segment was extended by. If the last ATL08 processing segment would be less than  
1465 10 km but greater than 3.4 km, a portion extending from the start of current ATL08  
1466 processing segment backwards into the previous ATL08 processing segment would



1467 be added to the current ATL08 processing segment to make it 10 km in length. The  
 1468 distance of this backward data gathering would be reported in last\_seg\_extend as a  
 1469 negative distance value. Only new 100 m ATL08 segment products generated from  
 1470 this backward extension would be reported. All other segments that are not extended  
 1471 will report a last\_seg\_extend value of 0.

1472 **2.4.21 Brightness\_flag**

1473 (parameter = brightness\_flag). Based upon the classification of the photons  
 1474 within each 100 m, this parameter flags ATL08 segments where the mean number of  
 1475 ground photons per shot exceed a value of 3. This calculation can be made as the total  
 1476 number of ground photons divided by the number of ATLAS shots within the 100 m  
 1477 segment. A value of 0 = indicates non-bright surface, value of 1 indicates bright  
 1478 surface, and a value of 2 indicates “undetermined” due to clouds or other factors. The  
 1479 brightness is computed initially on the 10 km processing segment. If the ground  
 1480 surface is determined to be bright for the entire 10 km segment, the brightness is then  
 1481 calculated at the 100 m segment size.

1482

1483 **2.5 Subgroup: Beam data**

1484 The subgroup for beam data contains basic information on the geometry and  
 1485 pointing accuracy for each beam.

1486 Table 2.5. Summary table for beam parameters for the ATL08 product.

Group	Data Type	Units	Description	Source
segment_id_beg	Integer		First along-track segment_id number in 100-m segment	ATL03
segment_id_end	Integer		Last along-track segment_id number in 100-m segment	ATL03
ref_elev	Float		Elevation of the unit pointing vector for the reference photon in the	ATL03

---

		local ENU frame in radians. The angle is measured from East-North plane and positive towards up	
<b>ref_azimuth</b>	Float	Azimuth of the unit pointing vector for the reference photon in the ENU frame in radians. The angle is measured from North and positive toward East.	ATL03
<b>atlas_pa</b>	Float	Off nadir pointing angle of the spacecraft	ATL03
<b>rgt</b>	Integer	The reference ground track (RGT) is the track on the earth at which the vector bisecting laser beams 3 and 4 is pointed during repeat operations	ATL03
<b>sigma_h</b>	Float	Total vertical uncertainty due to PPD and POD	ATL03
<b>sigma_along</b>	Float	Total along-track uncertainty due to PPD and POD knowledge	ATL03
<b>sigma_across</b>	Float	Total cross-track uncertainty due to PPD and POD knowledge	ATL03
<b>sigma_topo</b>	Float	Uncertainty of the geolocation knowledge due to local topography (Equation 1.3)	computed
<b>sigma_atlas_land</b>	Float	Total uncertainty that includes sigma_h plus the geolocation uncertainty due to local slope Equation 1.2	computed
<b>psf_flag</b>	integer	Flag indicating sigma_atlas_land (aka PSF) as computed in Equation 1.2 exceeds a value of 1m.	computed
<b>layer_flag</b>	Integer	Cloud flag indicating presence of clouds or blowing snow	ATL09

---

<b>cloud_flag_atm</b>	Integer	Cloud confidence flag from ATL09 indicating clear skies	ATL09
<b>msw_flag</b>	Integer	Multiple scattering warning product produced on ATL09	ATL09
<b>cloud_fold_flag</b>	integer	Cloud flag to indicate potential of high clouds that have “folded” into the lower range bins	ATL09
<b>asr</b>	Float	Apparent surface reflectance	ATL09
<b>snr</b>	Float	Background signal to noise level	Computed
<b>solar_azimuth</b>	Float	The azimuth (in degrees) of the sun position vector from the reference photon bounce point position in the local ENU frame. The angle is measured from North and is positive towards East.	ATL03g
<b>solar_elevation</b>	Float	The elevation of the sun position vector from the reference photon bounce point position in the local ENU frame. The angle is measured from the East-North plane and is positive Up.	ATL03g
<b>n_seg_ph</b>	Integer	Number of photons within each land segment	computed
<b>ph_ndx_beg</b>	Integer	Photon index begin	computed

1487

### 1488 2.5.1 Georeferenced\_segment\_number\_beg

1489 (parameter = segment\_id\_beg). The first along-track segment\_id in each 100-m  
1490 segment. Each 100-m segment consists of five sequential 20-m segments provided  
1491 from the ATL03 product, which are labeled as segment\_id. The segment\_id is a seven  
1492 digit number that uniquely identifies each along track segment, and is written at the  
1493 along-track geolocation segment rate (i.e. ~20m along track). The four digit RGT

1494 number can be combined with the seven digit segment\_id number to uniquely define  
1495 any along-track segment number. Values are sequential, with 0000001 referring to  
1496 the first segment after the equatorial crossing of the ascending node.

#### 1497 **2.5.2** Georeferenced\_segment\_number\_end

1498 (parameter = segment\_id\_end). The last along-track segment\_id in each 100-m  
1499 segment. Each 100-m segment consists of five sequential 20-m segments provided  
1500 from the ATL03 product, which are labeled as segment\_id. The segment\_id is a seven  
1501 digit number that uniquely identifies each along track segment, and is written at the  
1502 along-track geolocation segment rate (i.e. ~20m along track). The four digit RGT  
1503 number can be combined with the seven digit segment\_id number to uniquely define  
1504 any along-track segment number. Values are sequential, with 0000001 referring to  
1505 the first segment after the equatorial crossing of the ascending node.

#### 1506 **2.5.3** Beam\_coelevation

1507 (parameter = ref\_elev). Elevation of the unit pointing vector for the reference  
1508 photon in the local ENU frame in radians. The angle is measured from East-North  
1509 plane and positive towards up.

#### 1510 **2.5.4** Beam\_azimuth

1511 (parameter = ref\_azimuth). Azimuth of the unit pointing vector for the  
1512 reference photon in the ENU frame in radians. The angle is measured from North and  
1513 positive toward East.

#### 1514 **2.5.5** ATLAS\_Pointing\_Angle

1515 (parameter = atlas\_pa). Off nadir pointing angle (in radians) of the satellite to  
1516 increase spatial sampling in the non-polar regions.

#### 1517 **2.5.6** Reference\_ground\_track

1518 (parameter = rgt). The reference ground track (RGT) is the track on the earth  
1519 at which the vector bisecting laser beams 3 and 4 (or GT2L and GT2R) is pointed

1520 during repeat operations. Each RGT spans the part of an orbit between two ascending  
1521 equator crossings and are numbered sequentially. The ICESat-2 mission has 1387  
1522 RGTs, numbered from 0001xx to 1387xx. The last two digits refer to the cycle number.

### 1523 **2.5.7** Sigma\_h

1524 (parameter = sigma\_h). Total vertical uncertainty due to PPD (Precise Pointing  
1525 Determination), POD (Precise Orbit Determination), and geolocation errors.  
1526 Specifically, this parameter includes radial orbit error,  $\sigma_{orbit}$ , tropospheric errors,  
1527  $\sigma_{Trop}$ , forward scattering errors,  $\sigma_{forwardscattering}$ , instrument timing errors,  $\sigma_{timing}$ ,  
1528 and off-nadir pointing geolocation errors. The component parameters are pulled  
1529 from ATL03 and ATL09. Sigma\_h is the root sum of squares of these terms as detailed  
1530 in Equation 1.1. The sigma\_h reported here is the mean of the sigma\_h values reported  
1531 within the five ATL03 geosegments that are used to create the 100 m ATL08 segment.

### 1532 **2.5.8** Sigma\_along

1533 (parameter = sigma\_along). Total along-track uncertainty due to PPD and POD  
1534 knowledge. This parameter is pulled from ATL03.

### 1535 **2.5.9** Sigma\_across

1536 (parameter = sigma\_across). Total cross-track uncertainty due to PPD and  
1537 POD knowledge. This parameter is pulled from ATL03.

### 1538 **2.5.10** Sigma\_topo

1539 (parameter = sigma\_topo). Uncertainty in the geolocation due to local surface  
1540 slope as described in Equation 1.3. The local slope is multiplied by the 6.5 m  
1541 geolocation uncertainty factor that will be used to determine the geolocation  
1542 uncertainty. The geolocation error will be computed from a 100 m sample due to the  
1543 local slope calculation at that scale.

1544 **2.5.11 Sigma\_ATLAS\_LAND**

1545 (parameter = sigma\_atlas\_land). Total vertical geolocation error due to  
1546 ranging, and local surface slope. The parameter is computed for ATL08 as described  
1547 in Equation 1.2. The geolocation error will be computed from a 100 m sample due to  
1548 the local slope calculation at that scale.

1549 **2.5.12 PSF\_flag**

1550 (parameter = psf\_flag). Flag indicating that the point spread function  
1551 (computed as sigma\_atlas\_land) has exceeded 1m.

1552 **2.5.13 Layer\_flag**

1553 (parameter = layer\_flag). Flag is a combination of multiple ATL09 flags and  
1554 takes daytime/nighttime into consideration. A value of 1 means clouds or blowing  
1555 snow is likely present. A value of 0 indicates the likely absence of clouds or blowing  
1556 snow. If no ATL09 product is available for an ATL08 segment, an invalid value will be  
1557 reported. Since the cloud flags from the ATL09 product are reported at an along-track  
1558 distance of 250 m, we will report the highest value of the ATL09 flags at the ATL08  
1559 resolution (100 m). Thus, if a 100 m ATL08 segment straddles two values from  
1560 ATL09, the highest cloud flag value will be reported on ATL08. This reporting strategy  
1561 holds for all the cloud flags reported on ATL08.

1562 **2.5.14 Cloud\_flag\_atm**

1563 (parameter = cloud\_flag\_atm). Cloud confidence flag from ATL09 that indicates  
1564 the number of cloud or aerosol layers identified in each 25Hz atmospheric profile. If  
1565 the flag is greater than 0, aerosols or clouds could be present.

1566 **2.5.15 MSW**

1567 (parameter = msw\_flag). Multiple scattering warning flag with values from -1 to  
1568 5 as computed in the ATL09 atmospheric processing and delivered on the ATL09 data  
1569 product. If no ATL09 product is available for an ATL08 segment, an invalid value will  
1570 be reported. MSW flags:

1571 -1 = signal to noise ratio too low to determine presence of  
1572 cloud or blowing snow  
1573 0 = no\_scattering  
1574 1 = clouds at > 3 km  
1575 2 = clouds at 1-3 km  
1576 3 = clouds at < 1 km  
1577 4 = blowing snow at < 0.5 optical depth  
1578 5 = blowing snow at >= 0.5 optical depth

1579 **2.5.16 Cloud Fold Flag**

1580 (parameter = cloud\_fold\_flag). Clouds occurring higher than 14 to 15 km in the  
1581 atmosphere will be folded down into the lower portion of the atmospheric profile.

1582 **2.5.17 Computed\_Apparent\_Surface\_Reflectance**

1583 (parameter = asr). Apparent surface reflectance computed in the ATL09  
1584 atmospheric processing and delivered on the ATL09 data product. If no ATL09  
1585 product is available for an ATL08 segment, an invalid value will be reported.

1586 **2.5.18 Signal\_to\_Noise\_Ratio**

1587 (parameter = snr). The Signal to Noise Ratio of geolocated photons as  
1588 determined by the ratio of the superset of ATL03 signal and DRAGANN found signal  
1589 photons used for processing the ATL08 segments to the background photons (i.e.,  
1590 noise) within the same ATL08 segments.

1591 **2.5.19 Solar\_Azimuth**

1592 (parameter = solar\_azimuth). The azimuth (in degrees) of the sun position  
1593 vector from the reference photon bounce point position in the local ENU frame. The  
1594 angle is measured from North and is positive towards East.

1595 **2.5.20** Solar\_Elevation

1596 (parameter = solar\_elevation). The elevation of the sun position vector from  
1597 the reference photon bounce point position in the local ENU frame. The angle is  
1598 measured from the East-North plane and is positive up.

1599 **2.5.21** Number\_of\_segment\_photons

1600 (parameter = n\_seg\_ph). Number of photons in each land segment.

1601 **2.5.22** Photon\_Index\_Begin

1602 (parameter = ph\_ndx\_beg). Index (1-based) within the photon-rate data of  
1603 the first photon within this each land segment.

1604

1605



## 1606 3 ALGORITHM METHODOLOGY

1607 For the ecosystem community, identification of the ground and canopy surface  
1608 is by far the most critical task, as meeting the science objective of determining global  
1609 canopy heights hinges upon the ability to detect both the canopy surface and the  
1610 underlying topography. Since a space-based photon counting laser mapping system  
1611 is a relatively new instrument technology for mapping the Earth's surface, the  
1612 software to accurately identify and extract both the canopy surface and ground  
1613 surface is described here. The methodology adopted for ATL08 establishes a  
1614 framework to potentially accept multiple approaches for capturing both the upper  
1615 and lower surface of signal photons. One method used is an iterative filtering of  
1616 photons in the along-track direction. This method has been found to preserve the  
1617 topography and capture canopy photons, while rejecting noise photons. An advantage  
1618 of this methodology is that it is self-parameterizing, robust, and works in all  
1619 ecosystems if sufficient photons from both the canopy and ground are available. For  
1620 processing purposes, along-track data signal photons are parsed into  $L$ -km segment  
1621 of the orbit which is recommended to be 10 km in length.

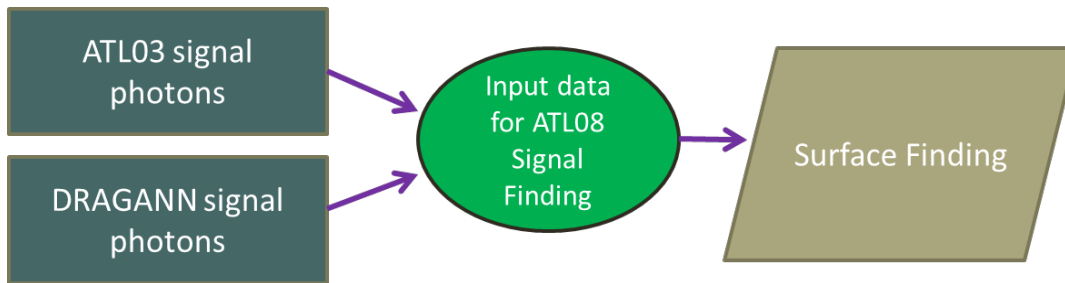
1622

### 1623 3.1 Noise Filtering

1624 Solar background noise is a significant challenge in the analysis of photon  
1625 counting laser data. Range measurement data created from photon counting lidar  
1626 detectors typically contain far higher noise levels than the more common photon  
1627 integrating detectors available commercially in the presence of passive, solar  
1628 background photons. Given the higher detection sensitivity for photon counting  
1629 devices, a background photon has a greater probability of triggering a detection event  
1630 over traditional integral measurements and may sometimes dominate the dataset.  
1631 Solar background noise is a function of the surface reflectance, topography, solar  
1632 elevation, and atmospheric conditions. Prior to running the surface finding  
1633 algorithms used for ATL08 data products, the superset of output from the GSFC  
1634 medium-high confidence classed photons (ATL03 signal\_conf\_ph: flags 3-4) and the

1635 output from DRAGANN will be considered as the input data set. ATL03 input data  
1636 requirements include the latitude, longitude, height, segment delta time, segment ID,  
1637 and a preliminary signal classification for each photon. The motivation behind  
1638 combining the results from two different noise filtering methods is to ensure that all  
1639 of the potential signal photons for land surfaces will be provided as input to the  
1640 surface finding software. The description of the methodology for the ATL03  
1641 classification is described separately in the ATL03 ATBD. The methodology behind  
1642 DRAGANN is described in the following section.

1643



1644

1645 Figure 3.1. Combination of noise filtering algorithms to create a superset of input data for  
1646 surface finding algorithms.

1647

### 1648 **3.1.1 DRAGANN**

1649 The Differential, Regressive, and Gaussian Adaptive Nearest Neighbor  
1650 (DRAGANN) filtering technique was developed to identify and remove noise photons  
1651 from the photon counting data point cloud. DRAGANN utilizes the basic premise that  
1652 signal photons will be closer in space than random noise photons. The first step of the  
1653 filtering is to implement an adaptive nearest neighbor search. By using an adaptive  
1654 method, different thresholds can be applied to account for variable amounts of  
1655 background noise and changing surface reflectance along the data profile. This search  
1656 finds an effective radius by computing the probability of finding P number of points  
1657 within a search area. For MABEL and mATLAS, P=20 points within the search area

1658 was empirically derived but found to be an effective and efficient number of  
1659 neighbors.

1660 There may be cases, however, where the value of P needs to be changed. For  
1661 example, during night acquisitions it is anticipated that the background noise rate will  
1662 be considerably low. Since DRAGANN is searching for two distributions in  
1663 neighborhood searching space, the software could incorrectly identify signal photons  
1664 as noise photons. The parameter P, however, can be determined dynamically from  
1665 estimations of the signal and noise rates from the photon cloud. In cases of low  
1666 background noise (night), P would likely be changed to a value lower than 20.  
1667 Similarly, in cases of high amounts of solar background, P may need to be increased  
1668 to better capture the signal and avoid classifying small, dense clusters of noise as  
1669 signal. In this case, however, it is likely that noise photons near signal photons will  
1670 also be misclassified as signal. The method for dynamically determining a P value is  
1671 explained further in section 4.3.1.

1672 After P is defined, a histogram of the number of neighbors within a search  
1673 radius for each point is generated. The distribution of neighbor radius occurrences is  
1674 analyzed to determine the noise threshold.

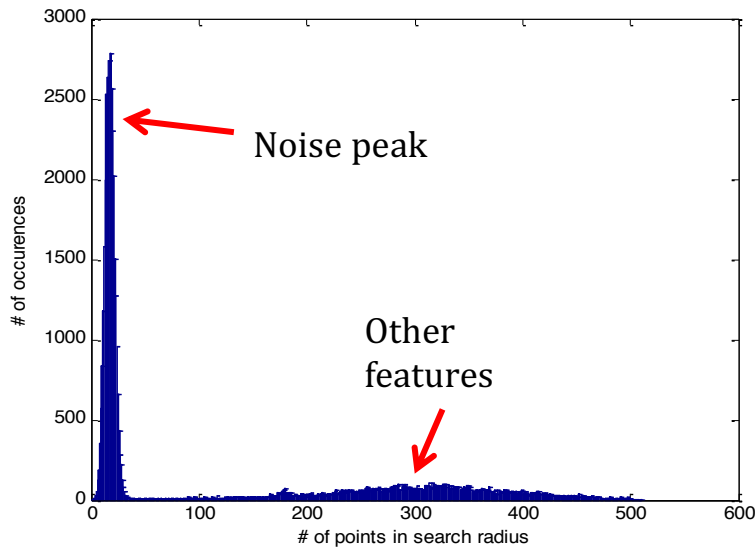
$$1675 \quad \frac{P}{N_{total}} = \frac{V}{V_{total}} \quad \text{Eqn. 3.1}$$

1676  
1677 where  $N_{total}$  is the total number of photons in the point cloud, V is the volume of the  
1678 nearest neighborhood search, and  $V_{total}$  is the bounding volume of the enclosed point  
1679 cloud. For a 2-dimensional data set, V becomes

$$1680 \quad V = \pi r^2 \quad \text{Eqn. 3.2}$$

1681  
1682  
1683 where r is the radius. A good practice is to first normalize the data set along each  
1684 dimension before running the DRAGANN filter. Normalization prevents the algorithm  
1685 from favoring one dimension over the others in the radius search (e.g., when the  
1686 latitude and longitude are in degrees and height is in meters).

1687



1688

1689 Figure 3.2. Histogram of the number of photons within a search radius. This histogram is  
1690 used to determine the threshold for the DRAGANN approach.

1691

1692 Once the radius has been computed, DRAGANN counts the number of points  
1693 within the radius for each point and histograms that set of values. The distribution of  
1694 the number of points, Figure 3.2, reveals two distinct peaks; a noise peak and a signal  
1695 peak. The motivation of DRAGANN is to isolate the signal photons by determining a  
1696 threshold based on the number of photons within the search radius. The noise peak  
1697 is characterized as having a large number of occurrences of photons with just a few  
1698 neighboring photons within the search radius. The signal photons comprise the broad  
1699 second peak. The first step in determining the threshold between the noise and signal  
1700 is to implement Gaussian fitting to the number of photons distribution (i.e., the  
1701 distribution shown in Figure 3.2). The Gaussian function has the form

1702

1703

$$g(x) = ae^{-\frac{(x-b)^2}{2c^2}} \quad \text{Eqn. 3.3}$$

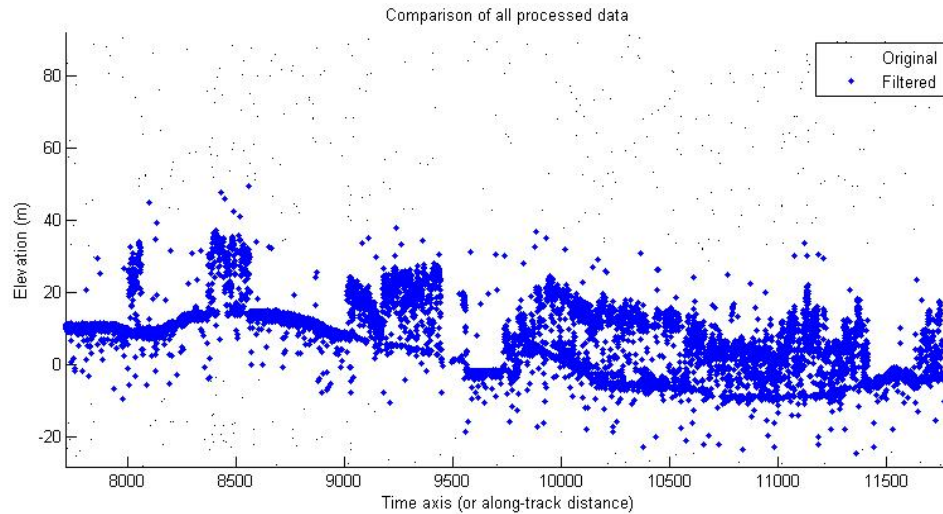
1704

1705 where  $a$  is the amplitude of the peak,  $b$  is the center of the peak, and  $c$  is the standard  
1706 deviation of the curve. A first derivative sign crossing method is one option to identify  
1707 peaks within the distribution.

1708 To determine the noise and signal Gaussians, up to ten Gaussian curves are fit  
1709 to the histogram using an iterative process of fitting and subtracting the max-  
1710 amplitude peak component from the histogram until all peaks have been extracted.  
1711 Then, the potential Gaussians pass through a rejection process to eliminate those with  
1712 poor statistical fits or other apparent errors (Goshtasby and O'Neill, 1994; Chauve et  
1713 al. 2008). A Gaussian with an amplitude less than  $1/5$  of the previous Gaussian and  
1714 within two standard deviations of the previous Gaussian should be rejected. Once the  
1715 errant Gaussians are rejected, the final two remaining are assumed to represent the  
1716 noise and signal. These are separated based on the remaining two Gaussian  
1717 components within the histogram using the logic that the leftmost Gaussian is noise  
1718 (low neighbor counts) and the other is signal (high neighbor counts).

1719 The intersection of these two Gaussians (noise and signal) determines a data  
1720 threshold value. The threshold value is the parameter used to distinguish between  
1721 noise points and signal points when the point cloud is re-evaluated for surface finding.  
1722 In the event that only one curve passes the rejection process, the threshold is set at  
1723  $1 \sigma$  above the center of the noise peak.

1724 An example of the noise filtered product from DRAGANN is shown in Figure  
1725 3.3. The signal photons identified in this process will be combined with the coarse  
1726 signal finding output available on the ATL03 data product.



1727

1728 Figure 3.3. Output from DRAGANN filtering. Signal photons are shown as blue.

1729 Figure 3.3 provides an example of along-track (profiling) height data collected  
 1730 in September 2012 from the MABEL (ICESat-2 simulator) over vegetation in North  
 1731 Carolina. The photons have been filtered such that the signal photons returned from  
 1732 vegetation and the ground surface are remaining. Noise photons that are adjacent to  
 1733 the signal photons are also retained in the input dataset; however, these should be  
 1734 classified as noise photons during the surface finding process. It is possible that some  
 1735 additional outlying noise may be retained during the DRAGANN process when noise  
 1736 photons are densely grouped, and these photons should be filtered out before the  
 1737 surface finding process. Estimates of the ground surface and canopy height can then  
 1738 be derived from the signal photons.

1739

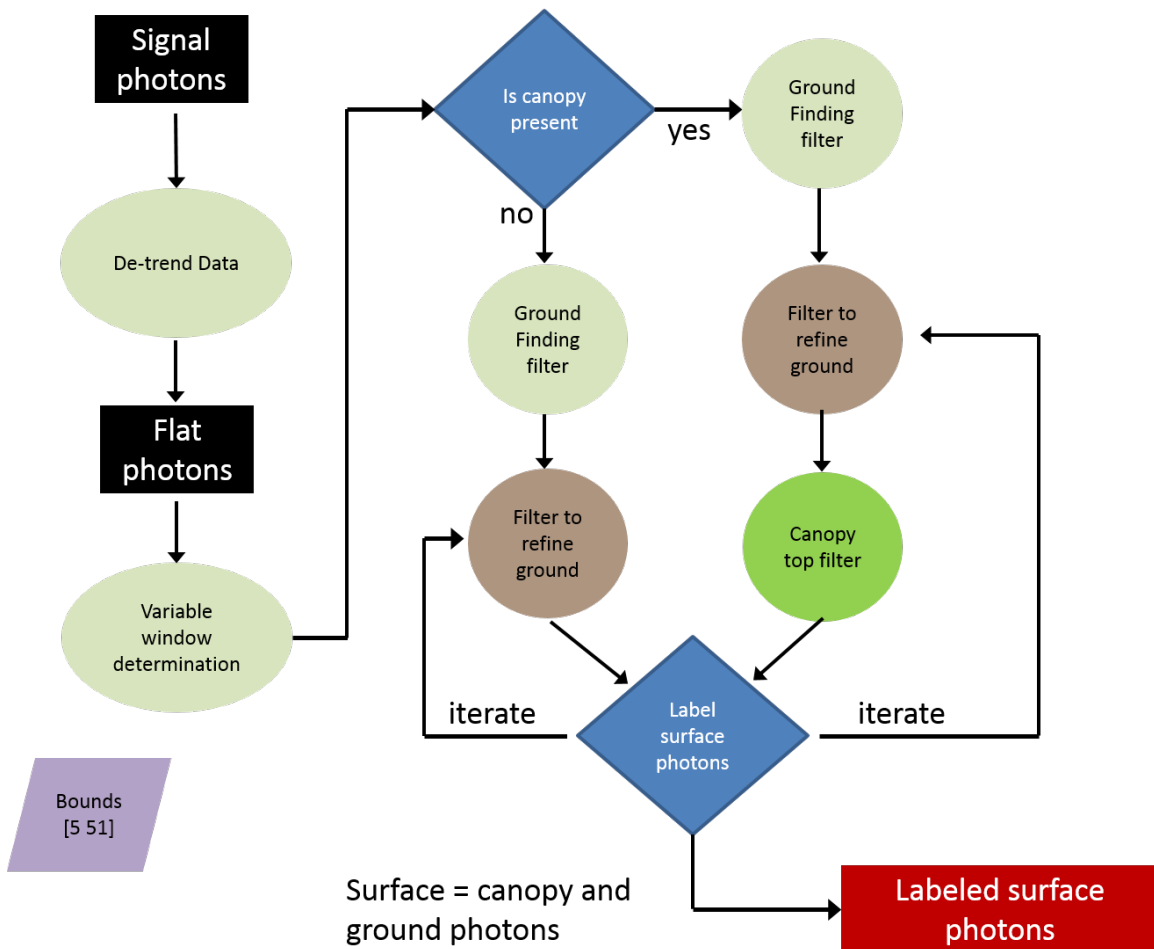
### 1740 **3.2 Surface Finding**

1741 Once the signal photons have been determined, the objective is to find the  
 1742 ground and canopy photons from within the point cloud. With the expectation that  
 1743 one algorithm may not work everywhere for all biomes, we are employing a  
 1744 framework that will allow us to combine the solutions of multiple algorithms into one  
 1745 final composite solution for the ground surface. The composite ground surface  
 1746 solution will then be utilized to classify the individual photons as ground, canopy, top

1747 of canopy, or noise. Currently, the framework described here utilizes one algorithm  
 1748 for finding the ground surface and canopy surface. Additional methods, however,  
 1749 could be integrated into the framework at a later time. Figure 3.4 below describes the  
 1750 framework.

1751

1752



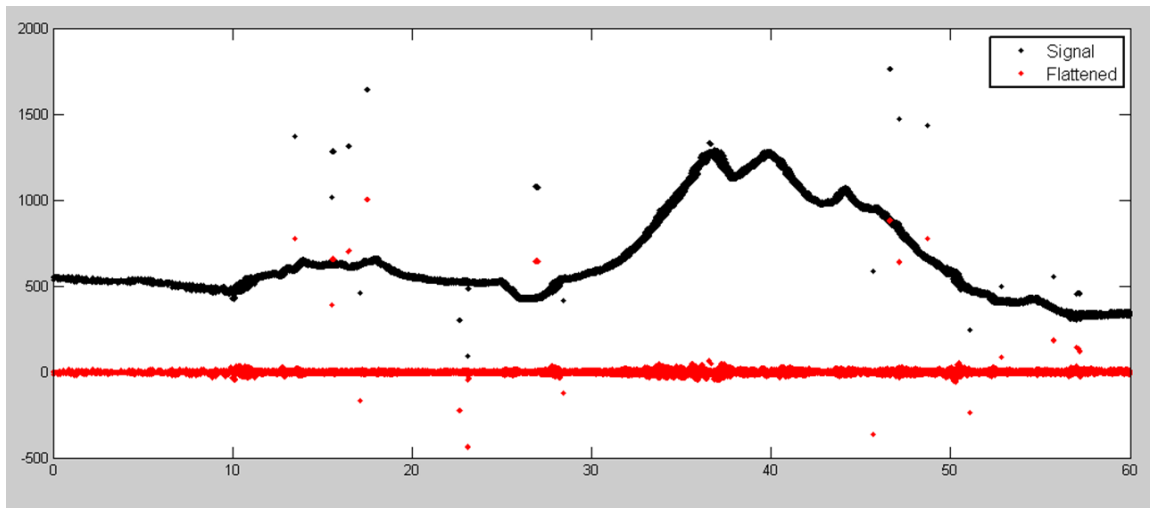
1753

1754 Figure 3.4. Flowchart of overall surface finding method.

1755

### 1756 3.2.1 De-trending the Signal Photons

1757 An important step in the success of the surface finding algorithm is to remove  
1758 the effect of topography on the input data, thus improving the performance of the  
1759 algorithm. This is done by de-trending the input signal photons by subtracting a  
1760 heavily smoothed “surface” that is derived from the input data. Essentially, this is a  
1761 low pass filter of the original data and most of the analysis to detect the canopy and  
1762 ground will subsequently be implemented on the high pass data. The amount of  
1763 smoothing that is implemented in order to derive this first surface is dependent upon  
1764 the relief. For segments where the relief is high, the smoothing window size is  
1765 decreased so topography isn’t over-filtered.



1766

1767 Figure 3.5. Plot of Signal Photons (black) from 2014 MABEL flight over Alaska and  
1768 de-trended photons (red).

1769

### 1770 3.2.2 Canopy Determination

1771 A key factor in the success of the surface finding algorithm is for the software  
1772 to automatically **account for the presence of canopy** along a given  $L$ -km segment.  
1773 Due to the large volume of data, this process has to occur in an automated fashion,  
1774 allowing the correct methodology for extracting the surface to be applied to the data.  
1775 In the absence of canopy, the iterative filtering approach to finding ground works



1776 extremely well, but if canopy does exist, we need to accommodate for that fact when  
1777 we are trying to recover the ground surface.

1778           Currently, the Landsat Tree Cover Continuous Fields dataset from the 2000  
1779 epoch is used to set a canopy flag within the ATL08 algorithm. Each of these Landsat  
1780 Tree Cover tiles contain 30 m pixels indicating the percentage canopy cover for  
1781 vegetation over 5 m high in that pixel area. The 2000 epoch is used over the newer  
1782 2005 epoch due to “striping” in the 2005 tiles, caused by the failure of the scan line  
1783 corrector (SLC) in 2003. The striping artifacts result in inconsistent pixel values  
1784 across a landscape which in turn can result in a tenfold difference in the average  
1785 canopy cover percentage calculated between the epochs for a flight segment. There is  
1786 currently available a 2015 Tree Cover Beta Release that utilizes Landsat 8 data. This  
1787 new release of the 2015 Tree Cover product will replace the 2000 epoch for setting  
1788 the canopy flag in the ATL08 algorithm. The Tree Cover data are available via ftp at  
1789 <http://glcf.umd.edu/data/landsatTreecover/>.

1790           For each  $L$ - $km$  segment of ATLAS data, a comparison is made between the  
1791 midpoint location of the segment and the midpoint locations of the WRS Landsat tiles  
1792 to find the closest tile that encompasses the  $L$ - $km$  segment. Using the closest found  
1793 tile, each signal photon’s X-Y location is used to identify the corresponding Landsat  
1794 pixel. Multiple instances of the same pixels found for the  $L$ - $km$  segment are discarded,  
1795 and the percentage canopy values of the unique pixels determined to be under the  $L$ -  
1796  $km$  segment are averaged to produce an average canopy cover percentage for that  
1797 segment. If the average canopy cover percentage for a segment is over 3% (threshold  
1798 subject to change under further testing), then the ATL08 algorithm will assume the  
1799 presence of canopy and identify both ground and vegetation photons in that  
1800 segment’s output. Else, the ATL08 algorithm uses a simplified calculation to identify  
1801 only ground photons in that segment.

1802           The canopy flag determines if the algorithm will calculate only ground photons  
1803 (canopy flag = 0) or both ground and vegetation photons (canopy flag = 1) for each  $L$ -  
1804  $km$  segment.

1805 For ATL08 product regions over Antarctica (regions 7, 8, 9, 10) and Greenland  
1806 (region 11), the algorithm will assume only ground photons (canopy flag = 0) (see  
1807 Figure 2.2).

1808

### 1809 **3.2.3 Variable Window Determination**

1810 The method for generating a best estimated terrain surface will vary depending  
1811 upon whether canopy is present. *L-km segments* without canopy are much easier to  
1812 analyze because the ground photons are usually continuous. *L-km segments* with  
1813 canopy, however, require more scrutiny as the number of signal photons from ground  
1814 are fewer due to occlusion by the vegetation.

1815 There are some common elements for finding the terrain surface for both cases  
1816 (canopy/no canopy) and with both methods. In both cases, we will use a variable  
1817 windowing span to compute statistics as well as filter and smooth the data. For  
1818 clarification, the window size is variable for each *L-km segment*, but it is constant  
1819 within the *L-km segment*. For the surface finding algorithm, we will employ a  
1820 Savitzky-Golay smoothing/median filtering method. Using this filter, we compute a  
1821 variable smoothing parameter (or window size). It is important to bound the filter  
1822 appropriately as the output from the median filter can lose fidelity if the scan is over-  
1823 filtered.

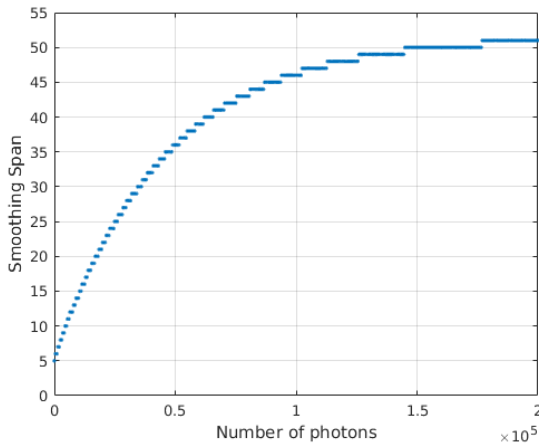
1824 We have developed an empirically-determined shape function, bound between  
1825 [5 51], that sets the window size (*Sspan*) based on the number of photons within each  
1826 *L-km segment*.

$$1827 \quad Sspan = \text{ceil}[5 + 46 * (1 - e^{-a*length})] \quad \text{Eqn. 3.4}$$

$$1828 \quad a = \frac{\log\left(1 - \frac{21}{51-5}\right)}{-28114} \approx 21 \times 10^{-6} \quad \text{Eqn. 3.5}$$

1829 where *a* is the shape parameter and *length* is the total number of photons in the *L-km*  
1830 segment. The shape parameter, *a*, was determined using data collected by MABEL and

1831 is shown in Figure 3.6. It is possible that the model of the shape function, or the  
1832 filtering bounds, will need to be adjusted once ICESat-2/ATLAS is on orbit and  
1833 collecting data.



1834

1835 Figure 3.6. Shape Parameter for variable window size.

1836

### 1837 3.2.4 Compute descriptive statistics

1838 To help characterize the input data and initialize some of the parameters used  
1839 in the algorithm, we employ a moving window to compute descriptive statistics on  
1840 the de-trended data. The moving window's width is the smoothing span function  
1841 computed in Equation 5 and the window slides  $\frac{1}{4}$  of its size to allow of overlap  
1842 between windows. By moving the window with a large overlap helps to ensure that  
1843 the approximate ground location is returned. The statistics computed for each  
1844 window step include:

- 1845 • Mean height
- 1846 • Min height
- 1847 • Max height
- 1848 • Standard deviation of heights
- 1849

1850           Dependent upon the amount of vegetation within each window, the estimated  
 1851 ground height is estimated using different statistics. A standard deviation of the  
 1852 photon elevations computed within each moving window are used to classify the  
 1853 vertical spread of photons as belonging to one of four classes with increasing amounts  
 1854 of variation: open, canopy level 1, canopy level 2, canopy level 3. The canopy indices  
 1855 are defined in Table 3.1.

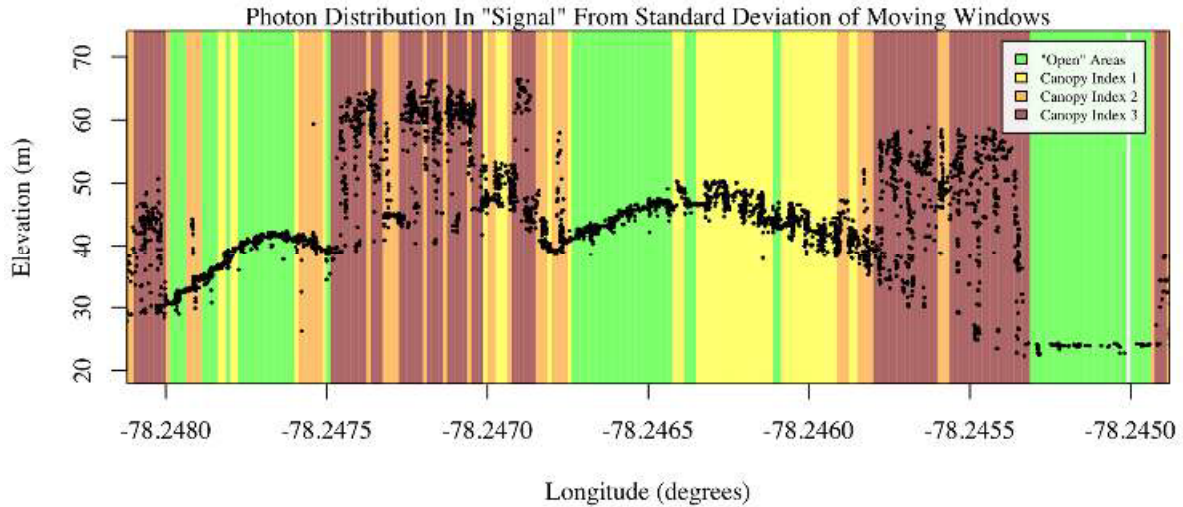
1856

1857 Table 3.1. Standard deviation ranges utilized to qualify the spread of photons within  
 1858 moving window.

Name	Definition	Lower Limit	Upper Limit
Open	Areas with little or no spread in signal photons determined due to low standard deviation	N/A	Photons falling within 1 <sup>st</sup> quartile of Standard deviation
Canopy Level 1	Areas with small spread in signal photons	1 <sup>st</sup> quartile	Median
Canopy Level 2	Areas with a medium amount of spread	Median	3 <sup>rd</sup> quartile
Canopy Level 3	Areas with high amount of spread in signal photons	3 <sup>rd</sup> quartile	N/A

1859

1860



1861

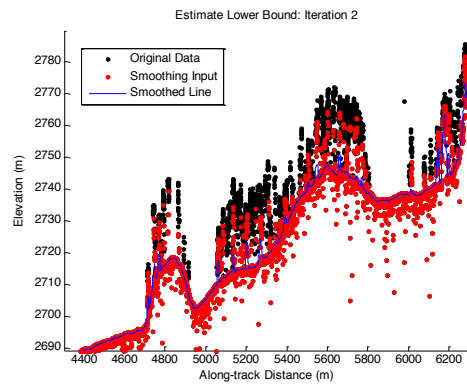
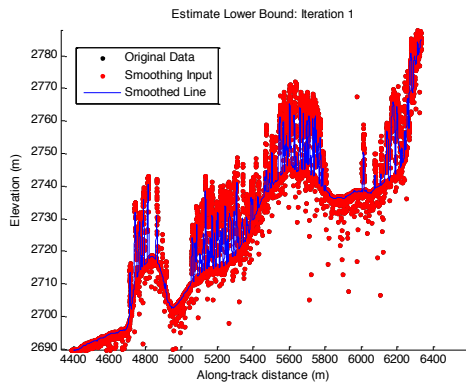
1862 Figure 3.7. Illustration of the standard deviations calculated for each moving window to  
 1863 identify the amount of spread of signal photons within a given window.

1864

### 1865 **3.2.5 Ground Finding Filter (Iterative median filtering)**

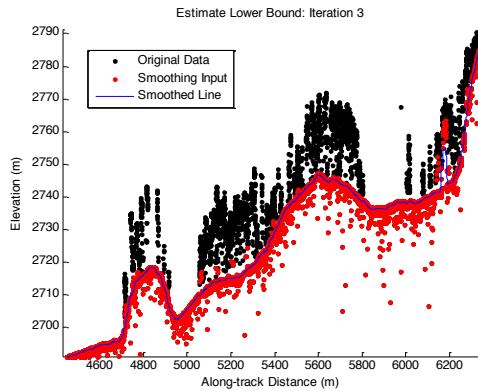
1866 A combination of an iterative median filtering and smoothing filter approach  
 1867 will be employed to derive the output solution of both the ground and canopy  
 1868 surfaces. The input to this process is the set of de-trended photons. Finding the  
 1869 ground in the presence of canopy often poses a challenge because often there are  
 1870 fewer ground photons underneath the canopy. The algorithm adopted here uses an  
 1871 iterative median filtering approach to retain/eliminate photons for ground finding in  
 1872 the presence of canopy. When canopy exists, a smoothed line will lay somewhere  
 1873 between the canopy top and the ground. This fact is used to iteratively label points  
 1874 above the smoothed line as canopy. The process is repeated five times to eliminate  
 1875 canopy points that fall above the estimated surface as well as noise points that fall  
 1876 below the ground surface. An example of iterative median filtering is shown in Figure  
 1877 3.8. The final median filtered line is the preliminary surface estimate. A limitation of  
 1878 this approach, however, is in cases of dense vegetation and few photons reaching the  
 1879 ground surface. In these instances, the output of the median filter may lie within the  
 1880 canopy.

1881



1882

1883



1884

1885 Figure 3.8. Three iterations of the ground finding concept for  $L$ -km segments with canopy.

1886

### 1887 3.3 Top of Canopy Finding Filter

1888 Finding the top of the canopy surface uses the same methodology as finding  
1889 the ground surface, except now the de-trended data are “flipped” over. The “flip”  
1890 occurs by multiplying the photons heights by -1 and adding the mean of all the heights  
1891 back to the data. The same procedure used to find the ground surface can be used to  
1892 find the indices of the top of canopy points.

1893

1894 **3.4 Classifying the Photons**

1895           Once a composite ground surface is determined, photons falling within the  
1896 point spread function of the surface are labeled as ground photons. Based on the  
1897 expected performance of ATLAS, the point spread function should be approximately  
1898 35 cm rms. Signal photons that are not labeled as ground and are below the ground  
1899 surface (buffered with the point spread function) are considered noise, but keep the  
1900 signal label.

1901           The top of canopy photons that are identified can be used to generate an upper  
1902 canopy surface through a shape-preserving surface fitting method. All signal photons  
1903 that are not labeled ground and lie above the ground surface (buffered with the point  
1904 spread function) and below the upper canopy surface are considered to be canopy  
1905 photons (and thus labeled accordingly). Signal photons that lie above the top of  
1906 canopy surface are considered noise, but keep the signal label.

1907

1908	FLAGS,	0 = noise
1909		1 = ground
1910		2 = canopy
1911		3 = TOC (top of canopy)

1912

1913           The final ground and canopy classifications are flags 1 – 3. The full canopy is  
1914 the combination of flags 2 and 3.

1915

1916 **3.5 Refining the Photon Labels**

1917           During the first iteration of the algorithm, it is possible that some photons are  
1918 mislabeled; most likely this would be noise photons mislabeled as canopy. To reject  
1919 these mislabeled photons, we apply three criteria:

- 1920           a) If top of canopy photons are 2 standard deviations above a
- 1921                 smoothed median top of canopy surface
- 1922           b) If there are less than 3 canopy indices within a 15m radius

1937 c) If, for 500 signal photon segments, the number of canopy photons  
1938 is  $< 5\%$  of the total (when  $SNR > 1$ ), or  $< 10\%$  of the total (when  $SNR$   
1939  $\leq 1$ ). This minimum number of canopy indices criterion implies a  
1940 minimum amount of canopy cover within a region.

1941 There are also instances where the ground points will be redefined. This  
1942 reassigning of ground points is based on how the final ground surface is determined.  
1943 Following the “iterate” steps in the flowchart shown in [Figure 3.4](#), if there are no  
1944 canopy indices identified for the  $L$ -km segment, the final ground surface is  
1945 interpolated from the identified ground photons and then will undergo a final round  
1946 of median filtering and smoothing.

1947 If canopy photons are identified, the final ground surface is interpolated based  
1948 upon the level/amount of canopy at that location along the segment. The final ground  
1949 surface is a composite of various intermediate ground surfaces, defined thusly:

**ASmooth** heavily smoothed surface used to de-trend the signal data

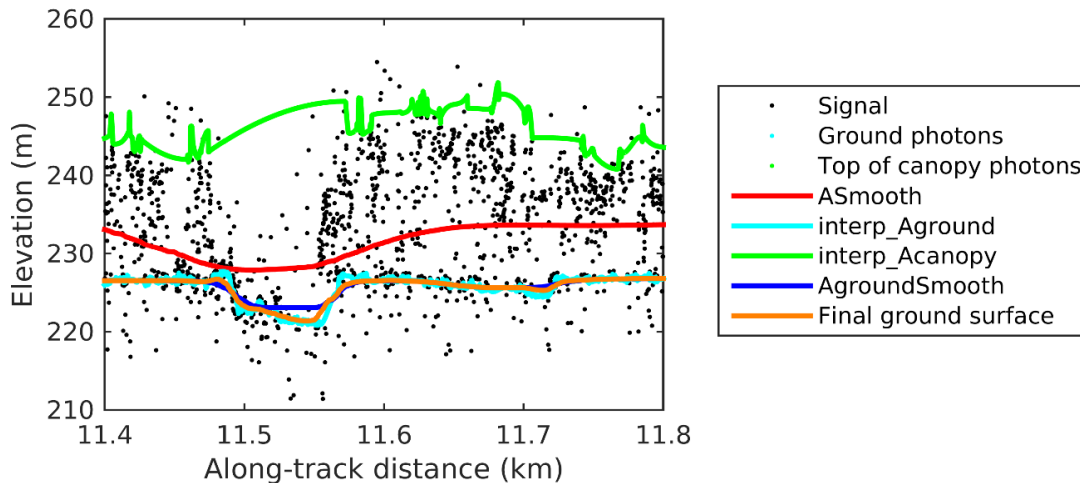
**Interp\_Aground** interpolated ground surface based upon the identified ground photons

**AgroundSmooth** median filtered and smoothed version of Interp\_Aground

1950

Deleted: Figure





1952

1953 Figure 3.9. Example of the intermediate ground and top of canopy surfaces calculated from  
 1954 MABEL flight data over Alaska during July 2014.

1955

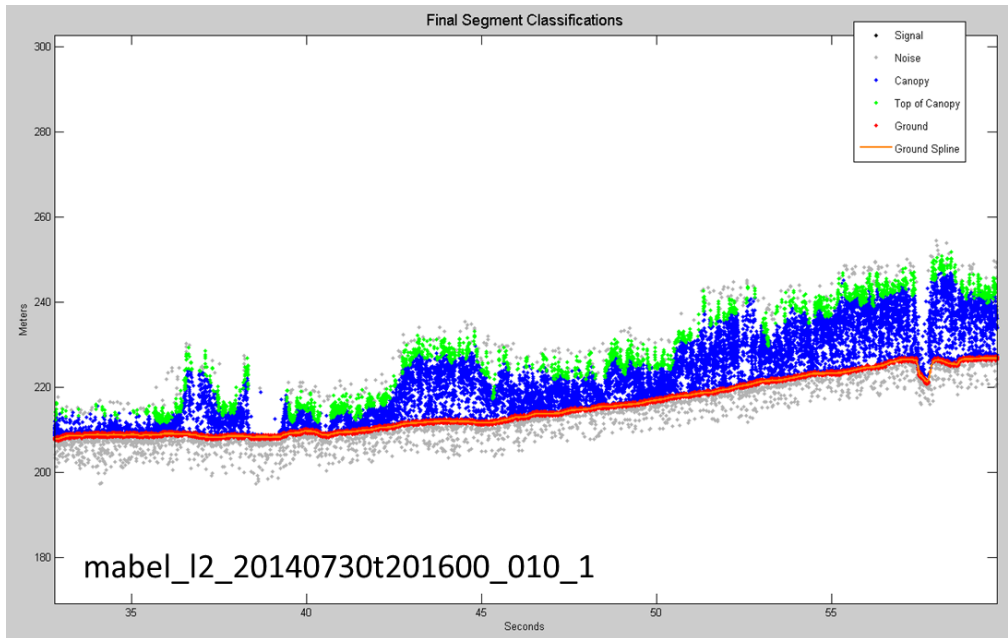
1956 During the first round of ground surface refinement, where there are canopy  
 1957 photons identified in the segment, the ground surface at that location is defined by  
 1958 the smoothed ground surface (AgroundSmooth) value. Else, if there is a location  
 1959 along-track where the standard deviation of the ground-only photons is greater than  
 1960 the 75% quartile for all signal photon standard deviations (i.e., canopy level 3), then  
 1961 the ground surface at that location is a weighted average between the interpolated  
 1962 ground surface (Interp\_Aground\*1/3) and the smoothed interpolated ground surface  
 1963 (AgroundSmooth\*2/3). For all remaining locations long the segment, the ground  
 1964 surface is the average of the interpolated ground surface (Interp\_Aground) and the  
 1965 heavily smoothed surface (ASmooth).

1966 The second round of ground surface refinement is simpler than the first.  
 1967 Where there are canopy photons identified in the segment, the ground surface at that  
 1968 location is defined by the smoothed ground surface (AgroundSmooth) value again.  
 1969 For all other locations, the ground surface is defined by the interpolated ground  
 1970 surface (Interp\_Aground). This composite ground surface is run through the median  
 1971 and smoothing filters again.

1972 The pseudocode for this surface refining process can be found in section 4.11.

1973 Examples of the ground and canopy photons for several MABEL lines are

1974 shown in Figures 3.10 – 3.12.



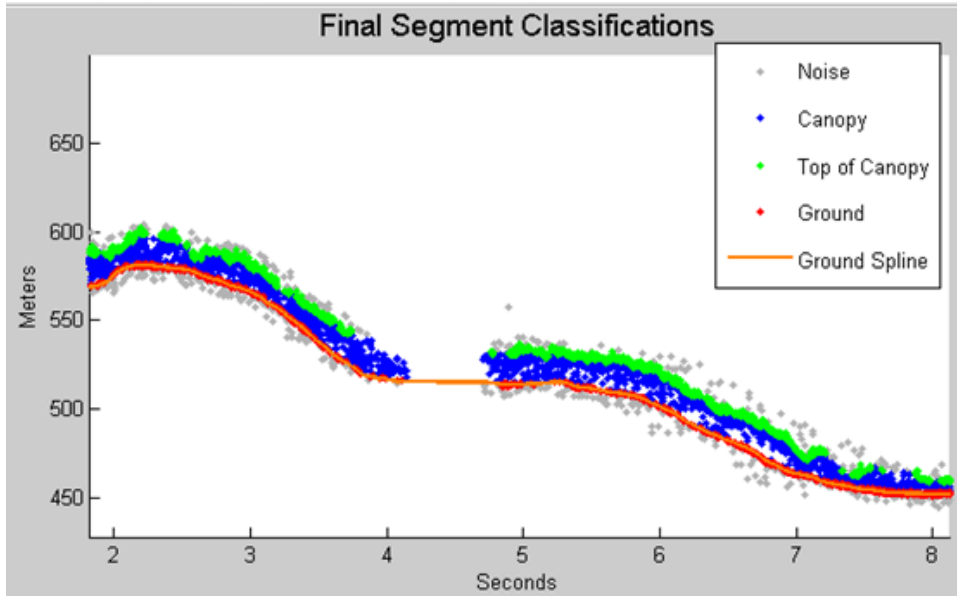
1975

1976 Figure 3.10. Example of classified photons from MABEL data collected in Alaska 2014.

1977 Red photons are photons classified as terrain. Green photons are classified as top of canopy.

1978 Canopy photons (shown as blue) are considered as photons lying between the terrain

1979 surface and top of canopy.



1980

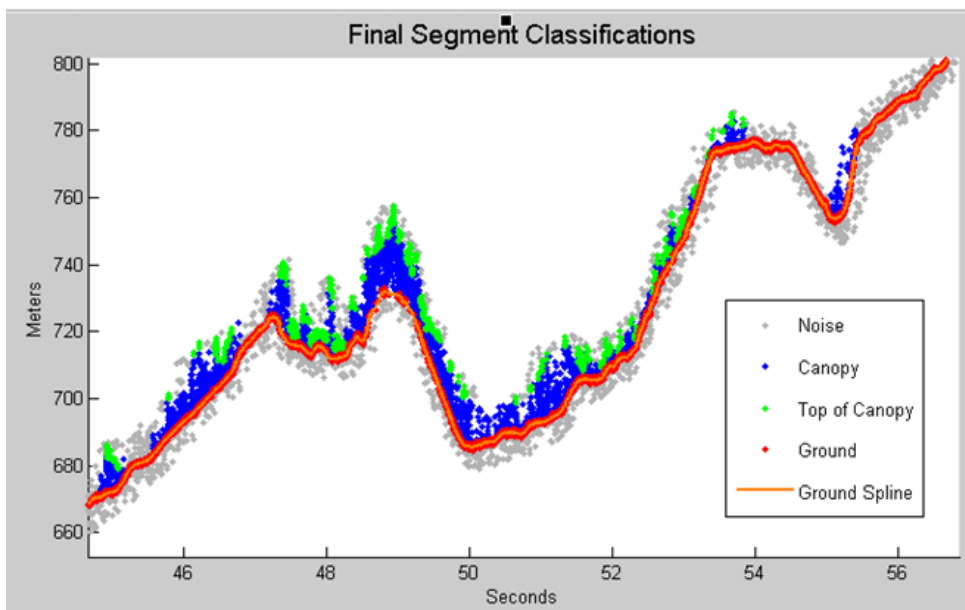
1981 Figure 3.11. Example of classified photons from MABEL data collected in Alaska 2014.

1982 Red photons are photons classified as terrain. Green photons are classified as top of canopy.

1983 Canopy photons (shown as blue) are considered as photons lying between the terrain

1984 surface and top of canopy.

1985



1986

1987 Figure 3.12. Example of classified photons from MABEL data collected in Alaska 2014.

1988 Red photons are photons classified as terrain. Green photons are classified as top of canopy.

1989 Canopy photons (shown as blue) are considered as photons lying between the terrain  
1990 surface and top of canopy.

1991

### 1992 **3.6 Canopy Height Determination**

1993 Once a final ground surface is determined, canopy heights for individual  
1994 photons are computed by removing the ground surface height for that photon's  
1995 latitude/longitude. These relative canopy height values will be used to compute the  
1996 canopy statistics on the ATL08 data product.

1997

### 1998 **3.7 Link Scale for Data products**

1999 The link scale for each segment within which values for vegetation parameters  
2000 will be derived will be defined over a fixed distance of 100 m. A fixed segment length  
2001 ensures that canopy and terrain metrics are consistent between segments, in addition  
2002 to increased ease of use of the final products. A size of 100 m was selected as it should  
2003 provide approximately 140 photons (a statistically sufficient number) from which to  
2004 make the calculations for terrain and canopy height.

2005

2006 **4. ALGORITHM IMPLEMENTATION**

2007 Prior to running the surface finding algorithms used for ATL08 data products, the  
 2008 superset of output from the GSFC medium-high confidence classed photons (ATL03  
 2009 signal\_conf\_ph: flags 3-4) and the output from DRAGANN will be considered as the input  
 2010 data set. ATL03 input data requirements include the along-track time, latitude, longitude,  
 2011 height, and classification for each photon. The motivation behind combining the results  
 2012 from two different noise filtering methods is to ensure that all of the potential signal  
 2013 photons for land surfaces will be provided as input to the surface finding software.

2014 Table 4.1. Input parameters to ATL08 classification algorithm.

Name	Data Type	Long Name	Units	Description	Source
<b>delta_time</b>	DOUBLE	GPS elapsed time	seconds	Elapsed GPS seconds since start of the granule for a given photon. Use the metadata attribute granule_start_seconds to compute full gps time.	ATL03
<b>lat_ph</b>	FLOAT	latitude of photon	degrees	Latitude of each received photon. Computed from the ECEF Cartesian coordinates of the bounce point.	ATL03
<b>lon_ph</b>	FLOAT	longitude of photon	degrees	Longitude of each received photon. Computed from the ECEF Cartesian coordinates of the bounce point.	ATL03
<b>h_ph</b>	FLOAT	height of photon	meters	Height of each received photon, relative to the WGS-84 ellipsoid.	ATL03
<b>sigma_h</b>	FLOAT	height uncertainty	m	Estimated height uncertainty (1-sigma) for the reference photon.	ATL03
<b>signal_conf_ph</b>	UINT_1_LE	photon signal confidence	counts	Confidence level associated with each photon event selected as signal (0-noise, 1- added to allow for buffer but algorithm classifies as background, 2-low, 3-med, 4-high).	ATL03
<b>segment_id</b>	UNIT_32	along-track	unitless	A seven-digit number uniquely identifying each along-track segment. These are sequential, starting with one for the first	ATL03

		segment ID number		segment after an ascending equatorial crossing node.	
<b>cab_prof</b>	FLOAT	Calibrated Attenuated Backscatter	unitless	Calibrated Attenuated Backscatter from 20 to -1 km with vertical resolution of 30m	ATL09
<b>dem_h</b>	FLOAT	DEM Height	meters	Best available DEM (in priority of GIMP/ANTARCTIC/GMTED/MS S) value at the geolocation point. Height is in meters above the WGS84 Ellipsoid.	ATL09
<b>Landsat tree cover</b>	UINT_8	Landsat Tree Cover Continuous Fields	percentage	Percentage of woody vegetation greater than 5 meters in height across a 30 meter pixel	Global Land Cover Facility (Sexton, 2013)

2015

2016 Table 4.2. Additional external parameters referenced in ATL08 product.

Name	Data Type	Long Name	Units	Description	Source
<b>atlas_pa</b>				Off nadir pointing angle of the spacecraft	
<b>ground_track</b>				Ground track, as numbered from left to right: 1 = 1L, 2 = 1R, 3 = 2L, 4 = 2R, 5 = 3L, 6 = 3R	
<b>dem_h</b>				Reference DEM height	ANC06
<b>ref_azimuth</b>	FLOAT	azimuth	radians	Azimuth of the unit pointing vector for the reference photon in the local ENU frame in radians. The angle is measured from north and positive towards east.	ATL03
<b>ref_elev</b>	FLOAT	elevation	radians	Elevation of the unit pointing vector for the reference photon in the local ENU frame in radians. The angle is measured from east-north plane and positive towards up.	ATL03
<b>rgt</b>	INTEGER_2	reference ground track	unitless	The reference ground track (RGT) is the track on the Earth at which a specified unit vector within the	ATL03

				observatory is pointed. Under nominal operating conditions, there will be no data collected along the RGT, as the RGT is spanned by GT2L and GT2R. During slews or off-pointing, it is possible that ground tracks may intersect the RGT. The ICESat-2 mission has 1,387 RGTs.	
<b>sigma_along</b>	DOUBLE	along-track geolocation uncertainty	meters	Estimated Cartesian along-track uncertainty (1-sigma) for the reference photon.	ATL03
<b>sigma_across</b>	DOUBLE	across-track geolocation uncertainty	meters	Estimated Cartesian across-track uncertainty (1-sigma) for the reference photon.	ATL03
<b>surf_type</b>	INTEGER_1	surface type	unitless	Flags describing which surface types this interval is associated with. 0=not type, 1=is type. Order of array is land, ocean, sea ice, land ice, inland water.	ATL03, Section 4
<b>layer_flag</b>	Integer	Consolidated cloud flag	unitless	Flag indicating the presence of clouds or blowing snow with good confidence	ATL09
<b>cloud_flag_asr</b>	Integer(3)	Cloud probability from ASR	unitless	Cloud confidence flag, from 0 to 5, indicating low, med, or high confidence of clear or cloudy sky	ATL09
<b>msw_flag</b>	Byte(3)	Multiple scattering warning flag	unitless	Flag with values from 0 to 5 indicating presence of multiple scattering, which may be due to blowing snow or cloud/aerosol layers.	ATL09
<b>asr</b>	Float(3)	Apparent surface reflectance	unitless	Surface reflectance as modified by atmospheric transmission	ATL09
<b>snow_ice</b>	INTEGER_1	Snow Ice Flag	unitless	NOAA snow-ice flag. 0=ice free water; 1=snow free land; 2=snow; 3=ice	ATL09

2017

#### 2018 **4.1 Cloud based filtering**

2019 It is possible for the presence of clouds to affect the number of surface photon  
2020 returns through signal attenuation, or to cause false positive classifications of  
2021 ground or canopy photons on low cloud returns. Either of these cases would reduce  
2022 the accuracy of the ATL08 product. To improve the performance of the ATL08  
2023 algorithm, ideally all clouds would be identified prior to processing through the  
2024 ATL08 algorithm. There will be instances, however, where low lying clouds (e.g.  
2025 <800 m above the ground surface) may be difficult to identify. Currently, ATL08  
2026 provides an ATL09 derived cloud flag (layer\_flag) on its 100 m product and  
2027 encourages the user to make note of the presence of clouds when using ATL08  
2028 output. Unfortunately at present, a review of on-orbit data from ATL03 and ATL09  
2029 indicate that the cloud layer flag is not being set correctly in the ATL09 algorithm.  
2030 Ultimately, the final cloud based filtering process used in the ATL08 algorithm will  
2031 most likely be derived from parameters/flag on the ATL09 data product. Until the  
2032 ATL09 cloud flags are proven reliable, however, a preliminary cloud screening  
2033 method is presented below. This methodology utilizes the calibrated attenuated  
2034 backscatter on the ATL09 data product to identify (and subsequently remove for  
2035 processing) clouds or other problematic issues (i.e. incorrectly telemetered  
2036 windows). Using this new method, telemetered windows identified as having either  
2037 low or no surface signal due to the presence of clouds (likely above the telemetered  
2038 band), **as well as photon returns suspected to be clouds instead of surface returns,**  
2039 will be omitted from the ATL08 processing. This process, however, will not identify  
2040 the extremely low clouds (i.e. <800 m). The steps are as follows:

- 2041 1. Match up the ATL09 calibrated attenuated backscatter (cab\_prof) columns to  
2042 the ATL03 granule being processed using segment ID.
- 2043 2. **Flip the matching cab\_prof vertical columns so that the elevation bins go**  
2044 **from low to high.**
- 2045 3. For each of the matching ATL09 cab\_prof vertical columns, perform a cubic  
2046 Savitsky-Golay smoothing filter with a span size of 15 vertical bins. Call this  
2047 cab\_smooth.



- 2048 4. Perform the same smoothing filter on each horizontal row of the cab\_smooth  
2049 output, this time using a span size of 7 horizontal bins. Call this  
2050 cab\_smoother.
- 2051 5. Create a low\_signal logical array the length of the number of matching ATL09  
2052 columns and set to false.
- 2053 6. For each column of cab\_smoother:
- 2054 a. Set any values below 0 to 0.
- 2055 b. Set a logical array of cab\_smoother bins that are below 15 km in  
2056 elevation to true. Call this cab15.
- 2057 c. Using the ATL09 dem\_h value for that column, find the ATL09  
2058 cab\_smoother bins that are 240 m above and 240 m below (~8 ATL09  
2059 vertical bins each direction) the dem\_h value. The bins found here that  
2060 are also within cab15 are designated as sfc\_bins.
- 2061 d. Find the maximum peak value of cab\_smoother within the sfc\_bins, if  
2062 any. This will represent the surface peak.
- 2063 e. Find the maximum value of cab\_smoother that is higher in elevation  
2064 than the sfc\_bins and within cab15, if any. This will represent the  
2065 cloud peak.
- 2066 f. If there is no surface peak, set the low\_signal flag to true.
- 2067 g. If there are both surface and cloud peak values returned, determine a  
2068 surface peak / cloud peak ratio. If that ratio is less than or equal to 0.4,  
2069 set low\_signal flag for that column to true.
- 2070 7. After each matching ATL09 column of cab\_smoother has been analyzed for  
2071 low signal, assign the low\_signal flag to an ATL03 photon resolution logical  
2072 array by matching up the ATL03 photon segment\_id values to the ATL09  
2073 range of segment IDs for each ATL09 cab\_prof column.
- 2074 8. For each ATL09 cab\_prof column where the low\_signal flag was not set, check  
2075 for any ATL03 photons greater than 800 meters (TBD) in elevation away  
2076 (higher or lower) from the ATL09 dem\_h value. Assign an ATL03 photon  
2077 resolution too\_far\_signal flag to true when this conditional is met.

2078 9. A logical array mask is created for any ATL03 photons that have either the  
2079 low\_signal flag or the too\_far\_signal flag set to true such that those photons  
2080 will not be further processed by the ATL08 function.

2081

#### 2082 4.2 Preparing ATL03 data for input to ATL08 algorithm

- 2083 1. Break up data into  $L$ -km segments. Segments equivalent of 10 km in along-  
2084 track distance of an orbit would be appropriate.
- 2085 a. If the last portion of an ATL03 granule being processed would result  
2086 in an  $L$ -km segment with less than 3.4 km (170 geosegments) worth of  
2087 data, that last portion is added to the previous  $L$ -km processing  
2088 window to be processed together as one extended  $L$ -km processing  
2089 segment.
    - 2090 i. The resulting **last\_seg\_extend** value would be reported as a  
2091 positive value of distance beyond 10 km that the ATL08  
2092 processing segment was extended by.
  - 2093 b. If the last  $L$ -km segment would be less than 10 km but greater than 3.4  
2094 km, a portion extending from the start of current  $L$ -km processing  
2095 segment backwards into the previous  $L$ -km processing segment would  
2096 be added to the current ATL08 processing segment to make it 10 km  
2097 in length. Only new 100 m ATL08 segment products generated from  
2098 this backward extension would be reported.
    - 2099 i. The distance of this backward data gathering would be  
2100 reported in **last\_seg\_extend** as a negative distance value.
  - 2101 c. All other segments that are not extended will report a last\_seg\_extend  
2102 value of 0.
- 2103 2. Add a buffer of 200 m (or 10 segment\_id's) to both ends of each  $L$ -km  
2104 segment. The total processing segment length is  $(L\text{-km} + 2*\text{buffer})$ , but will  
2105 be referred to as  $L$ -km segments for simplicity.

- 2106           a. The first  $L$ -km segment from an ATL03 granule would only have a  
2107           buffer at the end, and the last  $L$ -km segment from an ATL03 granule  
2108           would only have a buffer at the beginning.
- 2109        3. The input data for ATL08 algorithm is X, Y, Z, T (where T is time).

2110

### 2111   **4.3 Noise filtering via DRAGANN**

2112   DRAGANN will use ATL03 photons with all signal classification flags (0-4). These  
2113   will include both signal and noise photons. This section give a broad overview of the  
2114   DRAGANN function. See Appendix A for more details.

- 2115        1. Determine the relative along-track time, ATT, of each geolocated photon  
2116        from the beginning of each  $L$ -km segment.
- 2117        2. Rescale the ATT with equal-time spacing between each data photon, keeping  
2118        the relative beginning and end time values the same.
- 2119        3. Normalize the height and rescaled ATT data from 0 – 1 for each  $L$ -km  
2120        segment based on the min/max of each field. So,  $\text{normtime} = (\text{time} -$   
2121         $\text{mintime})/(\text{maxtime} - \text{mintime})$ .
- 2122        4. Build a kd-tree based on normalized Z and normalized and rescaled ATT.
- 2123        5. Determine the search radius starting with Equation 3.1.  $P$ =[determined by  
2124        preprocessor; see Sec 4.3.1], and  $V_{\text{total}} = 1$ .  $N_{\text{total}}$  is the number of photons  
2125        within the data  $L$ -km segment. Solve for  $V$ .
- 2126        6. Now that you know  $V$ , determine the radius using Equation 3.2.
- 2127        7. Compute the number of neighbors for each photon using this search radius.
- 2128        8. Generate a histogram of the neighbor count distribution. As illustrated in  
2129        Figure 3.2, the noise peak is the first peak (usually with the highest  
2130        amplitude).
- 2131        9. Determine the 10 highest peaks of the histogram.
- 2132        10. Fit Gaussians to the 10 highest peaks. For each peak,  
2133        a. Compute the amplitude,  $a$ , which is located at peak position  $b$ .

2134           b. Determine the width,  $c$ , by stepping one bin at a time away from  $b$  and  
2135           finding the last histogram value that is  $> \frac{1}{2}$  the amplitude,  $a$ .  
2136           c. Use the amplitude and width to fit a Gaussian to the peak of the  
2137           histogram, as described in Equation 3.3.  
2138           d. Subtract the Gaussian from the histogram, and move on to calculate  
2139           the next highest peak's Gaussian.  
2140           e. Reject Gaussians that are too near ( $< 2$  standard deviations) and  
2141           amplitude too low ( $< 1/5$  previous amplitude) from the previous  
2142           signal Gaussian.

2143   11. Reject any of the returned Gaussians with imaginary components.

2144   12. Determine if there is a narrow noise Gaussian at the beginning of the  
2145       histogram. These typically occur when there is little noise, such as during  
2146       nighttime passes.

2147       a. Search for the Gaussian with the highest amplitude,  $a$ , in the first 5%  
2148       of the histogram  
2149       b. Check if the highest amplitude is  $\geq 1/10$  of the maximum of all  
2150       Gaussian amplitudes  
2151       c. Check if the width,  $c$ , of the Gaussian with the highest amplitude is  $\leq$   
2152       4 bins  
2153       d. If these three conditions are met, save the  $[a,b,c]$  values as  $[a_0,b_0,c_0]$ .  
2154       e. If the three conditions are not met, search again within the first 10%.  
2155       Repeat the process, incrementing the percentage of histogram  
2156       searched by 5% up to 30%. As soon as the conditions are met, save  
2157       the  $[a_0,b_0,c_0]$  values and break out of the percentage histogram search  
2158       loop.

2159   13. If a narrow noise peak was found, sort the remaining Gaussians from largest  
2160       to smallest area, estimated by  $a*c$ , then append  $[a_0,b_0,c_0]$  to the beginning of  
2161       the sorted  $[a,b,c]$  arrays. If a narrow noise peak was not found, sort all  
2162       Gaussians by largest to smallest area.

- 2163 a. If a narrow noise peak was not found, check in sorted order if one of  
2164 the Gaussians are in the first 10% of the histogram. If so, it becomes  
2165 the first Gaussian.
- 2166 b. Reject any Gaussians that are fully contained within another.
- 2167 c. Reject Gaussians whose centers are within 3 standard deviations of  
2168 another, unless only two Gaussians remain
- 2169 14. If there are two or more Gaussians remaining, they are referred to as  
2170 Gaussian 1 and Gaussian 2, assumed to be the noise and signal Gaussians.
- 2171 15. Determine the threshold value that will define the cutoff between noise and  
2172 signal.
- 2173 a. If the absolute difference of the two Gaussians becomes near zero,  
2174 defined as  $< 1e-8$ , set the first bin index where that occurs, past the  
2175 first Gaussian peak location, as the threshold. This would typically be  
2176 set if the two Gaussians are far away from each other.
- 2177 b. Else, the threshold value is the intersection of the two Gaussians,  
2178 which can be estimated as the first bin index past the first Gaussian  
2179 peak location where there is a minimum absolute difference between  
2180 the two Gaussians.
- 2181 c. If there is only one Gaussian, it is assumed to be the noise Gaussian,  
2182 and the threshold is set to  $b + c$ .
- 2183 16. Label all photons having a neighbor count above the threshold as signal.
- 2184 17. Label all photons having a neighbor count below the threshold as noise.
- 2185 18. Reject noise photons.
- 2186 19. Retain signal photons for feeding into next step of processing.
- 2187 20. Use Logical OR to combine DRAGANN signal photons with ATL03 medium-  
2188 high confidence signal photons (flags 3-4) as ATL08 signal photons.
- 2189 21. Calculate a signal to noise ratio (SNR) for the  $L$ - $km$  segment by dividing the  
2190 number of ATL08 signal photons by the number of noise (i.e., all – signal)  
2191 photons.

#### 2192 **4.3.1 DRAGANN Quality Assurance**

2193 Based upon on-orbit data, there are instances where noise photons are selected as  
2194 signal photons following running through DRAGANN. These instances usually occur  
2195 to telemetered windows with low signal, signal attenuation near the surface due to  
2196 fog, haze (or other atmospheric properties). If any `d_flag` results in the 10 km = 1

- 2197 1. For each 20 m `segment_id` that has a `d_flag = 1`, build a histogram of 5 m  
2198 height bins using the height of only the DRAGANN-flagged photons  
2199 (`d_flag=1`)
- 2200 2. If the number of bins indicates that all `d_flag` photons fall within the same  
2201 vertical 60 m, do nothing and move to the next geosegment.
- 2202 3. If the `d_flag` photons fall outside of 60 m, calculate the median and  
2203 standard deviation of the histogram counts.
- 2204 4. If the maximum value of the histogram counts is greater than the median  
2205 + 3\*standard deviation, a surface peak has been detected based on the  
2206 relative photon density within the 5 meter steps. Else, set all `d_flag = 0`  
2207 for this geosegment.
- 2208 5. Set all `d_flag = 0` from 3 height bins below the detected peak to the bottom  
2209 of the telemetry window.
- 2210 6. Starting with the peak count bin (surface), step upwards bin by bin and  
2211 check if 12 bin counts (60 meters of height bins) above surface are less  
2212 than 0.5 \* histogram median. If so, for all photons above current height in  
2213 loop + 60 meters, set all `d_flag = 0` and exit bin-by-bin loop.
- 2214 7. Starting with one bin above the peak count bin (surface), again step  
2215 upwards bin by bin. For each iteration, calculate the standard deviation of  
2216 the bin counts including only the current bin to the highest height bin and  
2217 call this noise standard deviation. If all remaining vertical height bins  
2218 from current bin to highest height bin are less than 2\* histogram  
2219 standard deviation, or if the noise standard deviation is less than 1.0, or if  
2220 this bin and the next 2 higher bins each have counts less than the peak bin

2221 count (entire histogram) – 3\*histogram standard deviation, then set all  
2222 d\_flag = 0 for all heights above this level.  
2223 8. For a final check, construct a new histogram, with median and standard  
2224 deviation, using the corrected d\_flag results and only where d\_flag = 1. If  
2225 the histogram median is greater than 0.0 and the standard deviation is  
2226 greater than 0.75\*median, set all d\_flag in this geosegment = 0. This  
2227 indicates results not well constrained about a detectible surface.  
2228

#### 2229 **4.3.2 Preprocessing to dynamically determine a DRAGANN parameter**

2230 While a default value of P=20 was found to work well when testing with MABEL  
2231 flight data, further testing with simulated data showed that P=20 is not sufficient in  
2232 cases of very low or very high noise. Additional testing with real ATL03 data have  
2233 shown the ground signal to be much stronger, and the canopy signal to be much  
2234 weaker, than originally anticipated. Therefore, a preprocessing step for dynamically  
2235 calculating P and running the core DRAGANN function is described in this  
2236 subsection. This assumes *L-km* to be 10 km (with additional *L-km* buffering).

- 2237 1. Define a DRAGANN processing window of 170 segments (~3.4 km),  
2238 and a buffer of 10 segments (~200 m).
- 2239 2. The buffer is applied to both sides of each DRAGANN processing  
2240 window to create buffered DRAGANN processing windows  
2241 (referenced as “buffered window” for the rest of this section) that will  
2242 overlap the DRAGANN processing windows next to them.
- 2243 3. For each buffered window within the *L-km* segment, calculate a  
2244 histogram of points with 1 m elevation bins.
- 2245 4. For each buffered window histogram, calculate the median counts.
- 2246 5. Bins with counts below the buffered window median count value are  
2247 estimated to be noise. Calculate the mean count of noise bins.
- 2248 6. Bins with counts above the buffered window median count value are  
2249 estimated to be signal. Calculate the mean count of signal bins.
- 2250 7. Determine the time elapsed over the buffered window.

- 2251 8. Calculate estimated noise and signal rates for each buffered window  
 2252 by multiplying each window's mean counts of noise bins and signal  
 2253 bins, determined from steps 5 and 6 above, by 1/(elapsed time) to  
 2254 return the rates in terms of points/meter[elevation]/second[across].
- 2255 9. Calculate a noise ratio for each window by dividing the noise rate by  
 2256 the signal rate.
- 2257 10. If, for all the buffered windows in the *L-km* segment, the noise rate is  
 2258 less than 20 and the noise ratio is less than 0.15; OR any noise rate is  
 2259 0; OR any signal rate is greater than 1000: re-calculate steps 3-9  
 2260 using the entire *L-km* segment. Continue with the following steps  
 2261 using results from the one *L-km* window (instead of multiple buffered  
 2262 windows).
- 2263 11. Now, determine the DRAGANN parameter, P, for each buffered  
 2264 window based on the following conditionals:
- 2265 a. If the signal rate is NaN (i.e., an invalid value), set the signal  
 2266 index array to empty and move on to the next buffered  
 2267 window.
- 2268 b. If noise rate < 20 || noise ratio < 0.15:  
 2269 P = signal rate  
 2270 If signal rate is < 5, P = 5; if signal rate > 20, P = 20
- 2271 c. Else P = 20.
- 2272 12. Run DRAGANN on the buffered window points using the calculated P.
- 2273 13. If DRAGANN fails to find a signal (i.e., only one Gaussian found), run  
 2274 DRAGANN again with P = 10.
- 2275 14. If DRAGANN still fails to find a signal, try to determine P a second time  
 2276 using the following conditionals:
- 2277 a. If (noise rate >= 20) ...  
 2278 && (signal rate > 100) ...  
 2279 && (signal rate < 250),  
 2280 P = (signal rate)/2



```

2281         b. Else if signal rate >= 250,
2282             if noise rate >= 250,
2283                 P = (noise rate)*1.1
2284             else,
2285                 P = 250
2286         c. Else, P = mean(noise rate, signal rate)
2287 15. Run DRAGANN on the buffered window points using the newly
2288     calculated P.
2289     a. If still no signal points are found, set a dragannError flag.
2290 16. If signal points were found by DRAGANN, for each buffered window
2291     calculate a signal check by dividing the number of signal points found
2292     via DRAGANN by the number of total points in the buffered window.
2293 17. If dragannError has been set, or there are suspect signal statistics, the
2294     following snippet of pseudocode will check those conditionals and try
2295     to iteratively find a better P value to run DRAGANN with:
2296
2297     try_count = 0
2298
2299     While dragannError ...
2300     || ( (noise rate >= 30) ...
2301         && (signal check > noise ratio) ...
2302         && (noise ratio >= 0.15) ) ...
2303     || (signal check < 0.001):
2304
2305         if P < 3,
2306             break
2307         else,
2308             P = P*0.75
2309         end
2310
2311     if try_count < 2
2312         Clear out signal index results from previous DRAGANN run
2313         Re-run DRAGANN with new P value
2314         Recalculate the signal check
2315     end
2316
2317     if no signal index results are returned
2318         P = P*0.75
2319     end
2320

```

2321                   try\_count = try\_count + 1

2322

2323                   end

2324

2325

18. If no signal photons are found by DRAGANN because only one

2326

Gaussian was found, set the threshold as  $b+c$  (i.e., one standard

2327

deviation away from the Gaussian peak location) for a final DRAGANN

2328

run. Otherwise, set the signal index array to empty and move on to the

2329

next buffered window.

2330

19. Assign the signal values found from DRAGANN for each buffered

2331

window to the original DRAGANN processing window range of points.

2332

20. Combine signal points from each DRAGANN processing window back

2333

into one  $L-km$  array of signal points for further processing.

2334

### 2335 **4.3.3 Iterative DRAGANN processing**

2336

It is possible in processing segments with high noise rates that DRAGANN will

2337

incorrectly identify clusters of noise as signal. One way to reduce these false positive

2338

noise clusters is to run the alternative DRAGANN process (Sec 4.3.1) again with the

2339

input being the signal output photons from the first run through alternative

2340

DRAGANN. Note that this methodology is still being tested, so by default this option

2341

should not be set.

2342

1. If  $SNR < 1$  (TBD) from alternative DRAGANN run, run alternative DRAGANN

2343

process again using the output signal photons from first DRAGANN run as the

2344

input to the second DRAGANN run.

2345

2. Recalculate SNR based on output of second DRAGANN run.

2346

2347 **4.4 Is Canopy Present**

- 2348 1. If  $L$ -km segment is within an ATL08 region encompassing Antarctica (regions  
2349 7, 8, 9, 10) or Greenland (region 11), assume no canopy is present: canopy  
2350 flag = 0. Else:
- 2351 2. Determine the center Latitude/Longitude position for the  $L$ -km segment.
- 2352 3. Determine the corresponding tile from the Landsat continuous cover  
2353 product.
- 2354 4. For each unique XY position in the ATLAS segment, extract the canopy cover  
2355 value from the Landsat CC product
- 2356 5. Compute the average canopy cover value for the  $L$ -km segment (based on the  
2357 Landsat values).
- 2358 6. If canopy cover > 3%, set canopy flag = 1 (assumes canopy is present)
- 2359 7. If canopy cover ≤ 3%, set canopy flag = 0 (assumes no canopy is present)

2360

2361 **4.5 Compute Filtering Window**

- 2362 1. Next step is to run a surface filter with a variable window size (variable in  
2363 that it will change from  $L$ -km segment to  $L$ -km segment). The window-size is  
2364 denoted as Window.
- 2365 2.  $Window = \text{ceil}[5 + 46 * (1 - e^{-a*length})]$ , where  $length$  is the number of  
2366 photons in the segment.
- 2367 3.  $a = \frac{\log\left(1 - \frac{21}{51-5}\right)}{-28114} \approx 21 \times 10^{-6}$ , where  $a$  is the shape parameter for the window  
2368 span.

2369

2370 **4.6 De-trend Data**

- 2371 1. The input data are the signal photons identified by DRAGANN and the ATL03  
2372 classification (signal\_conf\_ph) values of 3-4.
- 2373 2. Generate a rough surface by connecting all unique (time) photons to each  
2374 other. Let's call this surface interp\_A.

- 2375 3. Run a median filter through interp\_A using the window size set by the  
2376 software. Output = Asmooth.  
2377 4. Define a reference DEM limit (ref\_dem\_limit) as 120 m (TBD).  
2378 5. Remove any Asmooth values further than the ref\_dem\_limit threshold from  
2379 the reference DEM, and interpolate the Asmooth surface based on the  
2380 remaining Asmooth values. The interpolation method to use is the shape  
2381 preserving piecewise cubic Hermite interpolating polynomial – hereafter  
2382 labeled as “pchip” (Fritsch & Carlson, 1980).  
2383 6. Compute the approximate relief of the *L-km* segment using the 95<sup>th</sup> - 5<sup>th</sup>  
2384 percentile heights of the signal photons. We are going to filter Asmooth again  
2385 and the smoothing is a function of the relief.  
2386 7. Define the SmoothSize using the conditional statements below. The  
2387 SmoothSize will be used to detrend the data as well as to create an  
2388 interpolated ground surface later.

2389 SmoothSize = 2 \* Window

- 2390 • If relief >= 900, SmoothSize = round(SmoothSize/4)
  - 2391 • If relief >= 400 && <= 900, SmoothSize = round(SmoothSize/3)
  - 2392 • If relief >= 200 && <= 400, SmoothSize = round(SmoothSize/2)
- 2393 8. Greatly smooth Asmooth by first running Asmooth 10 times through a  
2394 median filter then a smoothing filter with a moving average method on the  
2395 result. Both the median filter and the smoothing filter use a window size of  
2396 SmoothSize.

2397

#### 2398 **4.7 Filter outlier noise from signal**

- 2399 1. If there are any signal data that are 150 meters above Asmooth, remove them  
2400 from the signal data set.

- 2401 2. If the standard deviation of the detrended signal is greater than 10 meters,  
2402 remove any signal value from the signal data set that is 2 times the standard  
2403 deviation of the detrended signal below Asmooth.
- 2404 3. Calculate a new Asmooth surface by interpolating (pchip method) a surface  
2405 from the remaining signal photons and median filtering using the Window  
2406 size, then median filter and smooth (moving average method) 10 times again  
2407 using the SmoothSize.
- 2408 4. Detrend the signal photons by subtracting the signal height values from the  
2409 Asmooth surface height values. Use the detrended heights for surface finding.

2410

#### 2411 **4.8 Finding the initial ground estimate**

- 2412 1. At this point, the initial signal photons have been noise filtered and de-  
2413 trended and should have the following format: X, Y, detrended Z, T (T=time).  
2414 From this, the input data into the ground finding will be the ATD (along track  
2415 distance) metric (such as time) and the detrended Z height values.
- 2416 2. Define a medianSpan as  $\text{Window} * 2/3$ .
- 2417 3. Calculate the background neighbor density of the subsurface photons using  
2418 ALL available photons (the non-detrended data). This step is run on all  
2419 photons including noise photons. Histogram the photons in 0.5 m vertical  
2420 bins and a 60 m horizontal bin.
- 2421 4. To avoid including zero population bins in the histogram signal tracking  
2422 process, identify the bin with the maximum bin count among bins 3 - 7  
2423 (starting at the lowest height) across each 60 m within the 10-km processing  
2424 window.
- 2425 5. Calculate the mean of those maximum bin values to represent the noise count  
2426 for the 10-km window.
- 2427 6. The following steps are run on the detrended signal photons.

2428 7. Calculate the brightness of the surface for each 60 m to be histogrammed via  
2429 the calculation in Section 2.4.21. If a bright surface is detected, skip steps 7  
2430 and 8

2431 8. Determine the lowest 0.5 m histogram height bin for each 60 m along track,  
2432 in the detrended heights where:

2433 a. The neighbor density is 10 x greater than the background density and  
2434 b. The neighbor density is greater than the histogram population median  
2435 plus 1/3 of the population standard deviation.

2436 9. The photons with detrended heights above this bin are masked from  
2437 consideration in the initial ground height estimate. Detrended signal photons  
2438 implies that the d\_flag photons.

2439 10. Identifying the ground surface is an iterative process. Start by assuming that  
2440 all the input signal height photons are the ground. The first goal is the cut  
2441 out the lower height excess photons in order to find a lower bound for  
2442 potential ground photons. This process is done 5 times and an offset of 4  
2443 meters is subtracted from the resulting lower bound. The smoothing filter  
2444 uses a moving average again:

2445       for j=1:5

2446             cutOff = median filter (ground, medianSpan)

2447             cutOff = smooth filter (cutOff, Window)

2448             ground = ground( (cutOff - ground) > -1 )

2449       end

2450       lowerbound = median filter (ground, medianSpan\*3)

2451       middlebound = smooth filter (lowerbound, Window)

2452       lowerbound = smooth filter (lowerbound, Window) - 4

2453     end;

2454 11. Create a linearly interpolated surface along the lower bound points and only  
2455 keep input photons above that line as potential ground points:

2456       top = input( input > interp(lowerbound) )

2457 12. The next goal is to cut out excess higher elevation photons in order to find an  
2458 upper bound to the ground photons. This process is done 3 times and an  
2459 offset of 1 meter is added to the resulting upper bound. The smoothing filter  
2460 uses a moving average:

```
2461     for j = 1:3  
2462         cutOff = median filter (top, medianSpan)  
2463         cutOff = smooth filter (cutOff, Window)  
2464         top = top( (cutOff - top) > -1 )  
2465     end  
2466     upperbound = median filter (top, medianSpan)  
2467     upperbound = smooth filter (upperbound, Window) + 1
```

2468 13. Create a linearly interpolated surface along the upper bound points and  
2469 extract the points between the upper and lower bounds as potential ground  
2470 points:

```
2471     ground = input( ( input > interp(lowerbound) ) & ...  
2472                   ( input < interp(upperbound) ) )
```

2473 14. Refine the extracted ground points to cut out more canopy, again using the  
2474 moving average smoothing:

```
2475     For j = 1:2  
2476         cutOff = median filter (ground, medianSpan)  
2477         cutOff = smooth filter (cutOff, Window)  
2478         ground = ground( (cutOff - ground) > -1 )  
2479     end
```

2480 15. Run the ground output once more through a median filter using window side  
2481 medianSpan and a smoothing filter using window size Window, but this time  
2482 with the Savitzky-Golay method.

2483 16. Finally, linearly interpolate a surface from the ground points.

- 2512 17. The first estimate of canopy points are those indices of points that are  
2513 between 2 and 150 meters above the estimated ground surface. Save these  
2514 indices for the next section on finding the top of canopy.
- 2515 18. The output from the final iteration of ground points is temp\_interpA – an  
2516 interpolated ground estimate.
- 2517 19. Find ground indices that lie within 10 m below and 0.5 m above of  
2518 temp\_interpA only when the canopy\_flag indicates canopy should be present.  
2519 Otherwise, (i.e. no canopy) use a threshold of 0.5 m around temp\_interpA.
- 2520 20. Apply the ground indices to the original heights (i.e., not the de-trended data)  
2521 to label ground photons.
- 2522 21. Interpolate a ground surface using the pchip method based on the ground  
2523 photons. Output is interp\_Aground.

2524

#### 2525 **4.9 Find the top of the canopy (if canopy\_flag = 1)**

- 2526 1. The input are the ATD metric (i.e., time), and the de-trended Z values indexed  
2527 by the canopy indices extracted from step 4.8(17).
- 2528 2. Flip this data over so that we can find a canopy “surface” by multiplying the  
2529 de-trended canopy heights by -1.0 and adding the mean(heights).
- 2530 3. Finding the top of canopy is also an iterative process. Follow the same steps  
2531 described in 4.8(2) – 4.8(16), but use the canopy indexed and flipped Z  
2532 values in place of the ground input.
- 2533 4. Final retained photons are considered top of canopy photons. Use the indices  
2534 of these photons to define top of canopy photons in the original (not de-  
2535 trended) Z values.
- 2536 5. Build a kd-tree on canopy indices.
- 2537 6. If there are less than three canopy indices within a 15m radius, reassign  
2538 these photons to noise photons.

2539

Deleted: 10

Deleted: 9



2542 **4.10 Compute statistics on de-trended data**

- 2543 1. The input data have been noise filtered and de-trended and should have the  
2544 following input format: X, Y, detrended Z, T.
- 2545 2. The input data will contain signal photons as well as a few noise photons  
2546 near the surface.
- 2547 3. Compute statistics of heights in the along-track direction using a sliding  
2548 window. Using the window size (window), compute height statistics for all  
2549 photons that fall within each window. These include max height, median  
2550 height, mean height, min height, and standard deviation of all photon heights.  
2551 Additionally, in each window compute the median height and standard  
2552 deviation of just the initially classified top of canopy photons, and the  
2553 standard deviation of just the initially classified ground photon heights.  
2554 Currently only the median top of canopy, and all STD variables are being  
2555 utilized, but it's possible that other statistics may be incorporated as  
2556 changes/improvements are made to the code.
- 2557 4. Slide the window  $\frac{1}{4}$  of the window span and recompute statistics along the  
2558 entire *L-km* segment. This results in one value for each statistic for each  
2559 window.
- 2560 5. Determine canopy index categories for each window based upon the total  
2561 distribution of STD values for all signal photons along the *L-km* segment  
2562 based on STD quartiles.
- 2563 6. Open canopy have STD values falling within the 1<sup>st</sup> quartile.
- 2564 7. Canopy Level 1 has STD values falling from 1<sup>st</sup> quartile to median STD value.
- 2565 8. Canopy Level 2 has STD values falling from median STD value to 3<sup>rd</sup> quartile.
- 2566 9. Canopy Level 3 has STD values falling from 3<sup>rd</sup> quartile to max STD.
- 2567 10. Linearly interpolate the window STD values (both for all photons and  
2568 ground-only photons) back to the native along-track resolution and calculate  
2569 the interpolated all-photon STD quartiles to create an interpolated canopy  
2570 level index. This will be used later for interpolating a ground surface.  
2571

2572 **4.11 Refine Ground Estimates**

2573 1. Smooth the interpolated ground surface 10 times. All further ground surface  
2574 smoothing use the moving average method:

2575 For j= 1:10

2576           AgroundSmooth = median filter (interp\_Aground, SmoothSize\*5)

2577           AgroundSmooth = smooth filter (AgroundSmooth, SmoothSize)

2578 End

2579

2580 2. This output (AgroundSmooth) from the filtering/smoothing function is an  
2581 intermediate ground solution and it will be used to estimate the final  
2582 solution.

2583 3. If there are **no canopy indices** identified along the entire segment (OR  
2584 canopy\_flag = 0) AND relief >400 m

2585           FINALGROUND = median filter (Asmooth, SmoothSize)

2586           FINALGROUND = smooth filter (FINALGROUND, SmoothSize)

2587 Else

2588           FINALGROUND = AgroundSmooth

2589 end

2590 4. If there are **canopy indices** identified along the segment:

2591 If there is a canopy photon identified at a location along-track above the  
2592 ground surface, then at that location along-track

2593           FINALGROUND = AgroundSmooth

2594 else if there is a location along-track where the interpolated ground STD has  
2595 an interpolated canopy level >=3

2596           FINALGROUND = Interp\_Aground\*1/3 + AgroundSmooth\*2/3

2597 else

2598           FINALGROUND = Interp\_Aground\*1/2 + Asmooth\*1/2

2599 end

- 2600 5. Smooth the resulting interpolated ground surface (FINALGROUND) once  
 2601 using a median filter with window size of 9 then a smoothing filter twice with  
 2602 window size of 9. Select ground photons that lie within the point spread  
 2603 function (PSF) of FINALGROUND.
- 2604 6. PSF is determined by  $\sigma_{atlas\_land}$  (Eq. 1.2) calculated at the photon  
 2605 resolution and thresholded between 0.5 to 1 m.
- 2606 a. Estimate the terrain slope by taking the gradient of FINALGROUND.  
 2607 Gradient is reported at the center of  $((finalground(n+1)-$   
 2608  $finalground(n-1))/(dist\_x(n+1)-dist\_x(n-1))/2$
- 2609 b. Linearly interpolate the  $\sigma_h$  values to the photon resolution.
- 2610 c. Calculate  $\sigma_{topo}$  (Eq. 1.3) at the photon resolution.
- 2611 d. Calculate  $\sigma_{atlas\_land}$  at the photon resolution using the  $\sigma_h$   
 2612 and  $\sigma_{topo}$  values at the photon resolution.
- 2613 e. Set PSF equal to  $\sigma_{atlas\_land}$ .
- 2614 i. Any PSF < 0.5 m is set to 0.5 m as the minimum PSF.
- 2615 ii. Any PSF > 1 m is set to 1 m as the maximum PSF. Set `psf_flag` to  
 2616 true.

2617

#### 2618 **4.12 Canopy Photon Filtering**

- 2619 1. The first canopy filter will remove photons classified as top of canopy that  
 2620 are significantly above a smoothed median top of canopy surface. To  
 2621 calculate the smoothed median top of canopy surface:
- 2622 a. Linearly interpolate the median and standard deviation canopy  
 2623 window statistics, calculated from 4.10 (3), to the top of canopy  
 2624 photon resolution. Output variables: `interpMedianC`, `interpStdC`.
- 2625 b. Calculate a canopy window size using Eq. 3.4, where *length* = number  
 2626 of top of canopy photons. Output variable: `winC`.

2627           c. Create the median filtered and smoothed top of canopy surface,  
2628           smoothedC, using a locally weighted linear regression smoothing  
2629           method, “lowess” (Cleveland, 1979):

2630                       smoothedC = median filter ( interpMedianC, winC )  
2631  
2632                       if SNR > 1, canopySmoothSpan = winC\*2;  
2633                       else, canopySmoothSpan = smoothSpan;  
2634  
2635                       smoothedC = smooth filter ( smoothedC, canopySmoothSpan )

2636           d. Add the detrended heights back into the smoothedC surface:

2637                       smoothedC = smoothedC + Asmooth

2638       2. Set canopy height thresholds based on the interpolated top of canopy STD:

2639                       If SNR > 1, canopySTDthresh = 3; else, canopySTDthresh = 2;  
2640                       canopy\_height\_thresh = canopySTDthresh\*interpStdC

2641                       high\_cStd = canopy\_height\_thresh > 10

2642                       low\_cStd = canopy\_height\_thresh < 3

2643                       canopy\_height\_thresh(high\_cStd) =  
2644                       canopy\_height\_thresh(high\_cStd)/2

2645                       canopy\_height\_thresh(low\_cStd) = 3

2646       3. Relabel as noise any top of canopy photons that are higher than smoothedC +  
2647       canopy\_height\_thresh.

2648       4. Next, interpolate a top of canopy surface using the remaining top of canopy  
2649       photons (here we are trying to create an upper bound on canopy points). The  
2650       interpolation method used is pchip. This output is named interp\_Acanopy.

2651       5. Photons falling below interp\_Acanopy and above FINALGROUND+PSF are  
2652       labeled as canopy points.

2653 6. For 500 signal photon segments, if number of all canopy photons (i.e., canopy  
2654 and top of canopy) is:  
2655 < 5% of the total (when SNR > 1), OR  
2656 < 10% of the total (when SNR <= 1),  
2657 relabel the canopy photons as noise.

2658 7. Interpolate, using the pchip method, a new top of canopy surface from the  
2659 filtered top of canopy photons. This output is again named interp\_Acanopy.

2660 8. Again, label photons that lie between interp\_Acanopy and  
2661 FINALGROUND+PSF as canopy photons.

2662 9. Since the canopy points have been relabeled, we need to do a final  
2663 refinement of the ground surface:

2664 If canopy is present at any location along-track

2665 
$$\text{FINALGROUND} = \text{AgroundSmooth (at that location)}$$

2666 Else if canopy is not present at a location along-track

2667 
$$\text{FINALGROUND} = \text{interp\_Aground}$$

2668 Smooth the resulting interpolated ground surface (FINALGROUND) once  
2669 using a median filter with window size of SmoothSize (SmoothSize = 9), then  
2670 a moving average smoothing filter twice with window size of SmoothSize  
2671 (SmoothSize = 9)

2672 10. Relabel ground photons based on this new (and last) FINALGROUND solution  
2673 +/- a recalculated PSF (via steps in 4.11 (6)). Points falling below the buffer  
2674 are labeled as noise.

2675 11. Using Interp\_Acanopy and this last FINALGROUND solution + PSF buffer,  
2676 label all photons that lie between the two as canopy photons.

2677 12. Repeat the canopy cover filtering: For 500 signal photon segments, if  
2678 number of all canopy photons (i.e., canopy and top of canopy) is:  
2679 < 5% of the total (when SNR > 1), OR

2680 < 10% of the total (when SNR <= 1),  
2681 relabel the canopy photons as noise. This is the last canopy labeling step.

2682

#### 2683 **4.13 Compute individual Canopy Heights**

- 2684 1. At this point, each photon will have its final label assigned in  
2685 **classed\_pc\_flag**: 0 = noise, 1 = ground, 2 = canopy, 3 = top of canopy.
- 2686 2. For each individual photon labeled as canopy or top of canopy, subtract the Z  
2687 height value from the interpolated terrain surface, FINALGROUND, at that  
2688 particular position in the along-track direction.
- 2689 3. The relative height for each individual canopy or top of canopy photon will  
2690 be used to calculate canopy products described in Section 4.16. Additional  
2691 canopy products will be calculated using the absolute heights, as described in  
2692 Section 4.16.1.

2693

#### 2694 **4.14 Final photon classification QA check**

- 2695 1. Find any ground, canopy, or top of canopy photons that have elevations  
2696 further than the ref\_dem\_limit from the reference DEM elevation value.  
2697 Convert these to the noise classification.
- 2698 2. Find any relative heights of canopy or top of canopy photons that are greater  
2699 than 150 m above the interpolated ground surface, FINALGROUND. Convert  
2700 these to the noise classification.
- 2701 3. Find any FINALGROUND elevations that are further than the ref\_dem\_limit  
2702 from the reference DEM elevation value. Convert those FINALGROUND  
2703 elevations to an invalid value, and convert any classified photons at the same  
2704 indices to noise.
- 2705 4. If more than 50% of photons are removed in a segment, set ph\_removal\_flag  
2706 to true.

2707

2708 **4.15 Compute segment parameters for the Land Products**

- 2709 1. For each 100 m segment, determine the classed photons (photons classified  
2710 as ground, canopy, or top of canopy).
- 2711 a. If there are fewer than 50 classed photons in a 100 m segment, do not  
2712 calculate land or canopy products.
- 2713 b. If there are 50 or more classed photons in a 100 m segment, extract  
2714 the ground photons to create the land products.
- 2715 2. If the number of ground photons > 5% of the total number of classed photons  
2716 within the segment (this control value of 5% can be modified once on orbit):
- 2717 a. Compute statistics on the ground photons: mean, median, min, max,  
2718 standard deviation, mode, and skew. These heights will be reported  
2719 on the product as **h\_te\_mean**, **h\_te\_median**, **h\_te\_min**, **h\_te\_max**,  
2720 **h\_te\_mode**, and **h\_te\_skew** respectively described in Table 2.1.
- 2721 b. Compute the standard deviation of the ground photons about the  
2722 interpolated terrain surface, FINALGROUND. This value is reported as  
2723 **h\_te\_std** in Table 2.1.
- 2724 c. Compute the residuals of the ground photon Z heights about the  
2725 interpolated terrain surface, FINALGROUND. The product is the root  
2726 sum of squares of the ground photon residuals combined with the  
2727 **sigma\_atlas\_land** term in Table 2.5 as described in Equation 1.4. This  
2728 parameter reported as **h\_te\_uncertainty** in Table 2.1.
- 2729 d. Compute a linear fit on the ground photons and report the slope. This  
2730 parameter is **terrain\_slope** in Table 2.1.
- 2731 e. Calculate a best fit terrain elevation at the mid-point location of the  
2732 100 m segment:
- 2733 i. Calculate each terrain photon's distance along-track into the  
2734 100 m segment using the corresponding ATL03 20 m products  
2735 segment\_length and dist\_ph\_along, and determine the mid-  
2736 segment distance (expected to be 50 m ± 0.5 m).

2737 1. Use the mid-segment distance to linearly interpolate a  
2738 mid-segment time (**delta\_time** in Table 2.4). Use the  
2739 mid-segment time to linearly interpolate other mid-  
2740 segment parameters: interpolated terrain surface,  
2741 FINALGROUND, as **h\_te\_interp** (Table 2.1); **latitude**  
2742 and **longitude** (Table 2.4).

2743 ii. Calculate a linear fit, as well as 3<sup>rd</sup> and 4<sup>th</sup> order polynomial fits  
2744 to the terrain photons in the segment.

2745 iii. Create a slope-adjusted and weighted mid-segment variable,  
2746 weightedZ, from the linear fit: Use terrain\_slope to apply a  
2747 slope correction to each terrain photon by subtracting the  
2748 terrain photon heights from the linear fit. Determine the mid-  
2749 segment location of the linear fit, and add that height to the  
2750 slope corrected terrain photons. Apply a linear weighting to  
2751 each photon based on its distance to the mid-segment location:  
2752  $1 / \sqrt{(\text{photon distance along} - \text{mid-segment distance})^2}$ .  
2753 Calculate the weighted mid-segment terrain height, weightedZ:  
2754  $\text{sum}(\text{each adjusted terrain height} * \text{its weight}) / \text{sum}(\text{all}$   
2755  $\text{weights})$ .

2756 iv. Determine which of the three fits is best by calculating the  
2757 mean and standard deviation of the fit errors. If one of the fits  
2758 has both the smallest mean and standard deviations, use that  
2759 fit. Else, use the fit with the smallest standard deviation. If  
2760 more than one fit has the same smallest mean and/or standard  
2761 deviation, use the fit with the higher polynomial.

2762 v. Use the best fit to define the mid-segment elevation. This  
2763 parameter is **h\_te\_best\_fit** in Table 2.1.

2764 1. If **h\_te\_best\_fit** is farther than 3 m from **h\_te\_interp** (best  
2765 fit diff threshold), check if: there are terrain photons on  
2766 both sides of the mid-segment location; or the elevation  
2767 difference between weightedZ and **h\_te\_interp** is



2768 greater than the best fit diff threshold; or the number of  
2769 ground photons in the segment is  $\leq 5\%$  of total  
2770 number of classified photons per segment. If any of  
2771 those cases are present, use `h_te_interp` as the corrected  
2772 `h_te_best_fit`. Otherwise use `weightedZ` as the corrected  
2773 `h_te_best_fit`.

2774 f. Compute the difference of the median ground height from the  
2775 reference DTM height. This parameter is **`h_dif_ref`** in Table 2.4.

2776

2777 3. If the number of ground photons in the segment  $\leq 5\%$  of total number of  
2778 classified photons per segment,

2779 a. Report an invalid value for terrain products: **`h_te_mean`**,  
2780 **`h_te_median`**, **`h_te_min`**, **`h_te_max`**, **`h_te_mode`**, **`h_te_skew`**, **`h_te_std`**,  
2781 **and `h_te_uncertainty`** respectively as described in Table 2.1.

2782 b. If the number of ground photons in the segment is  $\leq 5\%$  of total  
2783 number of classified photons in the segment, compute **`terrain_slope`**  
2784 via a linear fit of the interpolated ground surface, `FINALGROUND`,  
2785 instead of the ground photons.

2786 c. Report the mid-segment interpolated terrain surface, `FinalGround`, as  
2787 **`h_te_interp`** as described in Table 2.1, and report **`h_te_best_fit`** as the  
2788 `h_te_interp` value.

2789

#### 2790 ***4.16 Compute segment parameters for the Canopy Products***

2791 1. For each 100 m segment, determine the classed photons (photons classified as  
2792 ground, canopy, or top of canopy).

2793 a) If there are fewer than 50 classed photons in a 100 m segment, do not  
2794 calculate land or canopy products.

2795 b) If there are 50 or more classed photons in a 100 m segment, extract all  
2796 canopy photons (i.e., canopy and top of canopy; henceforth referred to  
2797 as “canopy” unless otherwise noted) to create the canopy products.

2798 2. Only compute canopy height products if the number of canopy photons is >  
2799 5% of the total number of classed photons within the segment (this control  
2800 value of 5% can be modified once on orbit).

2801 a) If the number of ground photons is also > 5% of the total number of  
2802 classed photons within the segment, set **canopy\_rh\_conf** to 2.

2803 b) If the number of ground photons is < 5% of the total number of classed  
2804 photons within the segment, continue with the relative canopy height  
2805 calculations, but set canopy\_rh\_conf to 1.

2806 c) If the number of canopy photons is < 5% of the total number of classed  
2807 photons within the segment, regardless of ground percentage, set  
2808 canopy\_rh\_conf to 0 and report an invalid value for each canopy height  
2809 variable.

2810 3. Again, the relative heights (height above the interpolated ground surface,  
2811 FINALGROUND) have been computed already. All parameters derived in the  
2812 section are based on relative heights.

2813 4. Sort the heights and compute a cumulative distribution of the heights. Select  
2814 the height associated with the 98% maximum height. This value is **h\_canopy**  
2815 listed in Table 2.2.

2816 5. Compute statistics on the relative canopy heights. Min, Mean, Median, Max and  
2817 standard deviation. These values are reported on the product as  
2818 **h\_min\_canopy**, **h\_mean\_canopy**, **h\_max\_canopy**, and **canopy\_openness**  
2819 respectively in Table 2.2.

2820 6. Using the cumulative distribution of relative canopy heights, select the heights  
2821 associated with the **canopy\_h\_metrics** percentile distributions (25, 50, 60, 70,  
2822 75, 80, 85, 90, 95), and report as listed in Table 2.2.

2823 7. Compute the difference between h\_canopy and canopy\_h\_metrics(50). This  
2824 parameter is **h\_dif\_canopy** reported in Table 2.2 and represents an amount of  
2825 canopy depth.

2826 8. Compute the standard deviation of all photons that were labeled as Top of  
2827 Canopy (flag 3) in the photon labeling portion. This value is reported on the  
2828 data product as **toc\_roughness** listed in Table 2.2.

2829 9. The quadratic mean height, **h\_canopy\_quad** is computed by

$$2830 \quad qmh = \sqrt{\frac{\sum_{i=1}^{N_{ca}} h_i^2}{N_{ca}}}$$

2831 where  $N_{ca}$  is the number of canopy photons in the segment and  $h_i$  are the  
2832 individual canopy heights.

2833

#### 2834 **4.16.1 Canopy Products calculated with absolute heights**

- 2835 1. The absolute canopy height products are calculated if the number of canopy  
2836 photons is > 5% of the total number of classed photons within the segment.  
2837 No number of ground photons threshold is applied for these.
- 2838 2. The **centroid\_height** parameter in Table 2.2 is represented by all the classed  
2839 photons for the segment (canopy & ground). To determine the centroid  
2840 height, compute a cumulative distribution of all absolute classified heights  
2841 and select the median height.
- 2842 3. Calculate **h\_canopy\_abs**, the 98<sup>th</sup> percentile of the absolute canopy heights.
- 2843 4. Compute statistics on the absolute canopy heights: Min, Mean, Median, and  
2844 Max. These values are reported on the product as **h\_min\_canopy\_abs**,  
2845 **h\_mean\_canopy\_abs**, and **h\_max\_canopy\_abs**, respectively, as described in  
2846 Table 2.2.
- 2847 5. Again, using the cumulative distribution of absolute canopy heights, select  
2848 the heights associated with the **canopy\_h\_metrics\_abs** percentile  
2849 distributions (25, 50, 60, 70, 75, 80, 85, 90, 95), and report as listed in Table  
2850 2.2.

#### 2851 **4.17 Record final product without buffer**

- 2852 1. Now that all products have be determined via processing of the *L-km*  
2853 segment with the buffer included, remove the products that lie within the  
2854 buffer zone on each end of the *L-km* segment.
- 2855 2. Record the final *L-km* products and move on to process the next *L-km*  
2856 segment.

2857

2858

2859 **5 DATA PRODUCT VALIDATION STRATEGY**

2860 Although there are no Level-1 requirements related to the accuracy and precision  
2861 of the ATL08 data products, we are presenting a methodology for validating terrain  
2862 height, canopy height, and canopy cover once ATL08 data products are created.  
2863 Parameters for the terrain and canopy will be provided at a fixed size of 100 m along  
2864 the ground track referred to as a segment. Validation of the data parameters should  
2865 occur at the 100 m segment scale and residuals of uncertainties are quantified (i.e.  
2866 averaged) at the 5-km scale. This 5-km length scale will allow for quantification of  
2867 errors and uncertainties at a local scale which should reflect uncertainties as a  
2868 function of surface type and topography.

2869

2870 **5.1 Validation Data**

2871 Swath mapping airborne lidar is the preferred source of validation data for the  
2872 ICESat-2 mission due to the fact that it is widely available and the errors associated  
2873 with most small-footprint, discrete return data sets are well understood and  
2874 quantified. Profiling airborne lidar systems (such as MABEL) are more challenging to  
2875 use for validation due to the low probability of exact overlap of flightlines between  
2876 two profiling systems (e.g. ICESat-2 and MABEL). In order for the ICESat-2 validation  
2877 exercise to be statistically relevant, the airborne data should meet the requirements  
2878 listed in Table 5.1. Validation data sets should preferably have a minimum average  
2879 point density of 5 pts/m<sup>2</sup>. In some instances, however, validation data sets with a  
2880 lower point density that still meet the requirements in Table 5.1 may be utilized for  
2881 validation to provide sufficient spatial coverage.

2882 Table 5.1. Airborne lidar data vertical height (*Z* accuracy) requirements for validation data.

ICESat-2 ATL08 Parameter	Airborne lidar (rms)
Terrain height	<0.3 m over open ground (vertical) <0.5 m (horizontal)

---

Canopy height	<2 m temperate forest, < 3 m tropical forest
Canopy cover	n/a

---

2883

2884 Terrain and canopy heights will be validated by computing the residuals between the  
2885 ATL08 terrain and canopy height value, respectively, for a given 100 m segment and  
2886 the terrain height (or canopy height) of the validation data for that same  
2887 representative distance. Canopy cover on the ATL08 data product shall be validated  
2888 by computing the relative canopy cover ( $cc = \text{canopy returns}/\text{total returns}$ ) for the  
2889 same representative distance in the airborne lidar data.

2890 It is recommended that the validation process include the use of ancillary data sets  
2891 (i.e. Landsat-derived annual forest change maps) to ensure that the validation results  
2892 are not errantly biased due to non-equivalent content between the data sets.

2893 Using a synergistic approach, we present two options for acquiring the required  
2894 validation airborne lidar data sets.

2895

2896 **Option 1:**

2897 We will identify and utilize freely available, open source airborne lidar data as the  
2898 validation data. Potential repositories of this data include OpenTopo (a NSF  
2899 repository or airborne lidar data), NEON (a NSF repository of ecological monitoring  
2900 in the United States), and NASA GSFC (repository of G-LiHT data). In addition to  
2901 small-footprint lidar data sets, NASA Mission data (i.e. ICESat and GEDI) can also be  
2902 used in a validation effort for large scale calculations.

2903

2904 **Option 2:**

2905 Option 2 will include Option 1 as well as the acquisition of additional airborne lidar  
2906 data that will benefit multiple NASA efforts.

2907 GEDI: With the launch of the Global Ecosystems Dynamic Investigation  
2908 (GEDI) mission in 2018, there are tremendous synergistic activities for  
2909 data validation between both the ICESat-2 and GEDI missions. Since the  
2910 GEDI mission, housed on the International Space Station, has a  
2911 maximum latitude of 51.6 degrees, much of the Boreal zone will not be  
2912 mapped by GEDI. The density of GEDI data will increase as latitude  
2913 increases north to 51.6 degrees. Since the data density for GEDI would  
2914 be at its highest near 51.6 degrees, we would propose to acquire  
2915 airborne lidar data in a “GEDI overlap zone” that would ample  
2916 opportunity to have sufficient coverage of benefit to both ICESat-2 and  
2917 GEDI for calibration and validation.

2918 We recommend the acquisition of new airborne lidar collections that will meet our  
2919 requirements to best validate ICESat-2 as well as be beneficial for the GEDI mission.  
2920 In particular, we would like to obtain data over the following two areas:

- 2921 1) Boreal forest (as this forest type will NOT be mapped with GEDI)
- 2922 2) GEDI high density zone (between 50 to 51.6 degrees N). Airborne lidar data  
2923 in the GEDI/ICESat-2 overlap zone will ensure cross-calibration between  
2924 these two critical datasets which will allow for the creation of a global,  
2925 seamless terrain, canopy height, and canopy cover product for the  
2926 ecosystem community.

2927 In both cases, we would fly data with the following scenario:

2928 Small-footprint, full-waveform, dual wavelength (green and NIR), high point density  
2929 (>20 pts/m<sup>2</sup>) and, over low and high relief locations. In addition, the newly acquired  
2930 lidar data must meet the error accuracies listed in Table 5.1.

2931 Potential candidate acquisition areas include: Southern Canadian Rocky Mountains  
2932 (near Banff), Pacific Northwest mountains (Olympic National Park, Mt. Baker-  
2933 Snoqualmie National Forest), and Sweden/Norway. It is recommended that the

2934 airborne lidar acquisitions occur during the summer months to avoid snow cover in  
 2935 either 2016 or 2017 prior to launch of ICESat-2.

2936

2937 **5.2 Internal QC Monitoring**

2938 In addition to the data product validation, internal monitoring of data  
 2939 parameters and variables is required to ensure that the final ATL08 data quality  
 2940 output is trustworthy. Table 5.2 lists a few of the computed parameters that should  
 2941 provide insight into the performance of the surface finding algorithm within the  
 2942 ATL08 processing chain.

2943 Table 5.2. ATL08 parameter monitoring.

Group	Description	Source	Monitor	Validate in Field
<b>h_te_median</b>	Median terrain height for segment	computed		Yes against airborne lidar data. The airborne lidar data should have an absolute accuracy of <30 cm rms.
<b>n_te_photons</b> <b>n_ca_photons</b> <b>n_toc_photons</b>	Number of classed (sum of terrain, canopy, and top of canopy) photons in a 100 m segment	computed	Yes. Build an internal counter for the number of segments in a row where there aren't enough photons (currently a minimum of 50 photons	



---

<b>h_te_interp</b>	Interpolated terrain surface height, FINALGROUND	computed	per 100 m segment is used) Difference h_te_interp and h_te_median and determine if the value is > a specified threshold. 2 m is suggested as the threshold value. This is an internal check to evaluate whether the median elevation for a segment is roughly the same as the interpolated surface height.	
<b>h_dif_ref</b>	Difference between h_te_median and ref_dem	computed	This value will be computed and flagged if the difference is > 25 m. The reference DEM is the onboard DEM.	
<b>h_canopy</b>	95% height of individual canopy heights for segment	computed	Yes, > a specified threshold (e.g. 60 m)	Yes against airborne lidar data. The

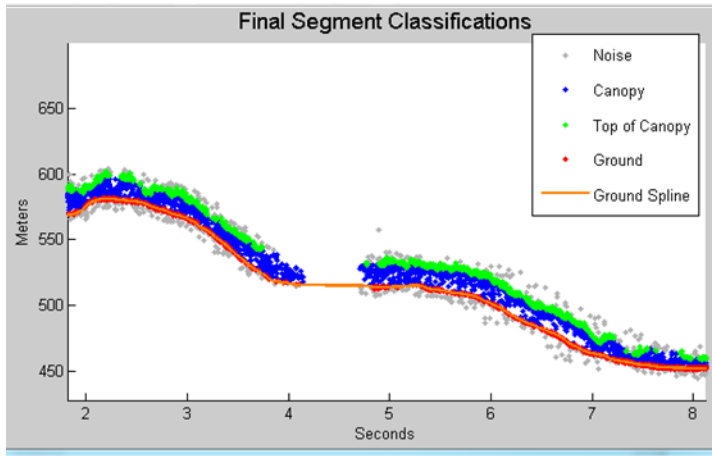
---

---

				canopy heights derived from airborne lidar data should have a relative accuracy <2 m in temperate forest, <3 m in tropical forest
<b>h_dif_canopy</b>	Difference between h_canopy and canopy_h_metrics(50)	computed	Yes, this is an internal check to make sure the calculations on canopy height are not suspect	
<b>psf_flag</b>	Flag is set if computed PSF exceeds 1m	computed	Yes, this is an internal check to make sure the calculations are not suspect	
<b>ph_removal_flag</b>	Flag is set if more than 50% of classified photons in a segment is removed during final QA check	computed		
<b>dem_removal_flag</b>	Flag is set if more than 20% of classified photons in a segment is removed due to a large distance from the reference DEM	computed	Yes, this will check if bad results are due to bad DEM values or because too much noise was labeled as signal	

---

2945 In addition to the monitoring parameters listed in Table 5.2, a plot such as what is  
2946 shown in Figure 5.1 would be helpful for internal monitoring and quality  
2947 assessment of the ATL08 data product. Figure 5.1 illustrates in graphical form what  
2948 the input point cloud look like in the along-track direction, the classifications of each  
2949 photon, and the estimated ground surface (FINALGROUND).



2950

2951 Figure 5.1. Example of *L-km* segment classifications and interpolated ground surface.

2952

2953 The following parameters are to be calculated and placed in the QA/QC group on the  
 2954 HDF5 data file, based on Table 5.2 of the ATL08 ATBD. Statistics shall be computed  
 2955 on a per-granule basis and reported on the data product. If any parameter meets the  
 2956 QA trigger conditional, an alert will be sent to the ATL08 ATBD team for product  
 2957 review.

2958 Table 5.3. QA/QC trending and triggers.

QA/QC trending description	QA trigger conditional
Percentage of segments with > 50 classed photons	None
Max, median, and mean of the number of contiguous segments with < 50 classed photons	None
Number and percentage of segments with difference in $h_{te\_interp} - h_{te\_median}$ is greater than a specified threshold (2 m TBD)	> 50 segments in a row
Max, median, and mean of $h_{diff\_ref}$ over all segments	None
Percentage of segments where $h_{diff\_ref} > 25$ m	Percentage > 75%
Percentage of segments where the $h_{canopy}$ is > 60m	None
Max, median, and mean of $h_{diff}$	None
Number and percentage of Landsat continuous tree cover pixels per processing (L-km) segment with values > 100	None
Percentage of segments where $psf\_flag$ is set	Percentage > 75%
Percentage of classified photons removed in a segment during final photon QA check	Percentage > 50% (i.e., $ph\_removal\_flag$ is set to true)

Percentage of classified photons removed in a segment during the reference DEM threshold removal process	Percentage > 20% (i.e., dem_removal_flag is set to true)
--	--

2959

2960

2961 **6 REFERENCES**

2962

2963 Carroll, M. L., Townshend, J. R., DiMiceli, C. M., Noojipady, P., & Sohlberg, R. A.  
2964 (2009). A new global raster water mask at 250 m resolution. *International Journal of*  
2965 *Digital Earth*, 2(4), 291–308. <http://doi.org/10.1080/17538940902951401>

2966 Channan, S., K. Collins, and W. R. Emanuel (2014). Global mosaics of the standard  
2967 MODIS land cover type data. University of Maryland and the Pacific Northwest  
2968 National Laboratory, College Park, Maryland, USA.

2969 Chauve, Adrien, et al. (2008). Processing full-waveform lidar data: modelling raw  
2970 signals. *International archives of photogrammetry, remote sensing and spatial*  
2971 *information sciences 2007*, 102-107.

2972 Cleveland, W. S. (1979). Robust Locally Weighted Regression and Smoothing  
2973 Scatterplots. *Journal of the American Statistical Association*, 74(368), 829–836.  
2974 <http://doi.org/10.2307/2286407>

2975 Friedl, M.A., D. Sulla-Menashe, B. Tan, A. Schneider, N. Ramankutty, A. Sibley and X.  
2976 Huang (2010). MODIS Collection 5 global land cover: Algorithm refinements and  
2977 characterization of new datasets, 2001-2012, Collection 5.1 IGBP Land Cover,  
2978 Boston University, Boston, MA, USA.

2979 Fritsch, F.N., and Carlson, R.E. (1980). Monotone Piecewise Cubic Interpolation.  
2980 *SIAM Journal on Numerical Analysis*, 17(2), 238–246.  
2981 <http://doi.org/10.1137/0717021>

2982 Goshtasby, A., and O’Neill, W.D. (1994). Curve fitting by a Sum of Gaussians.  
2983 *Graphical Models and Image Processing*, 56(4), 281-288.

2984 Goetz and Dubayah (2011). Advances in remote sensing technology and  
2985 implications for measuring and monitoring forest carbon stocks and change. *Carbon*  
2986 *Management*, 2(3), 231-244. doi:10.4155/cmt.11.18

2987 Hall, F.G., Bergen, K., Blair, J.B., Dubayah, R., Houghton, R., Hurtt, G., Kelldorfer, J.,  
2988 Lefsky, M., Ranson, J., Saatchi, S., Shugart, H., Wickland, D. (2011). Characterizing 3D  
2989 vegetation structure from space: Mission requirements. *Remote sensing of*  
2990 *environment*, 115(11), 2753-2775

2991 Harding, D.J., (2009). Pulsed laser altimeter ranging techniques and implications for  
2992 terrain mapping, in *Topographic Laser Ranging and Scanning: Principles and*  
2993 *Processing*, Jie Shan and Charles Toth, eds., CRC Press, Taylor & Francis Group, 173-  
2994 194.

2995 Neuenschwander, A.L. and Magruder, L.A. (2016). The potential impact of vertical  
2996 sampling uncertainty on ICESat-2/ATLAS terrain and canopy height retrievals for  
2997 multiple ecosystems. *Remote Sensing*, 8, 1039; doi:10.3390/rs8121039

2998 Neuenschwander, A.L. and Pitts, K. (2019). The ATL08 Land and Vegetation Product  
2999 for the ICESat-2 Mission. *Remote Sensing of Environment*, 221, 247-259.  
3000 <https://doi.org/10.1016/j.rse.2018.11.005>

3001 Neumann, T., Brenner, A., Hancock, D., Robbins, J., Saba, J., Harbeck, K. (2018). ICE,  
3002 CLOUD, and Land Elevation Satellite – 2 (ICESat-2) Project Algorithm Theoretical  
3003 Basis Document (ATBD) for Global Geolocated Photons (ATL03).

3004 Olson, D. M., Dinerstein, E., Wikramanayake, E. D., Burgess, N. D., Powell, G. V. N.,  
3005 Underwood, E. C., D'Amico, J. A., Itoua, I., Strand, H. E., Morrison, J. C., Loucks, C. J.,  
3006 Allnutt, T. F., Ricketts, T. H., Kura, Y., Lamoreux, J. F., Wettengel, W. W., Hedao, P.,  
3007 Kassem, K. R. (2001). Terrestrial ecoregions of the world: a new map of life on Earth.  
3008 *Bioscience*, 51(11), 933-938.

3009 Sexton, J.O., Song, X.-P., Feng, M. Noojipady, P., Anand, A., Huang, C., Kim, D.-H.,  
3010 Collins, K.M., Channan, S., DiMiceli, C., Townshend, J.R.G. (2013). Global, 30-m  
3011 resolution continuous fields of tree cover: Landsat-based rescaling of MODIS  
3012 Vegetation Continuous Fields with lidar-based estimations of error. *International*  
3013 *Journal of Digital Earth*, 130321031236007. doi:10.1080/17538947.2013.786146.

3014



3015 **Appendix A**

3016 **DRAGANN Gaussian Deconstruction**

3017 John Robbins

3018 20151021

3019

3020 Updates made by Katherine Pitts:

3021 20170808

3022 20181218

3023

3024 **Introduction**

3025 This document provides a verbal description of how the DRAGANN (Differential,  
3026 Regressive, and Gaussian Adaptive Nearest Neighbor) filtering system deconstructs  
3027 a histogram into Gaussian components, which can also be called *iteratively fitting a*  
3028 *sum of Gaussian Curves*. The purpose is to provide enough detail for ASAS to create  
3029 operational ICESat-2 code required for the production of the ATL08, Land and  
3030 Vegetation product. This document covers the following Matlab functions within  
3031 DRAGANN:

3032 • mainGaussian\_dragann

3033 • findpeaks\_dragann

3034 • peakWidth\_dragann

3035 • checkFit\_dragann

3036

3037 Components of the k-d tree nearest-neighbor search processing and histogram  
3038 creation were covered in the document, *DRAGANN k-d Tree Investigations*, and have  
3039 been determined to function consistently with UTexas DRAGANN Matlab software.

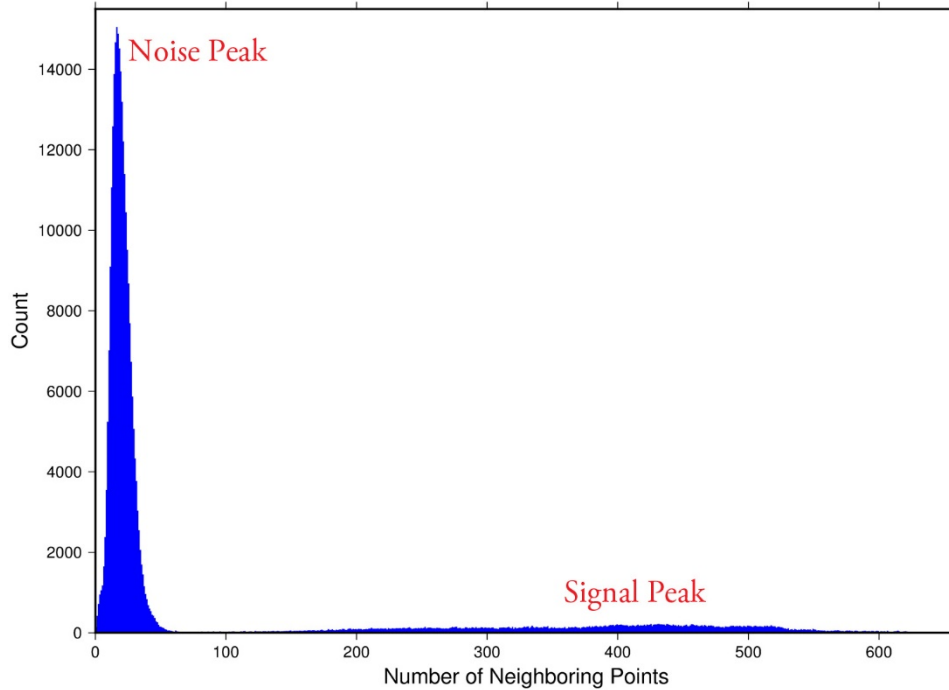
3040

3041 **Histogram Creation**

3042 Steps to produce a histogram of nearest-neighbor counts from a normalized photon  
3043 cloud segment have been completed and confirmed. Figure A.1 provides an example  
3044 of such a histogram. The development, below, is specific to the two-dimensional  
3045 case and is provided as a review.

3046 The histogram represents the frequency (count) of the number of nearby photons  
3047 within a specified radius, as ascertained for each point within the photon cloud. The  
3048 radius,  $R$ , is established by first normalizing the photon cloud in time (x-axis) and in  
3049 height (y-axis), i.e., both sets of coordinates (time & height) run from 0 to 1; then an  
3050 average radius for finding 20 points is determined based on forming the ratio of 20  
3051 to the total number of the photons in the cloud ( $N_{total}$ ):  $20/N_{total}$ .

3052



3053

3054 **Figure A.1.** Histogram for Mabel data, channel 43 from SE-AK flight on July 30, 2014  
 3055 at 20:16.

3056 Given that the total area of the normalized photon cloud is, by definition, 1, then this  
 3057 ratio gives the average area,  $A$ , in which to find 20 points. A corresponding radius is  
 3058 found by the square root of  $A/\pi$ . A single equation describing the radius, as a  
 3059 function of the total number of photons in the cloud (remembering that this is done  
 3060 in the cloud normalized, two-dimensional space), is given by

3061 
$$R = \sqrt{\frac{20/N_{total}}{\pi}} \quad (A.1)$$

3062 For the example in Figure A.1,  $R$  was found to be 0.00447122. The number of  
 3063 photons falling into this radius, at each point in the photon cloud, is given along the  
 3064 x-axis; a count of their number (or frequency) is given along the y-axis.

3065

3066 **Gaussian Peak Removal**

3067

3068 At this point, the function, `mainGaussian_dragann`, is called, which passes the  
 3069 histogram and the number of peaks to detect (typically set to 10).

3070 This function essentially estimates (i.e., fits) a sequence of Gaussian curves, from  
 3071 larger to smaller. It determines a Gaussian fit for the highest histogram peak, then  
 3072 removes it before determining the fit for the next highest peak, etc. In concept, the  
 3073 process is an iterative sequential-removal of the ten largest Gaussian components  
 3074 within the histogram.

3075 In the process of *sequential least-squares*, parameters are re-estimated when input  
3076 data is incrementally increased and/or improved. The present problem operates in  
3077 a slightly reverse way: the data set is fixed (i.e., the histogram), but components  
3078 within the histogram (independent Gaussian curve fits) are removed sequentially  
3079 from the histogram. The paper by *Goshtasby & O'Neill* (1994) outlines the concepts.

3080 Recall that a Gaussian curve is typically written as

$$3081 \quad y = a \cdot \exp(-(x - b)^2 / 2c^2) \quad (A.2)$$

3082 where  $a$  = the height of the peak;  $b$  = position of the peak; and  $c$  = width of the bell  
3083 curve.

3084 The function, `mainGaussian_dragann`, computes the  $[a, b, c]$  values for the ten  
3085 highest peaks found in the histogram. At initialization, these  $[a, b, c]$  values are set to  
3086 zero. The process begins by locating histogram peaks via the function,  
3087 `findpeaks_dragann`.

3088

### 3089 **Peak Finding**

3090 As input arguments, the `findpeaks_dragann` function receives the histogram and a  
3091 minimum peak size for consideration (typically set to zero, which means all peaks  
3092 will be found). An array of index numbers (i.e., the “number of neighboring points”,  
3093 values along x-axis of Figure A.1) for all peaks is returned and placed into the  
3094 variable `peaks`.

3095 The methodology for locating each peak goes like this: The function first computes  
3096 the derivatives of the histogram. In Matlab there is an intrinsic function, called `diff`,  
3097 which creates an array of the derivatives. `Diff` essentially computes the differences  
3098 along sequential, neighboring values. “ $Y = \text{diff}(X)$  calculates differences between  
3099 adjacent elements of  $X$ .” [from Matlab Reference Guide] Once the derivatives are  
3100 computed, then `findpeaks_dragann` enters a loop that looks for changes in the sign  
3101 of the derivative (positive to negative). It skips any derivatives that equal zero.

3102 For the  $k$ th derivative, the “*next*” derivative is set to  $k+1$ . A test is made whereby if  
3103 the  $k+1$  derivative equals zero and  $k+1$  is less than the total number of histogram  
3104 values, then increment “*next*” to  $k+2$  (i.e., find the next negative derivative). The test  
3105 is iterated until the start of the “down side” of the peak is found (i.e., these iterations  
3106 handle cases when the peak has a flat top to it).

3107 When a sign change (positive to negative) is found, the function then computes an  
3108 approximate index location (variable *maximum*) of the peak via

$$3109 \quad \text{maximum} = \text{round}\left(\frac{\text{next}-k}{2}\right) + k \quad (A.3)$$

3110 These values of *maximum* are retained in the peaks array (which can be *grown* in  
3111 Matlab) and returned to the function mainGaussian\_dragann.

3112 Next, back within mainGaussian\_dragann, there are two tests to determine whether  
3113 the first or last elements of the histogram are peaks. This is done since the  
3114 findpeaks\_dragann function will not detect peaks at the first or last elements, based  
3115 solely on derivatives. The tests are:

3116 If ( histogram(1) > histogram(2) && max(histogram)/histogram(1) < 20 ) then  
3117 insert a value of 1 to the very first element of the peaks array (again, Matlab can  
3118 easily “grow” arrays). Here, max(histogram) is the highest peak value across the  
3119 whole histogram.

3120 For the case of the last histogram value (say there are N-bins), we have

3121 If ( histogram(N) > histogram(N-1) && max(histogram)/histogram(N) < 4 ) then  
3122 insert a value of N to the very last element of the peaks array.

3123 One more test is made to determine whether there any peaks were actually found  
3124 for the whole histogram. If none were found, then the function,  
3125 mainGaussian\_dragann, merely exits.

3126

### 3127 **Identifying and Processing upon the Ten Highest Peaks**

3128 The function, mainGaussian\_dragann, now begins a loop to analyze the ten highest  
3129 peaks. It begins the  $n^{\text{th}}$  loop (where  $n$  goes from 1 to 10) by searching for the largest  
3130 peak among all remaining peaks. The index number, as well as the magnitude of the  
3131 peak, are retained in a variable, called maximum, with dimension 2.

3132 In each pass in the loop, the  $[a,b,c]$  values (see eq. 2) are retained as output of the  
3133 function. The values of  $a$  and  $b$  are set equal to the index number and peak  
3134 magnitude saved in maximum(1) and maximum(2), respectively. The  $c$ -value is  
3135 determined by calling the function, peakWidth\_dragann.

#### 3136 *Determination of Gaussian Curve Width*

3137 The function, peakWidth\_dragann, receives the whole histogram and the index  
3138 number (maximum(1)) of the peak for which the value  $c$  is needed, as arguments.  
3139 For a specific peak, the function essentially searches for the point on the histogram  
3140 that is about  $\frac{1}{2}$  the size of the peak and that is furthest away from the peak being  
3141 investigated (left and right of the peak). If the two sides (left and right) are  
3142 equidistant from the peak, then the side with the smallest value is chosen ( $> \frac{1}{2}$   
3143 peak).

3144 Upon entry, it first initializes  $c$  to zero. Then it initializes the index values left, xL and  
3145 right, xR as index-1 and index+1, respectively (these will be used in a loop,

3146 described below). It next checks whether the  $n^{\text{th}}$  peak is the first or last value in the  
3147 histogram and treats it as a special case.

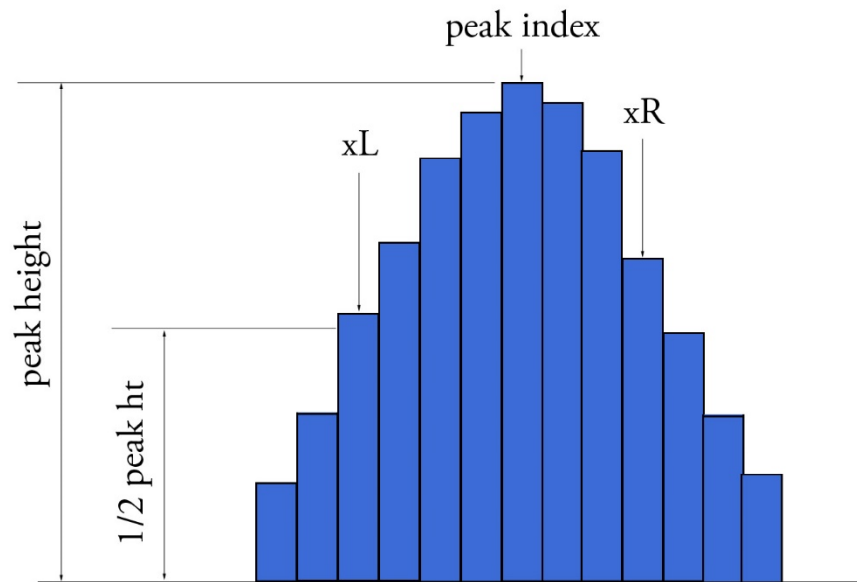
3148 At initialization, first and last histogram values are treated as follows:

3149 If first bin of histogram (peak = 1), set left = 1 and xL = 1.

3150 If last bin of histogram, set right =  $m$  and xR =  $m$ , where  $m$  is the final index of the  
3151 histogram.

3152 Next, a search is made to the left of the peak for a nearby value that is smaller than  
3153 the peak value, but larger than half of the peak value. A while-loop does this, with  
3154 the following conditions: (a) left > 0, (b) histogram value at left is  $\geq$  half of histo  
3155 value at peak and (c) histo value at left is  $\leq$  histo value at peak. When these  
3156 conditions are all true, then xL is set to left and left is decremented by 1, so that the  
3157 test can be made again. When the conditions are no longer met (i.e., we've moved to  
3158 a bin in the histogram where the value drops below half of the peak value), then the  
3159 program breaks out of the while loop.

3160 This is followed by a similar search made upon values to the right of the peak. When  
3161 these two while-loops are complete, we then have the index numbers from the  
3162 histogram representing bins that are above half the peak value. This is shown in  
3163 Figure A.2.



3164

3165 **Figure A.2.** Schematic representation of a histogram showing xL and xR parameters  
3166 determined by the function peakWidth\_dragann.

3167 A test is made to determine which of these is furthest from the middle of the peak. In  
3168 Figure A.2, xL is furthest away and the variable x is set to equal xL. The histogram

3169 “height” at  $x$ , which we call  $V_x$ , is used (as well as  $x$ ) in an inversion of Equation A.2  
3170 to solve for  $c$ :

$$3171 \quad c = \sqrt{\frac{-(x-b)^2}{2\ln\left(\frac{V_x}{a}\right)}} \quad (\text{A.4})$$

3172 The function, `peakWidth_dragann`, now returns the value of  $c$  and control returns to  
3173 the function, `mainGaussian_dragann`.

3174 The `mainGaussian_dragann` function then picks-up with a test on whether the  
3175 returned value of  $c$  is zero. If so, then use a value of 4, which is based on an *a priori*  
3176 understanding that  $c$  usually falls between 4 and 6. If the value of  $c$  is not zero, then  
3177 add 0.5 to  $c$ .

3178 At this point, we have the  $[a,b,c]$  values of the Gaussian for the  $n^{\text{th}}$  peak. Based on  
3179 these values, the Gaussian curve is computed (via Equation A.2) and it is removed  
3180 (subtracted) from the current histogram (and put into a new variable called  
3181 `newWave`).

3182 After a Gaussian curve is removed from the current histogram, the following peak  
3183 width calculations could potentially have a  $V_x$  value less than 1 from  $a$ . This would  
3184 cause the width,  $c$ , to be calculated as unrealistically large. Therefore, a check is put  
3185 in place to determine if  $a - V_x < 1$ . If so,  $V_x$  is set to a value of  $a - 1$ .

### 3186 *Numeric Optimization Steps*

3187 The first of the optimization steps utilizes a Full Width Half Max (*FWHM*) approach,  
3188 computed via

$$3189 \quad FWHM = 2c\sqrt{2\ln 2} \quad (\text{A.5})$$

3190 A left range,  $L_r$ , is computed by  $L_r = \text{round}(b - FWHM/2)$ . This tested to make sure it  
3191 doesn't go off the left edge of the histogram. If so, then it is set to 1.

3192 Similarly, a right range,  $R_r$ , is computed by  $R_r = \text{round}(b + FWHM/2)$ . This is also tested  
3193 to be sure that it doesn't go off the right edge of the histogram. If so, then it is set to  
3194 the index value for the right-most edge of the histogram.

3195 Using these new range values, create a temporary segment (between  $L_r$  and  $R_r$ ) of  
3196 the `newWave` histogram, this is called `errorWave`. Also, set three delta parameters  
3197 for further optimization:

3198 `DeltaC = 0.05;`      `DeltaB = 0.02;`      `DeltaA = 1`

3199 The temporary segment, `errorWave` is passed to the function `checkFit_dragann`,  
3200 along with a set of zero values having the same number of elements as `errorWave`,  
3201 the result, at this point, is saved into a variable called `oldError`. The function,  
3202 `checkFit_dragann`, computes the sum of the squares of the difference between two

3203 histogram segments (in this case, errorWave and zeros with the same number of  
3204 elements as errorWave). Hence, the result, oldError, is the sum of the squares of the  
3205 values of errorWave. This function is applied in optimization loops, to refine the  
3206 values of b and c, described below.

3207 *Optimization of the b-parameter.* The do-loop operates at a maximum of 1000 times.  
3208 It's purpose is to refine the value of  $b$ , in 0.02 increments. It increments the value of  
3209  $b$  by DeltaB, to the right, and computes a new Gaussian curve based on  $b+\Delta b$ , which  
3210 is then removed from the histogram with the result going into the variable  
3211 newWave. As before, checkFit\_dragann is called by passing the range-limited part of  
3212 newWave (errorWave) and returning a new estimate of the error (newError) which  
3213 is then checked against oldError to determine which is smaller. If newError is  $\geq$   
3214 oldError, then the value of  $b$  that produced oldError is retained, and the testing loop  
3215 is exited.

3216 *Optimization of the c-parameter.* Now the value of  $c$  is optimized, first to the left,  
3217 then to the right. It is performed independently of, but similarly, to the  $b$ -parameter,  
3218 using do-loops with a maximum of 1000 passes. These loops increment (to right) or  
3219 decrement (to left) by a value of 0.05 (DeltaC) and use checkFit\_dragann to, again,  
3220 check the quality of the fit. The loops (right and left) kick-out when the fit is found to  
3221 be smallest.

3222 The final, optimized Gaussian curve is now removed (subtracted) from the  
3223 histogram. After removal, a statement "corrects" any histogram values that may  
3224 drop below zero, by setting them to zero. This could happen due to any mis-fit of the  
3225 Gaussian.

3226 The  $n^{\text{th}}$  loop is concluded by examining the peaks remaining in the histogram  
3227 without the peak just processed by sending the  $n^{\text{th}}$ -residual histogram back into the  
3228 function findpeaks\_dragann. If the return of peak index numbers from  
3229 findpeaks\_dragann reveals more than 1 peak remaining, then the index numbers for  
3230 peaks that meet these three criteria are retained in an array variable called these:

- 3231 1. The peak must be located above  $b(n)-2*c(n)$ , and
  - 3232 2. The peak must be located below  $b(n)+2*c(n)$ , and
  - 3233 3. The height of the peak must be  $< a(n)/5$ .
- 3234

3235 The peaks meeting all three of these criteria are to be eliminated from further  
3236 consideration. What this accomplishes is eliminate the nearby peaks that have a size  
3237 lower than the peak just previously analyzed; thus, after their elimination, only  
3238 leaving peaks that are further away from the peak just processed and are  
3239 presumably "real" peaks. The  $n^{\text{th}}$  iteration ends here, and processing begins with the  
3240 revised histogram (after having removed the peak just analyzed).

3241



## 3242 **Gaussian Rejection**

3243 The function `mainGaussian_dragann` returns the  $[a,b,c]$  parameters for the ten  
3244 highest peaks from the original histogram. The remaining code in `dragann` examines  
3245 each of the ten Gaussian peaks and eliminates the ones that fail to meet a variety of  
3246 conditions. This section details how this is accomplished.

3247 First, an approximate area,  $area1=a*c$ , is computed for each found peak and  $b$ , for all  
3248 ten peaks, being the index of the peaks, are converted to an actual value via  
3249  $b+\min(\text{numptsinrad})-1$  (call this  $allb$ ).

3250 Next, a rejection is made for all peaks that have any component of  $[a,b,c]$  that are  
3251 imaginary (Matlab `isreal` function is used to confirm that all three components are  
3252 real, in which case it passes).

3253 To check for a narrow noise peak at the beginning of the histogram in cases of low  
3254 noise rates, such as during nighttime passes, a check is made to first determine if the  
3255 highest Gaussian amplitude,  $a$ , within the first 5% of the histogram is  $\geq 1/10$  \* the  
3256 maximum amplitude of all Gaussians. If so, that peak's Gaussian width,  $c$ , is checked  
3257 to determine if it is  $\leq 4$  bins. If neither of those conditions are met in the first 5%,  
3258 the conditions are rechecked for the first 10% of the histogram. This process is  
3259 repeated up to 30% of the histogram, in 5% intervals. Once a narrow noise peak is  
3260 found, the process breaks out of the incremental 5% histogram checks, and the  
3261 noise peak values are returned as  $[a0, b0, c0]$ .

3262 If a narrow noise peak was found, the remaining peak area values,  $area1 (a*c)$ , then  
3263 pass through a descending sort; if no narrow noise peak was found, all peak areas go  
3264 through the descending sort. So now, the  $[a,allb,c]$ -values are sorted from largest  
3265 "area" to smallest, these are placed in arrays  $[a1, b1, c1]$ . If a narrow noise peak was  
3266 found, it is then appended to the beginning of the  $[a1, b1, c1]$  arrays, such that  $a1 =$   
3267  $[a0 a1]$ ,  $b1 = [b0 b1]$ ,  $c1 = [c0 c1]$ .

3268 In the case that a narrow noise peak was not found, a test is made to check that at  
3269 least one of the peaks is within the first 10% of the whole histogram. It is done  
3270 inside a loop that works from peak 1 to the number of peaks left at this point. This  
3271 loop first tests whether the first (sorted) peak is within the first 10% of the  
3272 histogram; if so, then it simply kicks out of the loop. If not, then it places the loop's  
3273 current peak into a holder (`ihold`) variable, increments the loop to the next peak and  
3274 runs the same test on the second peak, etc. Here's a Matlab code snippet:

```
3275 inds = 1:length(a1);  
3276 for i = 1:length(b1)  
3277     if b1(i) <= min(numptsinrad) + 1/10*max(numptsinrad)  
3278         if i==1  
3279             break;  
3280         end  
3281         ihold = inds(i);  
3282         for j = i:-1:2  
3283             inds(j) = inds(j-1);  
3284         end  
3285         inds(1) = ihold;
```



```

3286         break
3287     end
3288 end
3289

```

3290 The j-loop expression gives the `init_val:step_val:final_val`. The semi-colon at the end  
3291 of statements causes Matlab to execute the expression without printout to the user's  
3292 screen. When this loop is complete, then the indexes (`inds`) are re-ordered and  
3293 placed back into the `[a1,b1,c1]` and `area1` arrays.

3294 Next, are tests to reject any Gaussian peak that is entirely encompassed by another  
3295 peak. A Matlab code snippet helps to describe the processing.

```

3296 % reject any gaussian if it is fully contained within another
3297 isR = true(1,length(a1));
3298 for i = 1:length(a1)
3299     ai = a1(i);
3300     bi = b1(i);
3301     ci = c1(i);
3302     aset = (1-(c1/ci).^2);
3303     bset = ((c1/ci).^2*2*bi - 2*b1);
3304     cset = -(2*c1.^2.*log(a1/ai)-b1.^2+(c1/ci).^2*bi^2);
3305     realset = (bset.^2 - 4*aset.*cset >= 0) | (a1 > ai);
3306     isR = isR & realset;
3307 end
3308 a2 = a1(isR);
3309 b2 = b1(isR);
3310 c2 = c1(isR);

```

3311

3312 The logical array `isR` is initialized to all be true. The i-do-loop will run through all  
3313 peaks. The computations are done in array form with the variables `aset,bset,cset` all  
3314 being arrays of `length(a1)`. At the bottom of the loop, `isR` remains "true" when  
3315 either of the conditions in the expression for `realset` is met (the single "|" is a logical  
3316 "or"). Also, the nomenclature, "." and ".", denote element-by-element array  
3317 operations (not matrix operations). Upon exiting the i-loop, the array variables  
3318 `[a2,b2,c2]` are set to the `[a1,b1,c1]` that remain as "true." [At this point, in our test  
3319 case from channel 43 of East-AK Mable flight on 20140730 @ 20:16, six peaks are  
3320 still retained: 18, 433, 252, 33, 44.4 and 54.]

3321 Next, reject Gaussian peaks whose centers lay within  $3\sigma$  of another peak, unless only  
3322 two peaks remain. The code snippet looks like this:

```

3323 isR = true(1, length(a2));
3324 for i = 1:length(a2)
3325     ai = a2(i);
3326     bi = b2(i);
3327     ci = c2(i);
3328     realset = (b2 > bi+3*ci | b2 < bi-3*ci | b2 == bi);
3329     realset = realset | a2 > ai;
3330     isR = isR & realset;
3331 end
3332 if length(a2) == 2
3333     isR = true(1, 2);
3334 end
3335 a3 = a2(isR);

```

```
3336     b3 = b2(isR);  
3337     c3 = c2(isR);
```

3338

3339 Once again, the isR array is initially set to “true.” Now, the array, realset, is tested  
3340 twice. In the first line, one of three conditions must be true. In the second line, if  
3341 realset is true or  $a2 > ai$ , then it remains true. At this point, we’ve pared down, from  
3342 ten Gaussian peaks, to two Gaussian peaks; one represents the noise part of the  
3343 histogram; the other represents the signal part.

3344 If there are less than two peaks left, a thresholding/histogram error message is  
3345 printed out. If the lastTryFlag is not set, DRAGANN ends its processing and an empty  
3346 IDX value is returned. The lastTryFlag is set in the preprocessing function which  
3347 calls DRAGANN, as multiple DRAGANN runs may be tried until sufficient signal is  
3348 found.

3349 If there are two peaks left, then set the array [a,b,c] to those two peaks. [At this  
3350 point, in our test case from channel 43 of East-AK Mable flight on 20140730 @  
3351 20:16, the two peaks are: 18 and 433.]

3352

### 3353 **Gaussian Thresholding**

3354 With the two Gaussian peaks identified as noise and signal, all that is left is to  
3355 compute the threshold value between the Gaussians.

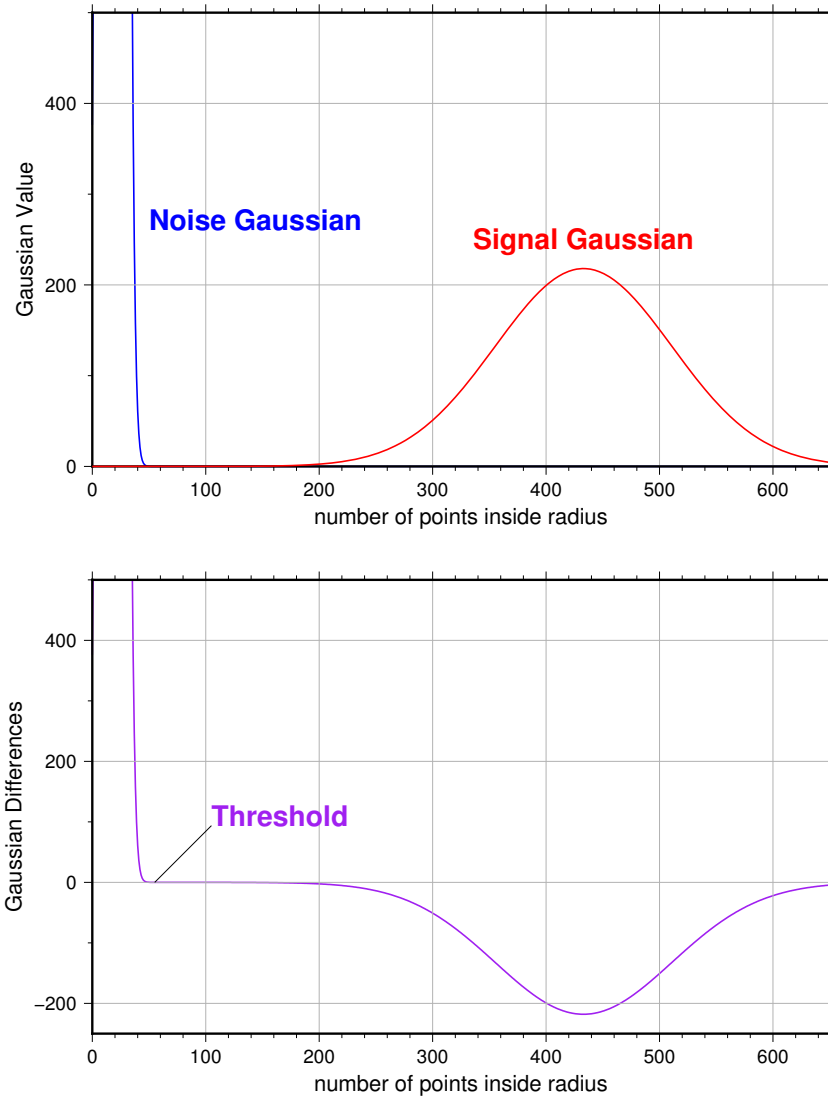
3356 An array of xvals is established running from min(numptsinrad) to  
3357 max(numptsinrad). In our example, xvals has indices between 0 and 653. For each  
3358 of these xvals, Gaussian curves (allGauss) are computed for the two Gaussian peaks  
3359 [a,b,c] determined at the end of the previous section. This computation is performed  
3360 via a function called gaussmaker which receives, as input, the xvals array and the  
3361 [a,b,c] parameters for the two Gaussian curves. An array of heights of the Gaussian  
3362 curves is returned by the function, computed with Equation A.2. In Matlab, the  
3363 allGauss array has dimension 2x654. An array, noiseGauss is set to be equal to the  
3364 1<sup>st</sup> column of allGauss.

3365 An if-statement checks whether the b array has more than 1 element (i.e., consisting  
3366 of two peaks), if so, then nextGauss is set to the 2<sup>nd</sup> column of allGauss, and a  
3367 difference, noiseGauss-nextGauss, is computed.

3368 The following steps are restricted to be between the two main peaks. First, the first  
3369 index of the absolute value of the difference that is near-zero (defined as 1e-8) is  
3370 found, if it exists, and put into the variable diffNearZero. This is expected to be found  
3371 if the two Gaussians are far away from each other in the histogram.

3372 Second, the point (i.e., index) is found of the minimum of the absolute value of the  
3373 difference; this index is put into variable, signchanges. This point is where the sign  
3374 changes from positive to negative as one moves left-to-right, up the Gaussian curve

3375 differences (noise minus next will be positive under the peak of the noise curve, and  
 3376 negative under the next (signal) curve). Figure A.3 (top) shows the two Gaussian  
 3377 curves. The bottom plot shows their differences.



3378

3379 **Figure A.3.** Top: two remaining Gaussian curves representing the noise (blue) and  
 3380 signal (red) portions of the histogram in F1gure A.1. Bottom: difference noise -  
 3381 signal of the two Gaussian curves. The threshold is defined as the point where the  
 3382 sign of the differences change.

3383 If there is any value stored in `diffNearZero`, that value is now saved into the variable  
 3384 `threshNN`. Else, the value of the threshold in `signchanges` is saved into `threshNN`,  
 3385 concluding the if-statement for `b` having more than 1 element.

3386 An else clause ( $b \neq 1$ ), merely sets threshNN to  $b+c$ , i.e., 1-standard deviation away  
3387 from mean of the (presumably) noise peak.

3388 The final step is mask the signal part of the histogram where all indices above the  
3389 threshNN index are set to logical 1 (true). This is applied to the numptsinrad array,  
3390 which represents the photon cloud. After application, dragann returns the cloud  
3391 with points in the cloud identified as “signal” points.

3392 The Matlab code has a few debug statements that follow, along with about 40 lines  
3393 for plotting.

3394

### 3395 **References**

3396 Goshtasby, A & W. D. O’Neill, Curve Fitting by a Sum of Gaussians, *CVGIP: Graphical*  
3397 *Models and Image Processing*, V. 56, No. 4, 281-288, 1994.